Universidade de Aveiro Departamento de Química

2019

Cristiana Martins Albuquerque

O papel do metabolismo das células dendríticas na imunidade anti-tumoral

The role of dendritic cell metabolism in antitumor immunity

Universidade de Aveiro Departamento de Química
2019

Cristiana Martins Albuquerque

O papel do metabolismo das células dendríticas naa imunidade anti-tumoral

Dissertação apresentada à Universidade de Aveiro para cumprimento dos requisitos necessários à obtenção do grau de Mestre em Bioquímica, ramo Métodos Biomoleculares, realizada sob a orientação científica da Doutora Iola Melissa Fernandes Duarte, Investigadora Principal do CICECO – Instituto de Materiais de Aveiro, Departamento de Química da Universidade de Aveiro, e da Doutora Catarina Rodrigues de Almeida, Professora Auxiliar do Departamento de Ciências Médicas da Universidade de Aveiro

This work was developed within the scope of the projects CICECO-Aveiro Institute of Materials, FCT Ref. UID/CTM/50011/2019, and iBiMED UID/BIM/04501/2019, project POCI-01-0145-FEDER-007628, financed by national funds through the FCT/MCTES. It was also supported by the projects StressIn (PTDC/IMI-IMU/3615/2014 and POCI-01-0145-FEDER-016768) and IDPhagy (PTDC/BIA-CEL/28791/2017 and POCI-01-0145-FEDER-028791), funded by FEDER, through COMPETE2020 - Programa Operacional Competitividade e Internacionalização (POCI), and by national funds (OE), through FCT/MCTES. The NMR spectrometers are part of the National NMR Network (PTNMR) and are partially supported by Infrastructure Project Nº 022161 (co-financed by FEDER through COMPETE 2020, POCI and PORL and FCT through PIDDAC).

Dedico este trabalho:

Aos meus pais, que me deram a capacidade de me superar e desejar o melhor em cada passo deste caminho árduo e difícil da vida. Agradeço por serem como são, porque a sua presença me tem ajudado a construir e a forjar a pessoa que sou hoje.

À minha família, orientadoras e amigos, que no andar da vida os encontrei, porque cada um deles motivou os meus sonhos e esperanças em consolidar as minhas ambições.

Obrigada a todos aqueles que percorreram comigo este caminho.

"100% de mim não é nada comparado com 1% da equipa inteira"
Eliud Kipchoge

o júri

presidente

Professora Doutora Diana Cláudia Gouveia Alves Pinto
Professora Auxiliar, Departamento de Química, Universidade de Aveiro

Professora Doutora Ana Maria Pissarra Coelho Gil
Professora Associada com Agregação, Departamento de Química, Universidade de Aveiro

Professora Doutora Catarina Rodrigues de Almeida
Professora Auxiliar, Departamento de Ciências Médicas, Universidade de Aveiro

agradecimentos

Foram 2 anos de uma aventura de autodescoberta e crescimento, tanto pessoal como profissional. Uma aventura de pesquisa científica, amadurecimento e consolidação da minha trajetória como Mestre em Bioquímica. Uma aventura com momentos de insegurança, angústia, mas também de superação de obstáculos que me fizeram tomar um caminho adulto em todos os sentidos. E, sem o apoio de muitas pessoas, este percurso não teria sido possível. Quero aqui aproveitar o espaço para agradecer profundamente à grande rede de apoio que tive para conseguir terminar esta parte importante do percurso marcado principalmente por encontros, abraços e trocas genuínas de conhecimento.

Em primeiro lugar quero agradecer à minha família. Sem vocês nada teria o mínimo sentido desde o princípio. Em momentos de dificuldades, reviravoltas e mudanças eu fui suportada emocionalmente e financeiramente por pais que, sustentaram a promessa de oferecer às suas duas meninas acesso ao estudo como herança. E cheguei ao segundo grau desse processo, unindo os meus sonhos com os sonhos dos meus pais. Obrigado por fazerem parte da minha vida e serem o meu porto seguro: pai, mãe, irmã e avós, obrigada por todo o carinho e fé em mim (um agradecimento especial à avó por me ter mantido bem alimentada).

Em segundo, um agradecimento especial às minhas orientadoras, Doutora Iola Duarte e Doutora Catarina Almeida, que confiaram em mim para desenvolver este trabalho. Agradeço a orientação exemplar com elevado rigor científico, um interesse permanente, uma visão crítica, um empenho exigente e, por fim e não menos importante, os pequenos puxões de orelhas. Tudo isto contribuiu para enriquecer com dedicação, passo a passo, todas as etapas subjacentes ao trabalho realizado.

Ao pessoal que integra os grupos de investigação do CICECO e iBiMED, que me receberam tão bem e me acompanharam nesta “aventura”, pela sua disponibilidade e interesse em transmitir o seu conhecimento. Um agradecimento especial ao Luís Mendes, pela sua ajuda indispensável na recolha e análise de amostras e pela partilha de conhecimentos preciosos para o meu trabalho.

Os últimos são os primeiros e, por isso, quero agradecer aos meus amigos de sempre, Daniel, Diana e Carolina, que me acompanharam durante 5 anos, cujo apoio tem sido crucial e cuja amizade é um verdadeiro porto de abrigo. Obrigada Daniel por me aturares 24h por dia durante este ano.

Obrigada a todos aqueles que contribuíram para esta longa viagem.

palavras-chave

Células dendríticas plasmacitóides, microambiente tumoral, interferão, metabolismo celular, metabolómica, espetroscopia de ressonância magnética nuclear

resumo

As células dendríticas plasmacitóides (pDCs) caracterizam-se pela produção de grandes quantidades de interferão tipo 1 (IFN-α/β) quando estimuladas nos recetores TLR7/9. Em cancro, contudo, as pDCs têm demonstrado uma diminuição da sua capacidade de ativação, diminuindo a produção de interferão e, assim, contribuindo para um ambiente imunossupressor. Nos últimos anos tem sido demonstrado que o metabolismo celular desempenha um papel fundamental no processo de ativação das pDCs, embora ainda falte uma compreensão abrangente da relação entre as adaptações metabólicas destas células e as suas funções estimuladoras ou reguladoras. O presente trabalho pretendeu contribuir para elucidar esta relação. Numa fase inicial, a linha celular de pDCs humanas CAL-1 foi cultivada *in vitro* e tratada com um agonista de TLR7 (CL307) em diferentes concentrações e tempos de incubação, com vista a otimizar as condições de ativação das células. De seguida, o trabalho focou-se nas respostas fenotípicas e metabólicas das pDCs ao CL307, sob a influência de fatores que mimetizam o microambiente tumoral (TNF-α+TGF-β). Para além da avaliação dos níveis de expressão de mRNA de IFN-β e TNF-α, as frações polares das células foram analisadas por espectroscopia de RMN de protão, tendo-se identificado cerca de 30 metabolitos intracelulares. Analisaram-se ainda os sobrenadantes dos meios de cultura para caracterizar os padrões de consumo e excreção das células. Os níveis de mRNA de IFN-β e TNF-α aumentaram significativamente após incubação das células durante 3h com CL307 a 1 µM. A exposição ao estímulo durante 3h resultou numa maior alteração dos níveis de expressão de mRNA de IFN-β e TNF-α, mas num menor impacto na composição e atividade metabólica das células do que durante 1h de exposição ao estímulo. As alterações metabólicas associadas à ativação com CL307 sugerem intensificação da glicólise e do ciclo do ácido tricarboxílico (TCA), que poderá estar correlacionada com o aumento das necessidades biosintéticas, inerente a um perfil imunogénico. Sob a influência de TNF-α e TGF-β, observou-se uma supressão da expressão de mRNA de IFN-β e TNF-α associada à ativação do TLR7, acompanhada por uma atenuação das alterações metabólicas. De uma forma geral, este estudo demonstrou que, na presença de um microambiente tumoral, as células dendríticas plasmacitóides CAL-1 alteram a sua resposta fenotípica e metabólica à estimulação do TLR7.

keywords

Plasmacytoid dendritic cells, tumor microenvironment, interferon, cell metabolism, metabolomics, nuclear magnetic resonance spectroscopy

abstract

Plasmacytoid dendritic cells (pDCs) are characterized by their ability to produce large amounts of interferon type I (IFN-α/β) when TLR7/9 receptors are stimulated. In cancer, however, pDCs have been shown to decrease their response, decreasing interferon production and thus contributing to an immunosuppressive environment. In recent years, cellular metabolism has been shown to play a key role in the activation process of pDCs, although a comprehensive understanding of the relation between metabolic adaptations on these cells and their stimulatory or regulatory functions is still lacking. The present work aims to further clarify this relation. Firstly, the human CAL-1 pDC cell line was cultured *in vitro* and treated with a TLR7 agonist (CL307) at different concentrations and incubation times, in order to optimize conditions for CAL-1 activation. Then, the work focused on the phenotypic and metabolic responses of pDCs to CL307, under the influence of factors that mimic the tumor microenvironment (TNF-α+TGF-β). In addition to the evaluation of IFN-β and TNF-α mRNA expression levels, the polar fractions of the cells were analyzed by ^{1}H-NMR spectroscopy and about 30 intracellular metabolites were identified. Culture media supernatants were further analyzed to characterize cell consumption and excretion patterns. The levels of IFN-β and TNF-α mRNA increased significantly upon incubation with CL307 1 µM for 3h. Exposure to the stimulus for 3h resulted in a greater change in IFN-β and TNF-α mRNA, but had a lower impact on cell composition and metabolic activity than an incubation of 1h. Metabolic changes associated with activation with CL307 resulted in intensification of glycolysis and the tricarboxylic acid (TCA) cycle, which may be correlated with the increased biosynthetic requirements inherent in an immunogenic profile. Under the influence of TNF-α and TGF-β, there was a suppression of IFN-β and TNF-α mRNA expression associated with activation, accompanied by attenuation of metabolic changes. Overall, this study demonstrated that, in the presence of a tumor microenvironment, CAL-1 plasmacytoid dendritic cells alter their phenotypic and metabolic response to TLR7 stimulation.

Abbreviations & Acronyms

1D	One-Dimensional
2-DG	2-Deoxyglucose
Acetyl-CoA	Acetyl Coenzyme A
AICAR	5-Aminoimidazole-4-Carboxamide Ribonucleotide
Akt	Protein Kinase B
AMPK	AMP-Activated Protein Kinase
APC	Antigen-Presenting Cell
ATP	Adenosine Triphosphate
BAD-LAMP	Brain and Dendritic cell (BAD)-Associated Lysosome-Associated Membrane Protein (LAMP)
BCAA	Branched-Chain Amino Acids
BMDC	Bone Marrow-Derived Dendritic Cell
BSA	Bovine Serum Albumin
CAF	Cancer-Associated Fibroblast
CCL22	C-C motif chemokine 22
cDC	Conventional Dendritic Cell
cDC1	Conventional Dendritic Cell Type 1
cDC2	Conventional Dendritic Cell Type 2
cDNA	Complementary DNA
CL307	N1-glycinyl [4-((6-amino-2-(butylamino)-8-hydroxy-9H-purin-9-yl)methyl) benzoyl] spermine
COX	Cyclooxygenase
CTL	Cytotoxic T Lymphocyte
CTLA	Cytotoxic T Lymphocyte Antigen
CXCL12	C-X-C Motif Chemokine 12
DAMP	Damage-Associated Molecular Pattern
DC	Dendritic Cell
DEX	Dexamethasone
dsDNA	Double-Strand DNA
DTT	Dithiothreitol
ECAR	Extracellular Acidification Rate
ECM	Extracellular Matrix
ER	Endoplasmatic Reticulum
$FADH_2$	Flavin Adenine Dinucleotide
FAO	Fatty Acid Oxidation
FAS	Fatty Acid Synthesis

FBS	Fetal Bovine Serum
Flt3L	FMS-like Tyrosine Kinase 3 Ligand
GAPDH	Glyceraldehyde 3-phosphate Dehydrogenase
GLUT	Glucose Transporter
GM-CSF	Granulocyte-Macrophage Colony-Stimulating Factor
GPR	G Protein-Coupled Receptor
HEPES	4-(2-hydroxyethyl)-1-piperazineethanesulfonic acid
HIF	Hypoxia-Inducible Factor
HLA-DR	Human Leukocyte Antigen – DR isotype
HMDB	Human Metabolome Database
HSC	Hematopoietic Stem Cell
ICOS	Inducible Costimulator
IDO	Indoleamine 2,3-Oxygenase
IFN	Interferon
IFNAR	Interferon-α/β Receptor
IKKε	IκB Kinase-ε
IkB	Inhibitory kappa B
IL	Interleukine
iNOS	Inducible Nitric Oxide Synthase
IRAK	Interleukin-1 Receptor-Associated Kinase
IRF	Interferon Regulatory Factor
Kyn	Kynurenine
LC-MS	Liquid Chromatograpgy-Mass Spectrometry
LD	Lipid Droplets
LPS	Lipopolysaccharide
MAPK	Mitogen-Activated Protein Kinase
MARCO	Macrophage Receptor with Collagenous Structure
MDSC	Myeloid-Derived Supressor Cell
MHC	Major Histocompatibility Complex
moDC	Monocyte-derived Dendritic Cell
MS	Mass Spectrometry
MSR	Macrophage Scavenger Receptor
MVA	Multivariate Analysis
mTOR	Mammalian Target of Rapamycin
MyD88	Myeloid Differentiation Primary Response 88
NADH	Nicotinamide Adenine Dinucleotide
NEAA	Non-Esstential Amino Acids

NF-κB	Nuclear Factor Kappa B
NK	Natural Killer
NMR	Nuclear Magnetic Resonance
NO	Nitric Oxide
OCR	Oxygen Consumption Rate
OXPHOS	Oxidative Phosphorylation
PAMP	Pathogen-Associated Molecular Patterns
PBMC	Peripheral Blood Mononuclear Cell
PBS	Phosphate-Buffered Saline
PCA	Principal Component Analysis
PD-1	Programmed Cell Death Protein 1
PD-L1	Programmed Cell Death-Ligand 1
pDC	Plasmacytoid Dendritic Cell
PGC	Peroxisome Proliferator-Activated Receptor Gamma Coactivator
PGE2	Prostaglandin E2
PI3K	Phosphoinositide 3-Kinase
PLS-DA	Partial Least Squares-Discriminant Analysis
Poly(I:C)	Polyinosinic:polycytidylic Acid
PPAR	Peroxisome Proliferator-Activated Receptor
PPP	Pentose Phosphate Pathway
PRR	Pattern Recognition Receptor
qRT-PCR	Quantitative Real-Time Polymerase Chain Reaction
R5P	Ribose-5-Phosphate
RIG-I	Retinoic Acid-Inducible Gene-I-Like Receptor
ROS	Reactive Oxygen Species
RPMI	Roswell Park Memorial Institute Medium
SHP	Src Homology Region 2 Domain-containing Phosphatase
SRC	Spare Respiratory Capacity
ssRNA	Single-Strand RNA
TAA	Tumor-Associated Antigens
TADC	Tumor-Associated Dendritic Cell
TAM	Tumor-Associated Macrophage
TBK1	TANK Binding Kinase 1
TCA	Tricarboxylic Acid
TdLN	Tumor-draining Lymph Nodes
TGF	Transforming Growth Factor
Th	T helper

TI	Tumor-Infiltrating
TIDC	Tumor-Infiltrating Dendritic Cell
TLR	Toll-Like Receptor
TME	Tumor Microenvironment
TNF	Tumor Necrosis Factor
TRAF	Tumor Necrosis Factor Receptor-Associated Factor
T_{reg}	T regulatory cell
Trp	Triptophan
TSP	3-(Trimethylsilyl) Propanoic Acid
UPR	Unfolded Protein Response
VEGF	Vascular Endothelial Growth Factor

Index

List of Figures

List of Tables

Supplementary Information

Figures

Tables

CHAPTER 1

INTRODUCTION

1. Introduction

1.1. Tumor microenvironment and the immune system

Cancer constitutes a major health burden worldwide, with 18.1 million new cases and 9.6 million deaths reported in 2018[1]. It comprises a set of diseases characterized by uncontrolled cell division and disrupted cell homeostasis, resulting from regulation failure due to genetic or epigenetic unrepaired alterations in normal cells. Despite all the diversity between and within cancer types, a number of crucial alterations in cell physiology have been highlighted as being present in all cancer types. These so-called cancer hallmarks were described in the year 2000 by Hanahan and Weinberg as self-sufficiency in growth signals, insensitivity to growth-suppressor signals, resistance to apoptosis, enabling replicative immortality, sustained angiogenesis, and tissue invasion and metastasis[2]. A decade later, two emerging hallmarks were added, reprogramming energy metabolism and evading immune response, together with two enabling characteristics: genome instability and inflammation[3]. Recently, the cellular properties underlying tumorigenesis have been re-organized and condensed into a framework of 7 cancer hallmarks: selective growth and proliferative advantage, altered stress response favouring overall survival, vascularization, invasion and metastasis, metabolic rewiring, an abetting microenvironment, and immune modulation[4]. Although during their development all cancer cells tend to acquire this same set of hallmark capacities, their mode of doing so varies mechanistically and chronologically[3].

The interactions between immune and cancer cells have been the object of numerous studies for many years, focusing on how the immune system protects the host against malignant cells and how it can be stimulated to repress tumor development[5]. The immune system can be described as the collection of cells, tissues and molecules that provide protection against potentially harmful threats like microbial infections, toxicants or abnormal cells[6]. In the context of cancer, the immune system plays a key role in shaping tumor development, that can be a tumoricidal role, whereby immune cells detect and destroy tumor cells, or a tumorigenic role, as a number of cancer variants can produce immunosuppressive factors that suppress antitumor immune cells[7,8]. During cancer immunoediting, the immunogenicity of tumors changes through three phases. In the first phase, elimination, transformed cells are destroyed by the immune system. After the elimination and equilibrium phases, the escape phase represents the progressively growth of tumor cells[7]. In brief, the immune system can recognize precursors of cancer during initial

transformation and, in most cases, destroy them in a process termed immunosurveillance[9,10]. This mechanism can destroy cells that are close to becoming malignant while selecting tumor cells that can survive an antitumor immune attack. Thus, tumor cells that survive immune system may enter the equilibrium phase where editing occurs, reducing the effectiveness of antitumoral therapies[11].

The stimulation of immune responses against cancer cells is being studied for many cancer types. Indeed, in recent years, cancer immunotherapy has emerged as a novel promising therapeutic strategy, with some approaches reaching some good results[12], mainly in melanoma, lung and ovarian cancers[13]. The general concept of cancer immunotherapy consists of modulating the patient's own immune response to eliminate tumor cells, leaving normal cells unaffected[14]. This is a great advantage compared to conventional chemotherapy, the first-line treatment for most malignancies, as anticancer drugs can lead to severe side effects related to systemic and local toxicity and/or to the development of drug resistance[14]. The main cancer immunotherapy approaches currently under clinical development include immune checkpoint blockade, that blocks inhibitory receptors such as cytotoxic T lymphocyte antigen (CTLA)-4 and programmed cell death protein 1 (PD-1)[15,16].

One of the factors limiting the success of cancer immunotherapies is the highly immunosuppressive nature of the tumor microenvironment (TME). Therefore, a deeper understanding of the mechanisms controlling immune cell responses in the TME is crucial. This work focuses on a specific type of innate immune cells present in the TME, dendritic cells, and addresses the role of metabolism in dendritic cell-mediated immunosuppressive or antitumor effects.

1.2. Immune cells in the tumor microenvironment

The tumor microenvironment (TME) is a complex ecosystem comprising various cell types, including neoplastic cells, endothelial cells, cancer-associated fibroblasts (CAFs) and infiltrating immune cells[17] (**Figure 1**). Moreover, extracellular matrix (ECM) components, responsible for signal transmission and regulation of growth factors[17], as well as cytokines and chemokines, growth factors, and hormones secreted by stromal and tumor cells, are also responsible for shaping stromal and cancer behaviour[18,19].

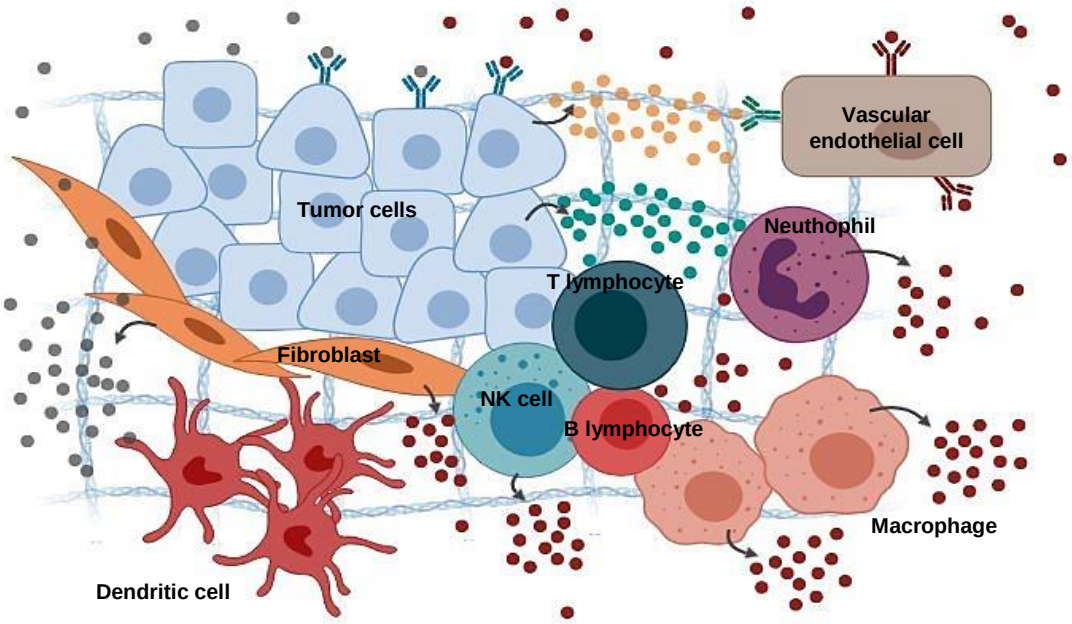

Figure 1 – Different immune cell types in the tumor microenvironment (TME). Apart from tumor cells, the TME contains endothelial cells, fibroblasts, immune cells and others. Immune cells in the TME include cells of the innate immune system, namely monocytes, macrophages, neutrophils, dendritic cells and natural killer cells, and cells of the adaptive immune system, including T and B lymphocytes. The arrows represent secretion of cytokines, chemokines, growth factors and hormones by stromal and tumor cells.

Immune cells in the TME comprise cells of the innate immune system, such as monocytes, macrophages, neutrophils, dendritic cells (DCs) and natural killer (NK) cells, and cells of the adaptive immune system, including T and B lymphocytes[8]. These immune cells have their own receptor expression restricted to the TME[17].

Innate immune cells, such as neutrophils, M1-like macrophages and DCs are part of the first line of defence[20]. When homeostasis is perturbed these cells respond through production of cytokines and chemokines that activate and recruit other immune cells, initiating an immune response[20]. During the early stages of cancer cell proliferation, cytotoxic immune cells such as NK cells and $CD8^+$ T lymphocytes promote tumor cell elimination through their rapid and potent cytotoxic activity[20]. T-helper (Th) 1 cells, on the other hand, are essential for tumor rejection since they produce interferon (IFN)-γ, tumor necrosis factor (TNF)-α and interleukine (IL)-2[20].

DCs are specialized and potent antigen-presenting cells (APCs) with an essential role in regulation of immunity, mostly due to their capacity to uptake, process and present antigens, including tumor antigens, to stimulate T cells, and also due to their ability to scavenge pathogens and to secrete different effector and regulatory cytokines[19]. Depending

on the inflammatory context and costimulatory signals, DCs can prime naïve and memory T cells and trigger an effector T cell response[8]. As a consequence, DCs are considered an important link between the innate and adaptive immune system[21,22], being found in many cancer types such as breast, lung, renal, head and neck, gastric, colorectal, bladder and ovarian cancers[23].

The functional states of DCs is influenced by a variety of stimuli. DC maturation controls the responses of cells such as T, B and NK cells, leading to a tumoricidal effector response[24]. In the absence of maturation stimuli, DCs are kept in an immature state, leading to immune tolerance[24]. Also, some cytokines released by immature DCs, such as IL-10 and transforming growth factor (TGF)-β, together with downregulation of costimulatory molecules (CD80 and CD86) and release of chemokines such as C-C motif chemokine 22 (CCL22) and C-X-C motif chemokine 12 (CXCL12) can also promote immunosuppression by activating regulatory T cells (T_{reg})[25–27]. Apart from the importance of DC maturation for the immune response, the tumor itself also influences DC maturation. Immunosuppressive molecules and physiological changes, such as hypoxia, low pH and nutrient unavailability, can inhibit antitumor immunity[16]. Various soluble factors present in the TME, such as vascular endothelial growth factor (VEGF), IL-6, IL-10 and IL-35, can induce tolerance in DCs[19,28]. IL-6 inhibits DC maturation and migration, inducing a tolerogenic phenotype, while IL-10 inhibit DC maturation, its antigen presentation capacity and production of IL-12[29,30], and priming of T cells, thus converting immunogenic into tolerogenic DCs, leading to an induction of anergy on $CD8^+$ T cells[31]. Furthermore, VEGF, TGF-β, IL-1β, IL-13, granulocyte-macrophage colony-stimulating factor (GM-CSF) and prostaglandins are involved in DC differentiation to myeloid-derived suppressor cells (MDSCs) and tumor-associated macrophages (TAMs)[32].

Other subsets of inflammatory cells promote immunosuppression and metastatic dissemination as the neoplastic tissue evolves to a clinically detectable tumor[8], as is the case of T_{reg} cells, M2-like macrophages and MDSCs[18]. Macrophages present in the TME are known for inhibiting lymphocytes and DC maturation through release of cytokines such as IL-10, prostaglandins and reactive oxygen species (ROS)[33,34] (**Figure 2**). On the other hand, fibroblasts, the major constituents of TME, can also be associated with an increase in tumor proliferation, drug resistance and decreased antitumor immunity[35].

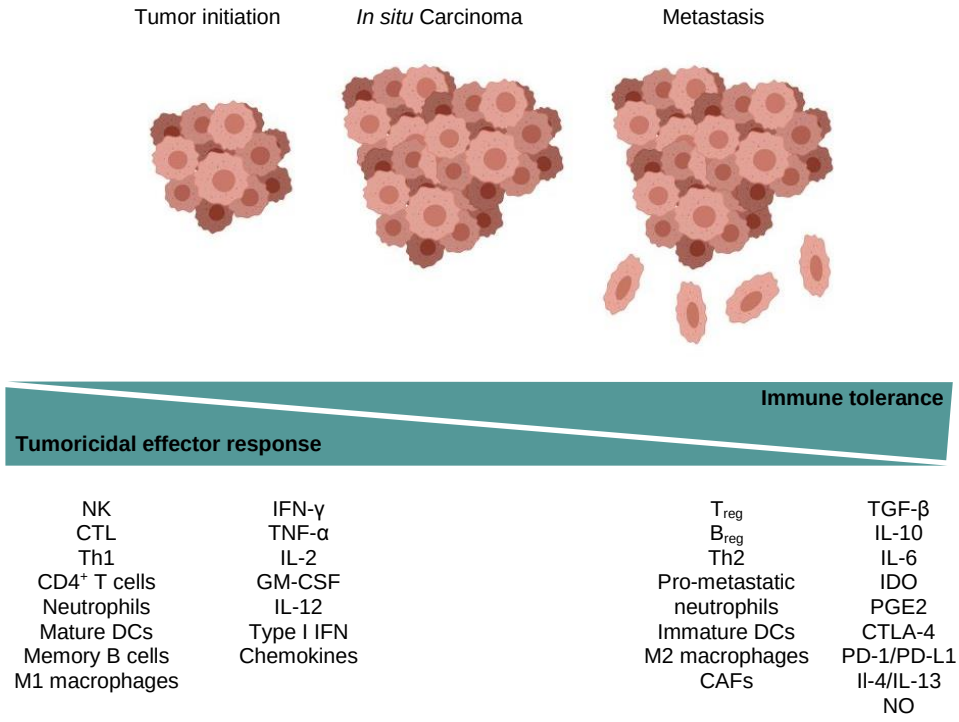

Figure 2 – Balance between tumoricidal and tolerogenic immune responses. In the early stages of tumor development, most infiltrating immune cells are innate cells. As the neoplastic tissue evolves to a clinically detectable tumor, other subsets of inflammatory and immunosuppressive immune cells promote metastatic dissemination. Legend: B_{reg} – Regulatory B cell; CAF – Cancer-associated fibroblasts; CTL – Cytotoxic T lymphocyte; CTLA – Cytotoxic T lymphocyte antigen; DC – Dendritic cell; GM-CSF – Granulocyte-macrophage colony-stimulating factor; IDO – Indoleamine 2,3-oxygenase; IL – Interleukine; IFN – Interferon; NK – Natural killer; NO – Nitric oxide; PD-1 – Programmed cell death protein 1; PD-L1 – Programmed cell death-ligand 1; PGE2 – Prostaglandin 2; Th – T helper cell; TNF – Tumor necrosis factor; T_{reg} – Regulatory T cell. Adapted from Gonzalez *et al.* (2018)[8] and Pitt *et al.* (2016)[20].

1.3. Dendritic cells

Due to their capacity to activate naïve lymphocytes, DCs are able to initiate and regulate adaptive immune responses, being considered the most efficient APCs[36]. Human DCs undergo activation from an immature state to an immunostimulatory phenotype after sensing pathogen-associated molecular patterns (PAMPs) or damage-associated molecular patterns (DAMPs) through pattern recognition receptors (PRRs)[36]. This contributes to activation of $CD8^+$ or $CD4^+$ T cells through expression of co-stimulatory molecules together with major histocompatibility complex (MHC) class I and II molecules, respectively[36]. Due to their crucial role, DCs can be found in almost all tissues, detecting homeostatic imbalances and modifying ongoing immune responses by processing antigens for presentation to T cells and secreting cytokines and growth factors[36], while also interacting with other immune cells, such as NK and innate lymphoid cells[37,38].

1.3.1. Origin and classification of DCs

DCs originate from bone marrow $CD34^+$ hematopoietic stem cells (HSCs)[39], which give rise to a series of precursors that migrate through the bloodstream to the target tissue. There are two main subsets of DCs: conventional DC (cDCs) and plasmacytoid dendritic cells (pDCs) [21].

cDCs are of myeloid lineage and are found in tissues and peripheral blood[40], being involved in the recognition of bacterial structures and production of pro-inflammatory cytokines, such as TNF-α, IL-6, IL-23, IL-1β and IL-12p70, activating different proinflammatory T helper cell subsets and cytotoxic T lymphocytes (CTLs)[41]. Based on their surface expression, location, cytokine secretion and the capacity to stimulate T and B cell responses, human cDCs can be further subdivided into two subsets: conventional dendritic cells type 1 (cDC1) and conventional dendritic cells type 2 (cDC2)[21,42,43].

pDCs are biologically distinct from cDCs in several aspects. pDCs are not of myeloid lineage markers and do not express CD11c. Instead, they express the surface markers BDCA2 (CD303), BDCA4 and CD123[44]. pDCs can be found in peripheral blood and several lymphoid organs[13,45] and are characterized by their extraordinary ability to produce interferons (IFNs)[47], being considered the main producers of IFN-α in the human body[48,49]. pDCs secrete cytokines after recognition of single-strand RNA (ssRNA) and double-strand DNA (dsDNA) by interaction with toll-like receptors (TLR) 7 and 9, being important anti-viral sentinels[21]. However, pDC present higher plasticity[50] and can also induce immune tolerance by different mechanisms such as secretion of immunoregulatory cytokines [51] or promoting T cell differentiation.

1.3.2. Pathways of DC activation

All DC subsets are equipped with PRRs that allow them to recognize danger signals. The most widely studied family of PRRs are TLRs, known for being critical in DC maturation to an immunogenic state and the priming of naïve T cells[52]. Different DC subsets express distinct TLRs coupled with distinct signalling pathways, which contribute to their functional specialization and induction of type I IFN responses[52]. Besides, by cell contact or soluble factors such as type I IFNs, TLR-induced activation of one DC subset can lead to the activation of the other subset, thus enhancing antitumor responses[40].

Generally, cDCs express TLR1, 2, 6 and 8; nevertheless, unlike human cDCs, mouse cDCs express TLR4 and TLR9. Among DCs, TLR3 and TLR10 are selectively expressed on the plasma membrane of cDCs[53–55]. In cDCs, TLR3 is expressed on the surface of the cells and recognize ligand polyinosinic:polycytidylic acid (poly(I:C))[56–58]. Activation initiates with recruitment of myeloid differentiation primary response 88 (MyD88), a crucial adapter that recruits interleukin-1 receptor-associated kinase (IRAK), tumor necrosis factor receptor-associated factor (TRAF)-6 and interferon regulatory factor (IRF)-5, leading to activation of the nuclear factor kappa B (NF-κB) to induce production of the cytokines TNF-α, IL-6, IL-8 and IL-12, whereas TICAM-1 (TRIF), another functional adapter, mediates activation of IRF-3 and IFN-β promoter[58]. Moreover, double-stranded RNA stimulate retinoic acid-inducible gene-I-like receptor (RIG-I) RNA helicase can also induce type I IFN production by activating IRF-3[59].

Activation of pDC is also triggered by TLR signalling after PAMP recognition[60]. In these cells, upon recognition of foreign DNA or RNA, TLR9 activation initiates with MyD88, a protein that forms a signalling complex with IRAK-4, TRAF-6 and IRAK-1[61]. The subsequent signalling cascade will result in IRF-7 activation, which is phosphorylated and translocated to the nucleus to induce transcription of type I IFN genes[61]. Through TRAF-6 signalling, NF-kB and mitogen-activated protein kinase (MAPK) pathways are also induced, leading to expression of inflammatory cytokines and chemokines, and upregulation of costimulatory molecules[61]. Moreover, association of NF-κB p65 and p50 subunits with IRF-5 appears to be the main inducer of IL-6 mRNA transcription[62]. Additionally, depending on the stimuli, TLR9 activation on distinct intracellular localizations can have different results on cytokine response[63]. The TLR ligand CpG-A signals through MyD88/IRF-7, inducing a strong IFN-I response, while CpG-B rapidly travels to the lysosomes to induce TNF, IL-6 and costimulatory molecules production[64], as well as upregulation of MHC II[65].

Additionally, pDCs can also control TLR access to different endosomes in order to achieve a coordinated DNA detection response[66]. The Brain and Dendritic Cell (BAD)-associated Lysosome-associated Membrane Protein (LAMP) (BAD-LAMP) is a molecule expressed on pDCs that controls TLR9 trafficking to $LAMP^+$ late endosomes, reducing IFN-I production upon activation with CpG DNA, favouring TNF-α[66]. Therefore, in breast tumor-associated pDCs, BAD-LAMP expression might contribute to the lack of IFN-α production, generally associated with immune tolerance [67,68].

1.3.3. The role of cDC and pDC in cancer

In consideration of their key role in the control of intrinsic and adaptive immunity, cDCs are essential to the induction of antitumor immunity. In the case of cancer, in the TME or after movement to tumor-draining lymph nodes, cDCs take antigens from tumor cells and present them to T cells[69]. Through their role in the activation of antigen-specific CTLs, cDCs can induce powerful cytotoxic immune responses towards tumor cells[69]. One clinical trial in melanoma patients who used naturally occurring cDC2s with tumor-associated antigens (TAAs) showed that the existence of TAA-specific T cells in peripheral blood was linked to progression-free survival[70]. In another study with melanoma mouse models, cDC1s were shown to transport TAAs to tumor-draining lymph nodes (TdLNs) and cross-present them to $CD8^+$ T cells[71]. While tumoral cDC1s stimulate activated $CD8^+$ T cells, and benefit T_{reg}-abundant tumors, cDC2s are more efficient in $CD4^+$ T cell stimulation and Th17 differentiation[72,73]. However, cDCs can also have tolerogenic properties, thus promoting tumor growth[21]. In mice, cDCs have been reported to cross-prime tolerogenic cells, although this is not well documented in humans[74,75].

Human pDCs are capable of infiltrating solid tumors, such as lung, breast, head and neck cancers and melanoma, where they are maintained in a tolerance-promoting state[67,76–78]. This blockage of pDC maturation can be reached through the secretion of immunosuppressive factors by tumor cells[79,80]. On the other hand, the release of DAMPs by tumor cells can stimulate TLR9 and activate pDCs[81]. In breast cancer, the presence of GM-CSF and its receptor expression activate tumor-infiltrating (TI)-pDCs[82]. Immature pDCs can also be found in tdLNs and suppress $CD8^+$ T cell responses by expression of indoleamine 2,3-oxygenase (IDO), inducible costimulatory (ICOS) ligand and granzyme B[83–85]. Interestingly, TI-pDCs decrease its IFN production capacity, and thus promoting a tolerogenic phenotype, under TLR stimulation due to the expansion of T_{reg} cells and induction of Th2 differentiation[82,86]. In melanoma, an increased expression of IDO has been observed in pDCs[87]. Also, pDCs can promote tumor growth, survival and drug resistance by influence of tumor-associated factors, such as TGF-β, TNF-α[88], IL-10[89], prostaglandin E2 (PGE2)[90], IL-3[91] and VEGF[92]. Therefore, several cancer types, such as breast cancer[67], ovarian cancer[93], multiple myeloma[91] and melanoma[86] are associated with immature pDCs.

1.3.4. DC-based cancer immunotherapy

The use of different DC subsets for vaccination and their specialized contribution to antitumor immunity is promising, however different cancer types might need different DC therapeutic strategies. Therefore, different DC-based strategies are being explored to induce immunological responses (**Figure 3**).

Manipulation of the immune system to control cancer is the key concept of cancer immunotherapy[36]. DC-based cancer immunotherapy depends on the crucial role that these cells induce antigen-specific T cell responses[94]. The use of DC vaccines for cancer has been extensively investigated. The majority of DC-based vaccines currently being tested consist of mature antigen-loaded autologous DC and are called *ex vivo* DC vaccines[95] (**Figure 3**). To generate these vaccines, patients DC precursor cells (i.e. peripheral blood monocytes, naturally occurring DCs or $CD34^+$ hematopoietic precursor cells) are firstly isolated and differentiated into DCs. The most used technique is the differentiation of DCs from peripheral blood mononuclear cells (PBMCs) (i.e. monocyte-derived DCs), by culturing cells in GM-CSF and IL-4. Then, these DCs are modified (maturation) to present tumor-specific antigens to T cells, using cytokines, TLR agonists, CD40 ligands or a cytokine mixture (TNF-α, IL-1β, IL-6 and prostaglandin E2). These cells are loaded with tumor antigens and infused back to the patient, to stimulate cytotoxic T cells[24,95].

When comparing to *in vitro* generated monocyte-derived dendritic cells (moDCs), naturally occurring DC subsets bear greater antigen-presentation capabilities due to the higher MHC molecule expression and specialized functions. In this sense, naturally occurring DCs are proposed as the basis of next-generation vaccines[96–98]. Preclinical studies showed that primary mouse pDCs can induce $CD8^+$ T cell activation[99]. Contrarily, mouse cDCs were more effective in terms of prolonging survival in a model of glioma[100], while another study reported that cDC1s are more effective in the induction of $CD8^+$ T cell responses, whereas cDC2s induce Th17 responses[72,101].

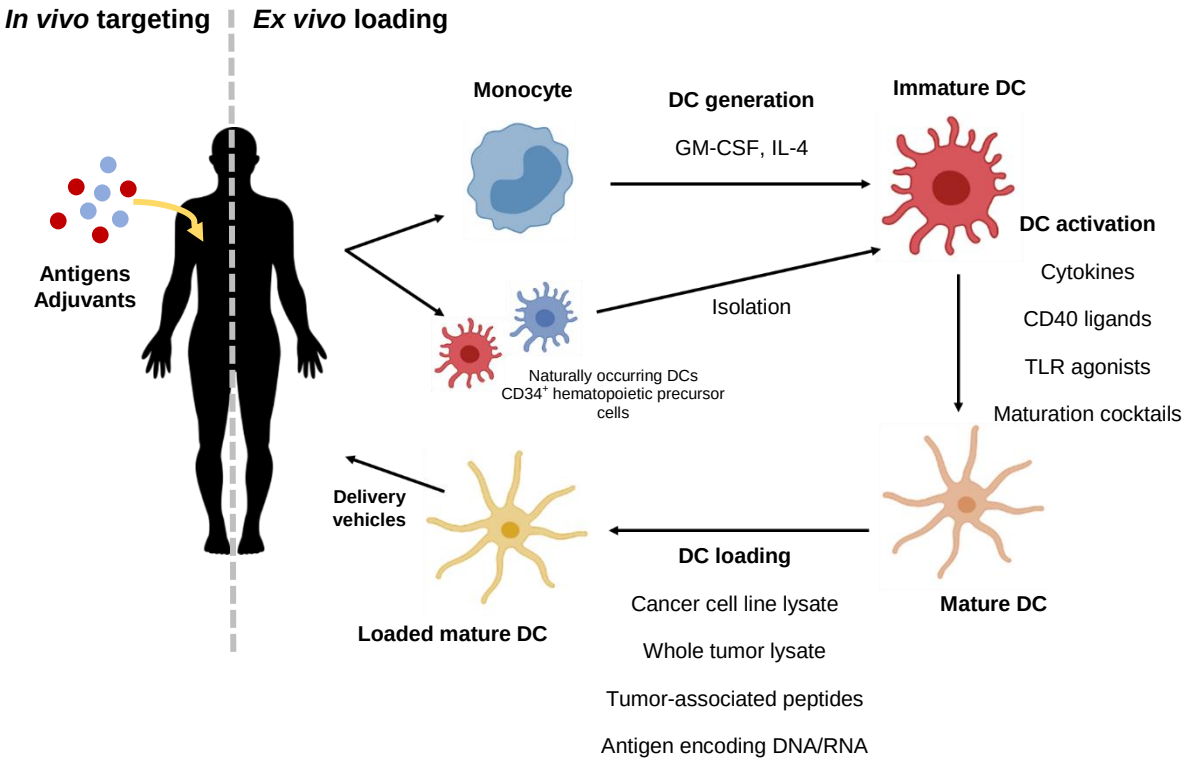

Figure 3 – DC-based immunotherapy approaches. By inducing antitumor immune responses by DCs activation, DC-based vaccines aim to stimulate antitumor immunity through DCs capacity to activate tumor-specific T cells. The most used strategy is vaccination based on monocyte-derived dendritic cells (right). Peripheral blood monocytes are differentiated into DCs in the presence of GM-CSF and IL-4, the most used combination. Then, DC activation can occur with different stimuli, including cytokines (TNF-α, IFN-γ), CD40 ligands, TLR agonists and maturation cocktails (TNF-α, IL-1β, IL-6 and prostaglandin E2). Lastly, mature DCs are loaded with tumor antigens and injected into the patient. On the other hand, activation of T cells responses can also be reached by targeting antigens and adjuvants directly to DCs *in vivo* (left). Legend: DC – Denditic cell; GM-CSF – Granulocyte-macrophage colony-stimulating factor; IL – Interleukine; TLR – Toll-like receptor. Adapted from Patente *et al.* (2019)[36].

Additionally, studies suggest that pDCs and cDCs act synergistically. In fact, combination vaccination with distinct DC subsets can promote $CD4^+$, $CD8^+$, T-cell and NK-cell responses[102]. cDCs and pDCs have been used in combination in clinical trials against melanoma, enhancing NK cell responses[103]. In mice, pDCs were shown to induce $CD8^+$ T-cell responses and promote the antigen capacity of cDCs[104,105]. In humans, cDCs and pDCs were shown to activate each other after TLR stimulation of one of the subsets[106]. In this way, combination vaccination might increase DC immunotherapeutic potential.

Activation of DCs can also be reached through cytokines, immunostimulatory adjuvants and agents that block immunosuppressive DC functions[107] (**Figure 3**). GM-CSF stimulates DC differentiation, activation and migration[96] by inducing antitumor immune

responses and increasing survival in patients with advanced melanoma[108]. Additionally, the administration of the cytokine and growth factor Flt3L also promotes antitumor immunity and $CD8^+$ T cell activation in tumor mouse models[71].

As mentioned above, tumors secrete modulatory factors that can influence the immunoregulatory capacities of pDCs and keep them in an immature state that promotes tolerance. However, when pDCs are TLR-stimulated they switch to a tolerogenic state. Thus, some of TLR-based approaches are currently under investigation.

Poly(I:C), a TLR3 agonist, has emerged as a potential adjuvant for cancer immunotherapy in human $CD141^+$ cDC1s[71,109,110]. Preclinical studies *in vitro* showed the efficacy of poly(I:C) in the activation of DCs and production of pro-inflammatory cytokines[71,111]. As concerning pDCs, treatment with the TLR7 agonist Imiquimod recruits mature pDC to the tumor site and increases their IFN production, leading to tumor regression in melanomas[112,113]. Besides, numerous clinical trials with TLR7/TLR8 agonists in cancer are ongoing (NCT02574377 and NCT026 92976). Moreover, a phase I clinical trial has demonstrated that tumor pDCs can be stimulated with CpG, thus promoting immunostimulatory capacities in pDCs in breast cancer and melanoma mouse models[114]. The same effect can also be observed stimulating pDCs with CpG before administration to the patient[115,116], since tumor cells secrete immunoregulatory antigens that inhibit IFN and pro-inflammatory cytokine production by pDCs, thus inhibiting antitumor responses[90,117].

Overcoming immunosuppression is another approach that enhances DC function. Potential solutions include controlling the production of type I IFN by blocking IDO, induced by TLRs, or suppressing other inhibitory molecules[118,119]. DC stimulation with Imiquimod, a TLR7 agonist, increased IDO expression and inhibited antitumor immune responses. In this sense, inhibition of IDO expression after activation could improve the efficacy of TLR-mediated therapy[120]. IDO is highly expressed on pDCs in leukemia[121]. Toho-1, an IDO inhibitor, was found to be efficient in promoting antigen-presentation in pDCs[121]. Moreover, BAD-LAMP modulation can control pDC responses in tumor development[66]. Indeed, recent studies show that higher expression of BAD-LAMP in pDCs exposed to the TME can lead to the impaired production of type I IFN. As the systemic type I IFN response produced by pDCs is critical to NK activation and subsequent inhibition of tumor metastasis[122], inhibiting BAD-LAMP expression could have a positive outcome.

In summary, the development of novel strategies still requires a better understanding of DC biology and functions. Some preclinical studies bring up DCs as efficient therapeutic treatments. Approaches to achieve this include administration of

cytokines that induce DC activation, immunostimulatory adjuvants and agents that block immunosuppressive DC functions as well as DC-based vaccines. However, we still need to learn more about how we can modulate DC subsets with specialized functions in order to improve antitumor immune responses.

1.4. Metabolism of DCs

The study of the molecular mechanisms that allow DCs to respond and initiate an immune response has been undergoing great advances. Moreover, it is becoming increasingly clear that external stimuli as well as the composition of the TME can alter the function of immune cells metabolism. The following sections address current knowledge on the metabolism of different DC subsets and its relation to the cell functional behaviour, especially in the tumor microenvironment. A general overview is given in **Figure 4**, while **Table 1** summarizes the studies addressing the relationship between metabolic pathways and innate immune function of cDC and pDC.

1.4.1. Glycolysis, Tricarboxylic Acid (TCA) cycle and Oxidative Phosphorylation (OXPHOS)

Glycolysis consists of a series of reactions occurring in the cytosol, which convert glucose into pyruvate, with the concomitant production of adenosine triphosphate (ATP) and nicotinamide adenine dinucleotide (NADH). Glycolysis may serve several purposes, such as the generation of energy under anaerobic conditions, or the fuelling of the TCA cycle to perform mitochondrial aerobic respiration. In cells with low oxygen availability, low mitochondria content or subject to certain stimuli, the pyruvate generated by glycolysis is mainly converted into lactate, recycling NAD^+ (important to keep the glycolytic flux). On the other hand, cells which rely mainly on aerobic respiration for energy generation, direct most pyruvate into the TCA cycle, whose products participate in oxidative phosphorylation (OXPHOS) to generate energy in mitochondria. The TCA cycle uses acetyl coenzyme A (Acetyl-CoA), produced by the oxidation of pyruvate, and, in a series of redox reactions, harvests much of its bond energy in the form of NADH, flavin adenine dinucleotide ($FADH_2$) and ATP molecules. The reduced electron carriers generated (NADH and $FADH_2$) will pass their electrons into the electron transport chain and, through OXPHOS, will generate most of the ATP produced in cellular respiration[123].

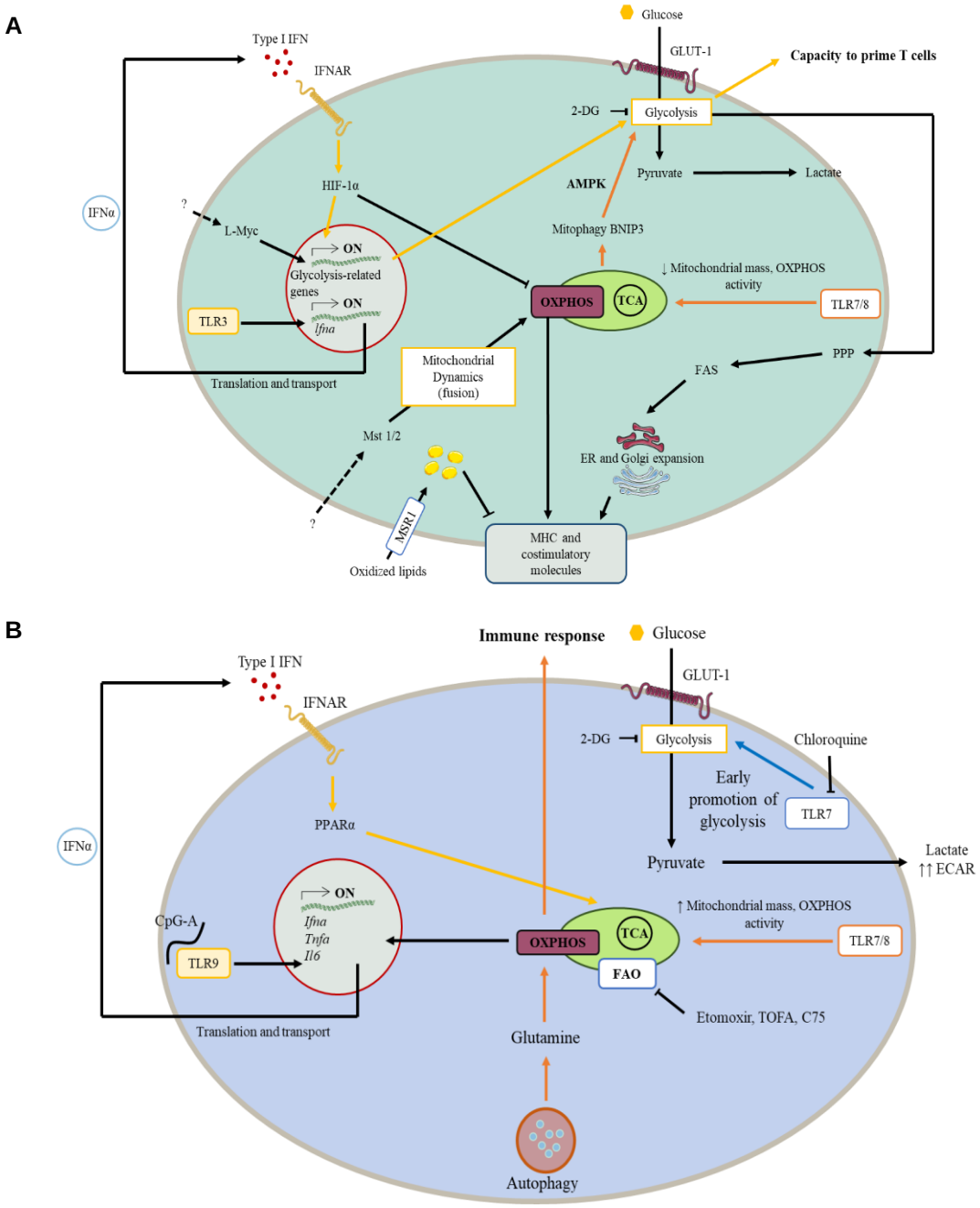

Figure 4 – Metabolic changes dictating (A) cDC and (B) pDC function. (A) Glycolytic metabolism supports the early activation of cDCs. At early stages of activation, glycolysis, tricarboxylic acid cycle and the pentose phosphate pathway support the expansion of the endoplasmatic reticulum and Golgi apparatus, leading to an increase in MHC and costimulatory molecules. Nevertheless, autocrine type I IFN signaling drive a glycolytic reprogramming dependent on HIF-1α. The kinases Mst1/2 promote mitochondrial fusion and L-Myc promotes glycolytic enzymes expression (may have a role in supporting mitochondrial dynamics by inducing glutaminolysis). (B) The endossomal TLR7 pathway in pDCs promote early glycolysis demonstrated by an increase in ECAR. In contrast, TLR9 pathway promotes, through an IFN/IFNAR loop, late glycolysis and fatty acid synthesis and oxidation coupled with oxidative phosphorylation to generate ATP in a PPARα-dependent mechanism. Specific inhibitors of these pathways are written. Legend: 2-DG – 2-Deoxyglucose; AMPK – AMP-activated protein kinase; ECAR – Extracellular acidification rate; ER – Endoplasmatic reticulum; FAO – Fatty acid oxidation; FAS – Fatty acid synthesis; GLUT-1 – Glucose transporter 1; IFN – Interferon; IFNAR – IFN-α receptor; MHC – Major histocompatibility complex; MSR – Macrophage scavenger receptor; OXPHOS – Oxidative phosphorylation; PPAR – Peroxisome proliferator-activated receptor; PPP – Pentose phosphate pathway; TCA – Tricarboxylic acid cycle; TLR – Toll-like receptor; Etomoxir, TOFA and C75 – FAO inhibitors. Based on Saas *et al.* (2017)[60], Giovanelli *et al.* (2019)[205], Basit et *al.* (2018)[127], Du et *al.* (2018)[134].

An early promotion of glycolysis is a metabolic hallmark of several activated DC subsets[124]. Glycolysis pathway is important not only for DC maturation, production of costimulatory molecules and cytokine secretion, and T cell stimulatory capacity[124], but also for DC development. It was shown that administration of glycolysis inhibitor 2-Deoxyglucose (2-DG) led to DC development inhibition in FMS-like tyrosine kinase 3 ligand (Flt3L)-induced mouse DC progenitor proliferation[125]. Furthermore, the presence of 2-DG in LPS-activated cDC1s and cDC2s decreased the expression of costimulatory molecules and activation of T cell responses[126]. Also, protamine-RNA complexes (pRNA)-stimulated human blood cDC2s require glycolysis for activation, evidenced by expression of TNF-α, CD86 and PD-L1[127].

It has also been shown that different cDC subsets differentially rely on glycolysis and oxidative metabolism. Analysis of mouse spleen $CD8\alpha^+$ DCs (cDC1) and $CD8\alpha^-$ DCs (cDC2) showed that $CD8\alpha^+$ DCs have a higher oxidative metabolism, when compared to cDC2, and abnormal mitochondrial function could affect the expansion of cDC1s, important for $CD8^+$ T cell antitumor responses[128].

Metabolic competition and glucose limitation are prevalent mechanisms in tumors which have been demonstrated to induce glycolytic and bioenergetic deficiencies in T cells[129]. In bone marrow-derived dendritic cells (BMDCs) and cDCs glucose deprivation has been shown to decrease DC trafficking to the lymph nodes[130]. In addition, low concentrations of glucose and glutamine in the tumor may trigger a decrease in protein glycosylation in the endoplasmatic reticulum (ER), causing aggregation of unfolded proteins and resulting in an ER stress response[131].

As previously mentioned, DCs detect invading pathogens or endogenous threat signals by TLRs, triggering innate and adaptive immune responses through promotion of antigen-specific T cell activation[132]. Inactive DCs generate energy primarily through OXPHOS and fatty acid oxidation (FAO), while TLR activation causes a shift to glycolysis[133]. This shift, analogous to the so-called Warburg effect in tumor cells, was shown to be important for the survival and maturation of BMDCs[133]. It has also been reported that, in cDCs, there is a late commitment to glycolysis after PRR stimulation, in a process dependent on the upregulation of hypoxia-inducible factor 1-alpha (HIF-1α) and autocrine type I IFN signalling[134,135], a process favoured by the activation of HIF-1α and phosphoinositide 3-kinase (PI3K)/Protein kinase B (Akt) pathways that leads to an increase in glucose uptake through glucose transporter 1 (GLUT-1), increased activity of glycolytic enzymes, increased lactate output, and decreased mitochondria oxidative metabolism and

FAO[136]. The mammalian target of rapamycin (mTOR) regulation mechanism also stimulates glycolysis via HIF-1α and induction of oncogenic transcription factor Myc, and, with increased production of GLUT-1, promotes an increase in glucose uptake[137].

On the other hand, mTORC is antagonized by AMP-activated protein kinase (AMPK) and induces the expression of peroxisome proliferator-activated receptor gamma coactivator (PGC)-1α, a key energy metabolism regulator that promotes mitochondrial oxidative metabolism[137,138]. Studies have suggested that AMPK downregulates NF-κB signals through multiple mechanisms[133]. In mouse BMDCs, lipopolysaccharide (LPS) activation caused phosphorylation decrease in AMPK, while AMPK knockdown promoted LPS activation, as observed by interleukin-12 p40 subunit (IL-12p40) and CD86 expression[133]. The administration of 5-aminoimidazole-4-carboxamide ribonucleotide (AICAR), an activator of AMPK, reduced IL-12p40 expression and promoted a shift to aerobic glycolysis, whereas IL-10 decreased the impact of LPS on AMPK phosphorylation[133].

As previously mentioned, non-activated DCs use OXPHOS and TCA cycle to produce ATP and fulfil the bioenergetic demands[126]. Upon stimulation, TCA cycle intermediates, such as citrate, succinate and fumarate, regulate inflammatory responses and cytokine production and the *de novo* fatty acid synthesis of DCs[139,140].

Citrate plays a key role in inflammatory pathways, serving as an important substrate for protein acetylation, NADPH production and fatty acid synthesis (FAS) in activated DCs[126,139]. Citrate is preferentially used in LPS-activated BMDCs for *de novo* fatty acid synthesis, increasing the glycolytic activity, which is mediated by kinases TANK binding kinase 1 (TBK1) and Akt, involved in the association of hexokinase 2 with the mitochondria[139]. Blocking the function of acetyl-CoA carboxylase or inhibiting fatty acid synthesis, results in the inhibition of LPS-activated DCs[139]. In this sense, DCs with a higher lipid content are more immunogenic whereas those with lower lipid concentrations acquire a tolerogenic phenotype[139]. So, citrate is critical for DCs activation by LPS, triggering T cell activation. Succinate, another TCA cycle intermediate, has also been found to be involved in DC activation. Mouse BMDCs detect extracellular succinate via G protein-coupled receptor 91 (GPR91), increasing the expression of TNF-α by poly(I:C) or Imiquimod activation[141].

The metabolic information available for pDCs is much scarcer than for cDCs and BMDCs. Still, a few studies have revealed useful information. Influenza A virus stimulation of human pDCs with 2-DG was found to reduce costimulatory molecules (CD80 AND

CD86), as well as human leukocyte antigen DR isotype (HLA-DR) and type I IFN expression[142]. In addition, as recently described in macrophages, 2-DG can impair TCA cycle, OXPHOS, and ATP levels[143]. Another study showed the involvement of TLR7 activation in glycolysis by the use of chloroquine, shown to disrupt endosomal acidification, which is a required component of TLR7 signalling[142,144]. These data support that glycolysis plays a role in the production of type I IFN, pro-inflammatory cytokines and co-stimulatory molecules by TLR7-stimulated pDCs.

Recently, it was also demonstrated that TLR stimulation in pDCs results in mitochondrial metabolic adaptations. Upon stimulation with pRNA, a TLR7/8 agonist, pDCs showed increased glutaminolysis and OXPHOS, while mitophagy and glycolysis were promoted in cDC[127]. Additionally, it was demonstrated that TLR-stimulated pDCs increased mitochondrial content and intracellular glutamine in an autophagy-dependent manner[127]. When glutaminolysis was inhibited by DON and BPTES pDC activation was prevented[127]. Contrarily, mitochondrial fragmentation inhibition with mdivi-1 and promotion of mitochondrial fusion with S3 impaired glycolysis and activation of TLR-stimulated $CD1c^+$ cDCs[116]. Deficiency of the kinase Mst1/2 can also inhibit antitumor immunity in cDCs, since it leads to a deregulation in mitochondrial dynamics[127].

Notably, based on the external stimuli, pDCs show distinctive mitochondrial energy metabolism patterns. While human pDCs, in the presence of an infection, decrease their OCR after 24h[142], they increase OXPHOS 6h after stimulation with pRNA, a process mediated by autophagy and glutaminolysis[127], which is required for the production and expression of IFN-α, CD80, and PD-L1[127]. On the other hand, a recent study has shown that pDC activation in response to CpGA (a TLR9 agonist) led to production of type I IFNs, which increased FAO and OXPHOS through an autocrine type I IFN receptor-dependent pathway[145].

Overall, early induction of glycolysis appears to be necessary for the maturation of most DC subsets, namely the upregulation of co-stimulatory surface molecules and the production of cytokines. However, no general conclusion on the function of mitochondrial energy metabolism in activated DCs can be reached, as it appears to be highly context-dependent and the DC subset considered.

1.4.2. Pentose phosphate pathway

The pentose phosphate pathway (PPP) is an alternative way of glucose-6-phosphate oxidation, running parallel to glycolysis to fulfil two main functions: the formation of ribose-5-phosphate (R5P) for the synthesis of nucleotides, supporting cell growth and proliferation, and the formation of NADPH, which carries reducing power, essential to the cellular anti-oxidant defence system and to many anabolic pathways, such as cholesterol and lipid synthesis[123].

In DCs, the Akt pathway activates hexokinase 2, the enzyme responsible for the production of glucose-6-phosphate, increasing the glycolytic metabolism and the TCA cycle and resulting in an increased PPP activity as well as the formation of citrate for FAS[132]. Of note, citrate and NADPH used for lipid synthesis in BMDCs have been shown to be linked to the expansion of the ER and Golgi apparatus[126], leading to an increase in the trafficking and secretion of effector cytokines upon DC activation[146].

It has also been observed a rapid decrease in NADPH and R5P intracellular concentrations in LPS-stimulated BMDCs[126]. When the expression of glucose-6-phosphate dehydrogenase, the first enzyme in the pentose phosphate pathway, was inhibited, it was observed a decrease in the pro-inflammatory cytokines IL-6 and IL-12, along with lipid accumulation. These results suggest that the flux of glucose into the pentose phosphate pathway plays a key role in DC activation, by promoting the generation of NADPH and, thus, fatty acid synthesis[126].

1.4.3. Amino acid metabolism

All tissues have some capability to synthesize non-essential amino acids and to convert them to other derivatives that contain nitrogen. The nitrogen of amino acids is eliminated via transamination, deamination, and urea formation, while the carbon skeletons are conserved as carbohydrates, via gluconeogenesis, or as fatty acids by fatty acid synthesis pathways. Glucogenic amino acids give rise to pyruvate or TCA cycle intermediates, such as α-ketoglutarate and oxaloacetate, acting as glucose precursors via gluconeogenesis. Ketogenic amino acids give rise to acetyl-CoA. Besides, amino acids have a possible fate for energy production through anaplerotic fuelling of the TCA cycle[123].

The catabolism of some amino acids has been associated with the tolerogenic phenotype of DCs such as the upregulation of surface molecules, receptors and cytokines

that lead to the induction of regulatory T cell responses[124,147]. Tryptophan (Trp) is an amino acid involved in immune tolerance and antitumor immune responses. Trp depletion is induced by the enzyme IDO1, which has an immunoregulatory effect, and the generation of kynurenine (Kyn), which has as role in controlling acute inflammation. IDO is also associated with the induction of a tolerogenic microenvironment in tumors[148]. In this sense, IDO could be an attractive target for cancer immunotherapy[148], since its catabolic effect on Trp can lead to the generation of T_{reg}[148]. A recent study in a model of melanoma demonstrated that β-catenin induction of FAO led to the production of IDO, generating T_{reg} responses[149]. Products from Trp catabolism, such as Kyn, may serve as signalling molecules that suppress antitumor immune responses[150]. In a model of murine mammary carcinoma, Kyn is required to preserve IDO in $CD11c^+$ TADCs, leading to an increase in T_{reg}[151]. In addition, the interaction between CTLA-4 and CD80 induce NF-kB signaling and controls IDO expression in cDC1s[152]. Besides, TGF-β stimulates Trp catabolism leading to an increase in kynurenines and promoting tolerance[152].

Arginine is another immunomodulatory amino acid required for T-cell activation. In immune cells, arginine is metabolized to L-citruline and nitric oxide (NO) by inducible nitric oxide synthase (iNOS) under inflammatory conditions[153], and by arginases 1 and 2 to ornithine, which is involved in tumor cell proliferation[153,154]. Arginase 1 has been reported to control the production of IDO in $CD11c^+$ DCs under TGF-β stimulation[155], inhibiting T cell antitumor responses by depletion of arginine. Besides, the production of polyamine spermidine leads to the activation of IDO1, promoting a tolerogenic phenotype[155,156]. In addition, the release of polyamines by myeloid-derived suppressor cells can also inhibit IDO1 expression by DCs, leading to immunosuppression[155]. Moreover, cDC2s have been shown to control T cell function by modulating arginine levels in the TME in a murine model of mammary carcinoma, decreasing $CD8^+$ T cell proliferation and IFN-γ production[157].

In pDCs, when in a TGF-β-dominated environment, IDO interacts with the tyrosine phosphatases Src homology region 2 domain-containing phosphatase (SHP)-1 and SHP-2, activating the NF-κB pathway and the transcription of *Ido1* and *Tgfb1* genes, thus promoting an immunoregulatory response[60]. Notably, IDO expression by a type of tumor-associated pDCs leads to antigen-specific T cell responses that contribute to tumor progression[85,158]. Besides, cytokines such as IFN-γ and TGF-β[159–162], immunosuppressive drugs such as dexamethasone (DEX)[159], and CTLA-4-expressing T_{regs}[160,161] can also induce IDO expression in pDCs.

1.4.4. Lipid metabolism

Fatty acids are main constituents of many lipids, which play several key roles in cells, such as membrane composition, energy storage and intracellular communication. Their metabolism comprises the reverse processes of fatty acid synthesis (FAS) and oxidation (FAO). In the former, fatty acids are generated in the cytosol from acetyl-CoA and NADPH, through the action of fatty acid synthases. In the latter, activated fatty acids (FA-CoA) are broken down in the mitochondria into acetyl-CoA, which can be processed by the TCA cycle and oxidative phosphorylation for energy production[123].

Lipid metabolism also appears to be intimately related to DC phenotype and function. While FAS supports DC maturation, FAO inhibits their pro-inflammatory functions. During DC development and maturation, there is an increase in cytosolic lipid droplets (LD)[163]. This lipid accumulation in DCs is due to the expression of high levels of receptors, such as macrophage receptor with collagenous structure (MARCO)/macrophage scavenger receptor (MSR) 1[163]. There is strong evidence suggesting that lipid accumulation in human and mouse tumor-infiltrating myeloid cells reduces antitumor immunity in several cancer types like melanoma, lymphoma, mammary and colon adenocarcinomas and ovarian cancer[164–169]. In cDCs isolated from various types of tumors, lipids from the extracellular milieu can be imported in higher levels by the receptor MSR1, leading to a decrease in the antigen-presenting capacity[170]. This increase can be prevented through inactivation of genes involved in the regulation of lipid assembly, or the use of diacylglycerol acyltransferase inhibitors[171]. Additionally, administration of the FAO inhibitor TOFA also decrease FAS and lipid content, leading to a decrease of cDC to initiate an immune response and expression of TNF-α and IL-6[172]. Moreover, inhibition of FAO with etomoxir did not affect cDC development but increased IRF4 levels in cDC2 cells, while decreased IRF8 in cDC1 cells[173]. Moreover, since FAO produces citrate to fuel TCA cycle for *de novo* FAS and LD formation, the inhibition of FAS or lipid catabolism could be a promising approach to increase immune responses[174].

In the TME, due to the high levels of ROS, DCs accumulate oxidized lipids and activate ER stress responses, reducing their ability to induce immune responses[172]. Indeed, ER stress can promote IL-23 production in zymosan-stimulated human moDCs trough IRE1a and X-box binding protein 1 (XBP1)[175]. It was also demonstrated that the activation of XBP1 protein by unfolded protein responses (UPR) results in a production of LDs and, as a consequence, in DC dysfunction[164]. So, the inhibition of XBP1 restores DC function and thus T cell activation[147]. Besides, it was shown in a model of metastatic ovarian cancer

that inhibition of LDs can be reached by disabling IRE1α-XBP1 signaling, leading to an effective immune response[164].

The protein β-catenin also plays a role in fatty acids metabolism. Recent studies have shown that Wnt5 protein induce β-catenin signaling in a melanoma model of mouse TADCs, triggering peroxisome proliferator-activated receptor (PPAR) and promoting FAO[149]. This activation of β-catenin can result in induction of IDO, thus promoting T_{reg} responses[149]. Nevertheless, in a murine model of melanoma, $CD11c^+$ cells with decreased levels of β-catenin were associated with increased antitumor immunity[149]. Moreover, β-catenin was shown to induce vitamin A metabolism and production of retinoic acid, involved in T_{reg} generation[176].

Additional studies have demonstrated a correlation between lipids and immunosuppressive phenotypes in various DC subsets. PGE2, a bioactive eicosanoid lipid, plays a role in tumor progression and metastasis in melanoma, colon, breast, head and neck and lung cancers[177,178]. In cDCs, PGE2 deregulates the production IL-12, activating $CD8^+$, Th1 and NK cells responses[179]. Furthermore, in a melanoma model of cDCs incapable of producing PGE2, since they lack cyclooxygenase (COX) enzymes, it was observed and increase in antitumor immunity by increased expression of co-stimulatory molecules and IL-12[180].

As for pDCs, it has been demonstrated that FAO is favoured over FAS. This increase in FAO is due to the IFN-I signaling through IFN receptor (IFNAR) induced by TLR9, which increases pyruvate uptake[145]. In this mouse model of Flt3L-sorted pDCs, a late increase in ECAR after CpG (TLR9 agonist) or IFN-α stimulation was associated with increased FAS, fueling FAO in order to maintain an increased OXPHOS[145]. The administration of TOFA, etomoxir and C75 inhibit FAO metabolism and influenced the activation of these cells, by preventing IFN-α, TNF-α and IL-6 production[145]. The PPAR network also plays a role in pDCs metabolism since activation of FAO and OXPHOS by CpGA is somehow dependent on PPARα[60].

As described in the previous sections (and summarised in **Table 1**), some patterns are starting to emerge regarding metabolic adaptations of different DC subsets upon their development and stimulation. Still, further efforts are necessary to better understand the regulation processes involved in the immunogenic and tolerogenic DC metabolism. In particular, the influence of tumor microenvironmental factors on the regulation of signalling pathways and metabolic adaptions of DCs should be further explored in the future. Untargeted metabolic profiling approaches (metabolomics) may be especially useful in this

respect, namely to identify unanticipated changes in the levels of metabolites involved in central metabolic pathways.

Table 1 – Summary of studies addressing the relationship between metabolic pathways and innate immune function of cDC and pDC. The main metabolic and functional alterations resulting from cell activation with specific stimuli and/or treatment of activated cells with pharmacological agents are presented. The experimental approach used is also described. Legend: 2-DG (2-Deoxyglucose) – glycolysis inhibitor; 3-MA – autophagy inhibitor; AMPK – AMP-activated protein kinase; Arg – Arginase; BPTES – glutaminase inhibitor; C75 – fatty acid oxidation inhibitor; cDC – Conventional Dendritic Cell; DON – glutamine antagonist; ECAR – extracellular acidification rate; ELISA – enzyme linked immunosorbent assay; Etomoxir – fatty acid oxidation inhibitor; FACS – Fluorescence activated cell sorting; FAO – fatty acid oxidation; FAS – fatty acid synthesis; Flt3L – FMS-like tyrosine kinase 3 ligand; HLA-DR – Human leukocyte antigen DR isotype; IDO – Indoleamine 2,3-oxygenase; IFN – Interferon; IL – Interleukine; IRF – Interferon regulatory factor LPS – Lipopolysaccharide; Mdivi-1 – mitochondrial fission inhibitor; mROS – Mitochondrial reactive oxygen species; mTORC1 – Mammalian target of rapamycin complex 1; OCR – oxygen consumption rate; Olomoucine – BNIP3 inhibitor; pDC – Plasmacytoid Dendritic Cell; PD-L1 – Programmed death-ligand 1; PPP – Pentose Phosphate Pathway; pRNA – Protamine-RNA complexes; qRT-PCR – quantitative real time polymerase chain reaction; Rapamycin – mTOR inhibitor; S3 – mitochondrial fusion promoter; SRC – spare respiratory capacity; TCA – Tricarboxylic acid; TLR – Toll-like receptor; TGF – Transforming growth factor; TNF – Tumor necrosis factor; TOFA – fatty acid oxidation inhibitor.

Metabolic pathway	Cell type	Stimulus	Pharmacological agent	Experimental approach	Metabolic alteration	Affected innate immune functions	Reference
Glycolysis, TCA cycle and OXPHOS	$CD1c^+$ cDC	pRNA (TLR7/8)	Olomoucine, 3-MA	Extracellular flux analysis, flow cytometry, qPCR	↑ AMPK1α	TNF-α, CD80, PD-L1	[127]
	$CD1c^+$ cDC	pRNA (TLR7/8)	S3, Mdivi-1	Extracellular flux analysis, flow cytometry, qPCR	↓ ECAR, glucose uptake	TNF-α, CD80, PD-L1	[127]
	$CD1c^+$ cDC	pRNA (TLR7/8)	S3, Mdivi-1	Mito Tracker Green FM, flow cytometry, qPCR	↑ OCR, mitochondrial mass	TNF-α, CD80, PD-L1	[127]
	Human blood-sorted pDC	Guardiquimod (TLR7)	2-Deoxyglucose	XF-24 Analyzer (ECAR, OCR), ELISA, flow cytometry	↓ 2-glucose-6-phosphate	Type I IFN, expression of HLA-DR, CD80 and CD86	[142]
	pDCs sorted from Flt3L bone marrow cultures	CpGA (TLR9)		XF-96 Extracellular Flux Analyzer, qRT-PCR, flow cytometry	↑ Basal OCR and SRC	IFN-α, IL-6, TNF-α and CD86	[145]
	pDCs	Imiquimod (TLR7)			↑ Basal OCR	↓ IFN-α ↑ IL-6, TNF-α	[145]

Table 1 (Cont.)

Metabolic pathway	Cell type	Stimulus	Pharmacological agent	Experimental approach	Metabolic alteration	Affected innate immune functions	Reference
Glycolysis, TCA cycle and OXPHOS	Human blood-sorted or mouse spleen-sorted pDC	CpGA (TLR9)	Rapamycin		↓ mTORC1	Type I IFN, IL-6 and TNF-α	61
	pDC	pRNA (TLR7/8)	BPTES, 3-MA	Extracellular flux analysis, flow cytometry, qPCR	↓ OCR, mitochondrial mass	IFN-α, CD80, and PD-L1	127
	pDC	TLR7 (R848)		mROS measurement by fluorescence, qRT-PCR, flow cytometry	↑ mROS	Induction of cross-presentation and generation of $CD8^+$ T cell responses in vivo	181
PPP	cDC	LPS	Suppression of the expression of glucose-6-phosphate dehydrogenase	MicroBeta Liquid Scintillation Counter, qRT-PCR, flow cytometry	↓ Lipid accumulation	Pro-inflammatory cytokines (IL-6, IL-12 and TNF)	126
Amino acid metabolism	$cDC11c^+$ DCs	TGF-β, IL-4		qRT-PCR, Western Blott	↑ Arg1, IDO1	Tolerogenic phenotype	155
	pDC	pRNA (TLR7/8)	DON, 3-MA	Extracellular flux analysis, flow cytometry, qPCR	↓ Glutamine	IFN-α, CD80, and PD-L1	127
Lipid metabolism	cDC		TOFA	BODIPY staining, HCS LipidTOX Red neutral lipid staining, FACS, flow cytometry	↓ FAS and lipid content	TNF-α, IL-6 and TLRs, functional impairments for activating antigen-restricted $CD4^+$ T or NK cells	172
	$cD11c^+$ cDCs and pDCs		Etomoxir	Flow cytometry, immunofluorescence microscopy	FAO	DC development not affected	173

Table 1 (Cont.)

Metabolic pathway	Cell type	Stimulus	Pharmacological agent	Experimental approach	Metabolic alteration	Affected innate immune functions	Reference
Lipid metabolism	cDC2		Etomoxir		↑ FAO	↑ IRF4 ↑ CD71	173
	cDC1		Etomoxir		↓ FAO	↑ IRF8	173
	pDC	CpGA (TLR9)	Etomoxir	XF-96 Extracellular Flux Analyzer, qRT-PCR, flow cytometry	↓ Basal OCR, SRC and FAO	↓ IFN-α, IL-6, TNF-α and CD86	145
	Mouse pDC (sorted from Flt3L ligand-stimulated bone marrow cultures)	CpGA (TLR9)	TOFA, C75	XF-96 Extracellular Flux Analyzer, qRT-PCR, flow cytometry	↓ FAS ↓ Basal OCR	Type I IFN, IL-6, TNF-α and CD86	145

1.5. Metabolomics of DCs

1.5.1. The metabolomics approach

The term metabolomics corresponds to the quantitative measurement of variations in the concentrations of low-molecular weight metabolites (<1-2 kDa)[182] in biological samples (e.g. tissues, cells, biofluids), resulting from pathophysiologic/external stimuli and/or changes in the pattern of gene/protein expression in an organism[183]. Cell metabolism is a complex network of highly ordered and interconnected reactions, so that even small changes in regulating proteins can cause noticeable changes in the concentration of tens to hundreds of metabolites. By employing a holistic measurement of metabolic variations, metabolomics has the potential to disclose hidden biological events, being a suitable technique for studying physiological and pathological processes and for testing the effects of drugs or other exogenous compounds[183]. Indeed, metabolomics studies have been performed in several fields of biological and biomedical research, for instance to identify biomarkers of pathologies, help understanding the occurrence and nature of pathologies, discover new therapeutic targets, elucidate the mechanisms of drug action, assess the efficacy and safety of drug candidates in preclinical studies, select and stratify patients during clinical trials, and monitor treatment responses. Cancer research is a particular area highly impacted by metabolomics, as numerous studies of tissues, cells and body fluids have been performed over more than one decade[184,185].

Nowadays, Nuclear Magnetic Resonance (NMR) spectroscopy and Mass Spectrometry (MS) are the most commonly used analytical methods to characterize the metabolome, mainly due to their ability to assess variations in tens to hundreds of metabolites in a single measurement[186]. Ideally, the choice of the most adequate analytical platform(s) to be used in a particular metabolomics should be based on the biological questions under study, as well on the nature and number of samples to be analysed[187].

NMR spectroscopy offers several advantages that are important in the field of metabolomics[186,188]. It is non-destructive, highly reproductive and quantitative, requires minimum sample manipulation, and potentially enables the identification of unknown metabolites, which is important considering that many metabolites in complex biological mixtures are not known *a priori*. Moreover, the metabolic profiles obtained are virtually independent of the operator and the instrument, providing a high degree of reliability[186]. On the other hand, NMR has some important limitations, namely in terms of resolution (difficulty to distinguish overlapped signals in very complex samples) and sensitivity (inability to detect

metabolites present at concentrations lower than the µM-mM range)[186]. In reality, no single analytical platform can be applied to detect all metabolites in a biological sample due to the complexity of the metabolome. In this sense, the combined use of NMR and MS can provide a more sensitive coverage of detected metabolites[189].

To deal with the complex metabolic profiles derived from NMR and/or MS data, multivariate analysis (MVA) is typically employed, enabling the multiparametric comparison of sample groups, i.e., the assessment of differences/similarities between spectra of several samples[190]. The two most common MVA methods used in metabolomics are principal component analysis (PCA) and partial least squares discriminant analysis (PLS-DA). The first is a non-supervised method, that shows clusters of samples based on their similarity. PCA does not discard any variables, but reduces the number of dimensions, offering a general idea of separation patterns arising from the various sources of variability within the dataset. On the other hand, PLS-DA maximizes the separation between pre-defined sample groups and highlights the variables (metabolites) responsible for class discrimination[190,191].

1.5.2. Application of metabolomics to DC profiling

Metabolomics of dendritic cells offers many opportunities to reveal their metabolic adaptations in different pathophysiological conditions. However, there are also many challenges, mainly related to low numbers of immune cells available and rapid turnover rates of the cellular metabolites[186,192]. As such, there are still few studies on the application of NMR- or MS-based metabolomics to DC profiling.

Using untargeted liquid chromatography-mass spectrometry (LC-MS) profiling in moDCs in a model of yellow fever, Li *et al.* (2013) observed a shift in the metabolism of nucleotides, glutathione and amino acids[193]. Later, Ravindran *et al.* (2014) used LC-MS to analyze the intracellular concentration of amino acids in human moDCs in a model of yellow fever[194]. Furthermore, flux studies have been important for the interpretation of differences in the metabolite profiles. This technique has been applied in many studies concerning immunometabolism, such as one that defined metabolic fluxes in DCs (tracing ^{13}C-glucose)[126]. It was found that TLR-activation of DCs led to rapid metabolic changes, by increasing glycolysis and TCA cycle, determined by untargeted MS metabolic profiling[126]. Finally, using stable-isotope tracing LC-MS metabolomics, Vanherwegen *et al.* (2019) have shown the importance of vitamin D in imprinting human moDCs with tolerogenic properties by reprogramming their glucose metabolism[195].

However, comprehensive profiling of metabolic responses of dendritic cells using NMR metabolomics has not been reported before. In this thesis, this platform is employed for the first time to asses dendritic cell metabolic alteration upon stimulation in order to advance in understanding their mode of action.

1.6. Objectives of this work

The dual role of dendritic cell sub-populations in tumor progression and response to therapy calls for a deeper understanding of the factors that trigger and/or regulate DC stimulatory (antitumor) and regulatory (pro-tumoral) functions. These functions appear to be associated with distinct metabolic programs. Hence, it is important to characterize the metabolic adaptations associated with DC functional plasticity. For that purpose, comprehensive, untargeted metabolomics may constitute a uniquely useful approach.

This project aims at characterizing the metabolic profile of pDCs and at assessing the metabolic changes associated with: i) TLR7 stimulation (activated immunogenic profile) and ii) immunosuppression induced by a tumor-mimicking microenvironment. A human leukemic cell line (CAL-1) was used as *in vitro* model. Activation of pDCs was performed through incubation with the TLR7 agonist CL307, while the soluble factors TNF-α+TGF-β were used to decrease secretion of type I interferons and, in this way, to induce a more tolerogenic phenotype (typically observed in tumors). The assays performed involved evaluation of the mRNA expression levels of selected cytokines (IFN-β and TNF-α), in parallel with metabolic profiling through ^{1}H-NMR analysis of cell extracts and culture medium supernatants. Overall, we expect to gain new insights on the role of metabolism in pDCs phenotypic modulation.

CHAPTER 2

MATERIALS AND METHODS

2. Materials and Methods

2.1. Reagents

Stock solutions of CL307 (InvivoGen), TNF-α (PrepoTech) and TGF-β (PrepoTech) were prepared as follows. CL307 was prepared at 1 mg/mL in RNase-free water. TNF-α was prepared at 0.1 mg/mL in 0.1% BSA with PBS. TGF-β was reconstituted for a final concentration of 0.1 mg/mL in 0.1% BSA with 10 mM citric acid. All stock solutions were stored in aliquots at -20ºC. TNF-α and TGF-β concentrations were chosen according to the range used in Sisirak *et al*.[88].

2.2. Cell culture maintenance

CAL-1 cells, a human blastic plasmacytoid dendritic cell neoplasm cell line, were a gift of Dr. Takahiro Maeda from Nagasaki University Graduate school of Biomedical Science, Japan. These cells were cultured in suspension at 37ºC and 5% CO_2 atmosphere, in RPMI 1640 (Roswell Park Memorial Institute Medium, Gibco) culture medium supplemented with 1% NEAA (non-essential amino acids) (InvitroGen), 1% sodium pyruvate (InvitroGen) and 1% HEPES (InvitroGen), and containing 10% FBS (fetal bovine serum) (Sigma). The cells were maintained in suspension in T175 flasks (final volume of 30 mL and $2x10^5$ cell/mL density). When cells were incubated for 2 days, the cell culture media containing the cells was split into new T175 flasks, to which fresh culture media was added. All experiments were performed with cells from passages 9-11.

2.3. Cell stimulation and collection

For the stimulation experiments, cells were harvested from T175 flasks and centrifuged at 300 xg for 6 min. The medium supernatant was discarded and the cell pellet resuspended in 10-20 mL of RPMI media containing 1% FBS, 1% NEAA, 1% HEPES and 1% sodium pyruvate. The cells were counted using a Neubauer Chamber and adjusted with RPMI 1% FBS until the desired density was obtained. Using a 6-well plate, the cell suspension was divided in order to obtain 5.5 $x10^6$ cells per well. To note that each sample had two corresponding wells, leading to a final number of $11x10^6$ cells per sample. Of these,

$1x10^6$ cells were collected for quantitative real-time polymerase chain reaction (qRT-PCR) and $10x10^6$ cells for NMR, as shown schematically in **Figure 5**.

The activation stimulus used in this work was CL307 (chemical structure in Supplementary **Figure S1**), a potent TLR7 agonist. At an initial phase, cells were incubated for 1h, 3h, 6h and 24h with either 1 µM or 2 µM of CL307 per well, in order to optimize the concentration and incubation time with this stimulus. For the second part of this work, the cells were stimulated with CL307 in the presence of TNF-α together with TGF-β to mimic the tumor microenvironment. CAL-1 cells were incubated for 16h, with or without TNF-α (1 ng/mL per well) and TGF-β (1 ng/mL per well), as in Sisirak *et al.*[88], followed by CL307 at 1 µM for 1h or 3h (**Figure 6**). A well with RPMI medium with 1% FBS without cells was included as a control.

After incubation, samples were collected (11 mL final volume per sample). Then, 1 mL of each sample was separated for future qRT-PCR analysis. Next, samples were centrifuged at 300 xg for 6 min, 4ºC, and the supernatant collected. Thereafter, cell pellets were washed twice with cold PBS by centrifuging at 300 xg for 6 min at 4ºC. Finally, cell pellets and supernatant media were stored at -80ºC for further qRT-PCR and NMR metabolomics analysis. The medium from the wells without cells was also collected and stored at -80ºC.

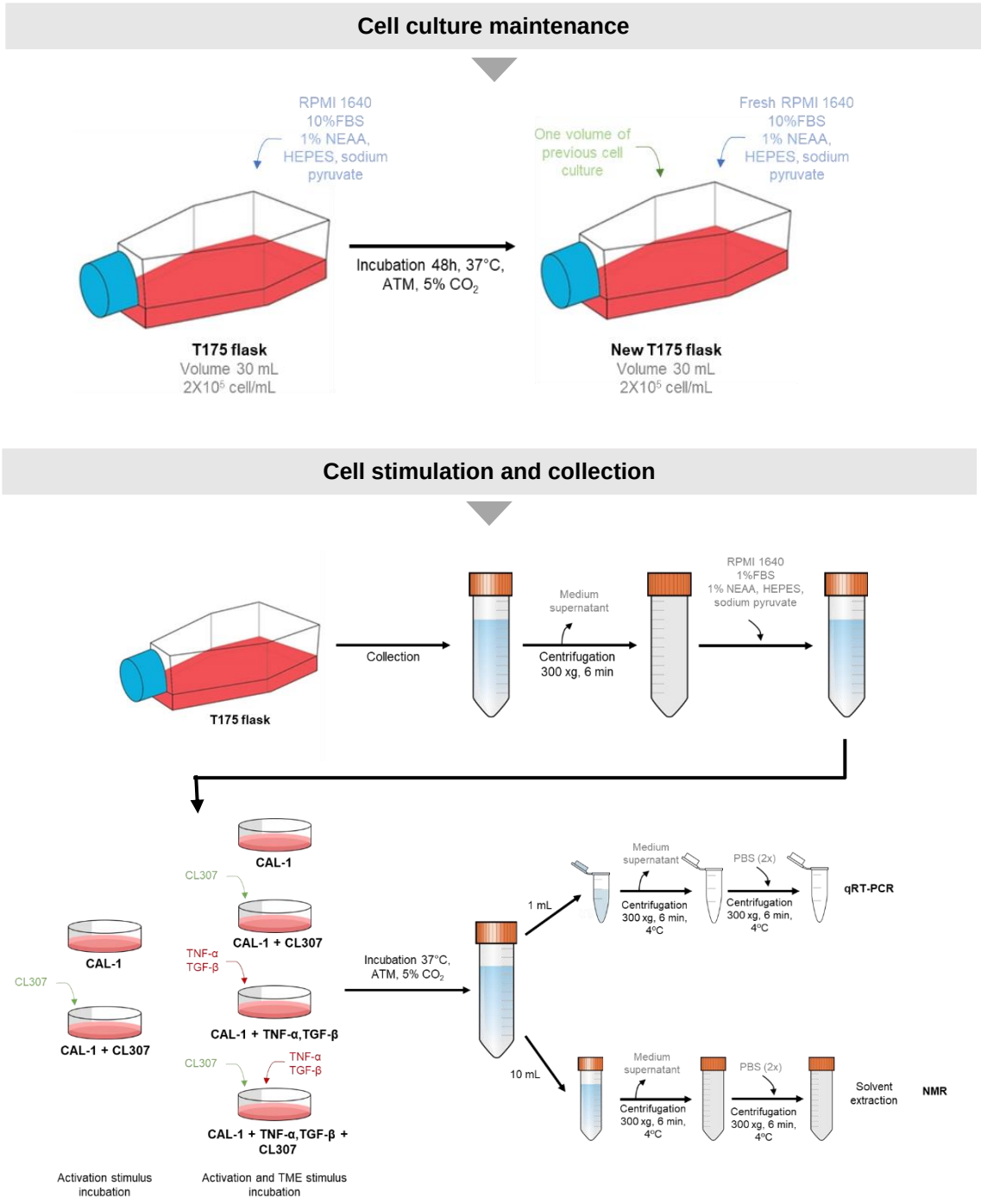

Figure 5 – Schematic representation of the experimental protocol used to obtain the cell pellet samples for qRT-PCR analysis and the polar extracts and cell media samples for NMR metabolomics. CAL-1 were maintained in RPMI 10% FBS for proliferation and growth. Then, cells were cultured *in vitro* in RPMI 1% FBS and stimulated with CL307 and/or TNF-α+TGF-β. After incubation, the cells were collected for qRT-PCR and prepared for NMR metabolomics.

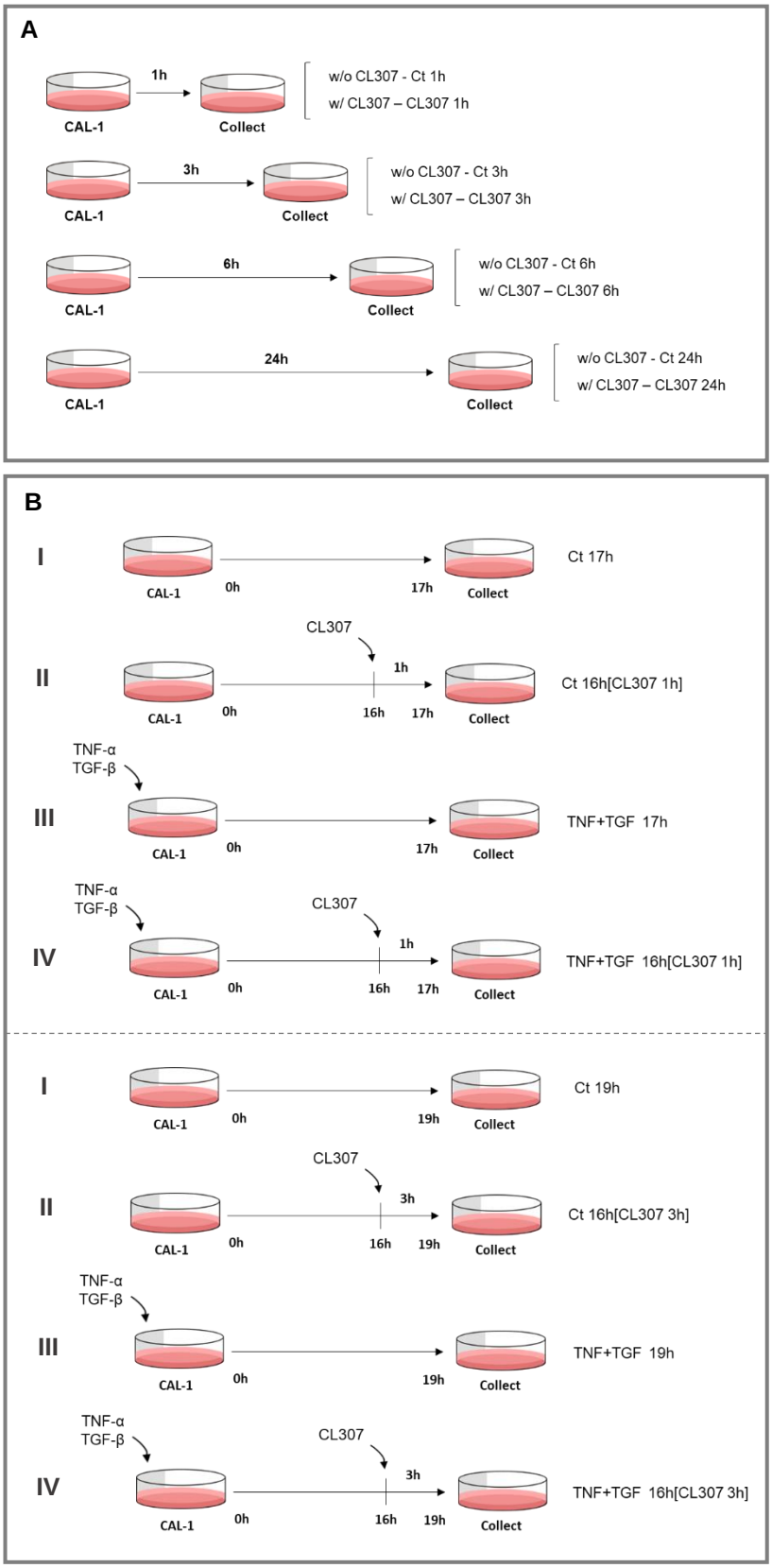

Figure 6 – Scheme of the experimental approach. (A) In the first part of the work, cells were incubated with CL307 at 1 or 2 µM during 1, 3, 6 or 24h. (B) In the second part of the work, cells were incubated alone, without any stimulus (I), incubated with TNF-α and TGF-β stimuli (III), activated with CL307 1 µM for 1h or 3h upon 16h of prior incubation alone (II) or with TNF-α and TGF-β (IV).

2.4. Quantitative mRNA expression analysis

2.4.1. RNA extraction and quantification

Total RNA extraction was performed using the RNeasy Mini Kit (Qiagen) according to manufacturer's instructions. Briefly, cell pellets were thawed on ice before adding 350 µL of buffer RLT with β-mercaptoethanol to each sample and vortexing for 1 min. Then, 350 µL of 70% ethanol was added to the samples. Next, the sample was transferred to a RNeasy spin column placed in a 2 mL collection tube and centrifuged for 20 sec at 11,000 xg. In order to remove any genomic DNA present in the samples, a treatment with DNAse was performed. A volume of 350 µL of buffer RW1 was added to the column, which was then centrifuged 20 sec at 11,000 xg. Then, 80 µL of a DNAse mix was added directly to the spin column and incubated at room temperature for 15 min. After that, 350 µL of buffer RW1 was added to the column, and then centrifuged at 11,000 xg for 20 sec. Thereafter, 500 µL of RPE buffer were added to the column, followed by centrifugation 20 sec at 11,000 xg and at full speed for 1 min. The RNeasy spin column was then placed in a 1.5 mL Eppendorf. Total RNA was eluted with 20 µL of RNase-free water by centrifugation at 11,000 xg for 1 min. The RNA was stored at -80ºC or kept on ice to proceed directly for quantification and cDNA synthesis. RNA quantification was performed in a DeNoVix DS-11 spectrophotometer (Frilabo).

2.4.2. cDNA synthesis

For gene expression analysis, cDNA was synthetized using the enzyme SuperScript II Reverse Transcriptase (Invitrogen). In each tube, on ice, 500 ng of total RNA, RNase-free water, 1 µL of dNTP mix (10 mM) and 2 µL of random hexamers (50 mM) were added to complete a total volume of 12 µL. To note that, in this protocol a negative control was added, containing the control sample which was treated the same way as the other samples. This no reverse transcriptase control (-RT) is used to monitor genomic DNA contamination when the target sample is cDNA. After that, all the components were gently mixed and incubated at 65ºC for 10 min in a C1000 Thermal Cycler (Bio-Rad), followed by a quick chill on ice for 2 min. Samples were mixed and added to a mix containing 4 µL 5x first-strand buffer, 2 µL of 0.1 M DTT and 40 U/µL RNase inhibitor per reaction, followed by incubation at 25ºC for 2 min. Thereafter, 1 µL of Superscript II Reverse Transcriptase was added to each sample, completing a total volume of 20 µL. Finally, samples were incubated at 25ºC for 10 min followed by 42ºC for 50 min. The reaction was inactivated by heating at 70ºC for 15 min,

followed by 4ºC. This incubation was performed in the same C1000 Thermal Cycler (Bio-Rad) mentioned previously. The samples were kept at -20ºC or on ice to proceed directly for qRT-PCR analysis.

2.4.3. Quantitative Real-Time PCR (qRT-PCR)

IFN-β and TNF-α transcripts were quantified by qRT-PCR. The assays were performed using primers for IFN-β (10 µM, InvitroGen) and TNF-α (10 µM, InvitroGen) and the endogenous control GAPDH (10 µM, InvitroGen) (details in **Table 2**). Firstly, cDNA samples were diluted 10x in RNase-free water. Then, a mix for each primer was prepared, containing 2x SyBR Green qPCR Master Mix (10 µL per reaction), Primer Forward (0.6 µL per reaction), Primer Reverse (0.6 µL per reaction) and RNase-free water (6.8 µL per reaction). The volumes used take into account the number of samples, in triplicates, and the -RT and blank wells. A volume of 2 µL of the diluted samples were added to each well of the 96-well qPCR plate (2 µL of RNase-free water to the blank wells), followed by 18 µL of the above primer mixture (total volume of 20 µL). Finally, the plate was sealed and centrifuged at 1,000 xg, 2 min. The expression assays were performed in a 7500 real time PCR system (Applied Biosystems). The qRT-PCR conditions were: 95ºC, 5 min (holding stage), 95ºC, 15 sec and 60ºC, 60 sec (cycling stage, 40 cycles), 95ºC, 15 sec, followed by 60ºC, 60 sec and 95ºC, 15 sec (melt curve). The run took about 2 hours.

To normalize the absolute quantification according to a single reference gene, the mean quantity of IFN-β and TNF-α expression levels were normalized against the mean quantity of the endogenous control GAPDH expression levels for the corresponding sample. For each target gene sample, the relative quantity (RQ) value obtained was divided by the value derived from the control sequence in the corresponding target gene. Results were further presented as fold variation in comparison to the experimental control.

Table 2 – qRT-PCR primers features: target gene, sequence and amplicon size.

Target gene	Sequence (5' → 3')	Amplicon size (bp)
GAPDH	CAATGACCCCTTCATTGACC GACAAGCTTCCCGTTCTCAG	106
TNF-α	CCCTCAGCAAGGACAGCAGA AGCCGTGGGTCAGTATGTGAG	139
IFN-β_1	TGCTTGGATTCCTACAAAGA GGATGTCAAAGTTCATCCTG	108

2.5. NMR metabolomics assay

2.5.1. Cell culture supernatants

Medium aliquots were collected from each well, including medium without cells incubated under the same conditions. To remove interfering proteins, thawed supernatants were subjected to a protein precipitation protocol described by Kostidis and colleagues[196]. Briefly, 600 µL of cold methanol 100% (v/v) (precooled at -80ºC) were added to 300 µL of supernatant. The aliquots were then kept at -20ºC for 30 min, after which they were centrifuged at 13,000 xg for 20 min. The supernatant was transferred to another vial, vacuum dried (SpeedVac, Eppendorf) and stored at -80ºC until NMR acquisition.

At the time of analysis, the samples were resuspended in 600 µL of deuterated phosphate buffer (PBS 100 mM, pH 7, containing 0.1 mM 3-(trimethylsilyl) propanoic acid (TSP-d4)), and 550 µL of each sample were transferred to 5 mm NMR tubes.

2.5.2. Cell extracts

The intracellular metabolites were extracted using a biphasic extraction protocol with methanol:choloroform:water (1:1:0.7). A volume of 800 µL of cold methanol (80% v/v) was added to each cell pellet. Then, the cells suspension was transferred to a vial with 150 mg of glass beads (to aid in cell disruption) and vortexed for 2 min. Next, 320 µL of cold

chloroform (-20ºC) was added to the tube and vortexed for 2 min, followed by the addition of 320 µL of choloroform and 280 µL of cold milli-Q water. The samples were vortexed, rested on ice for 10 min and then centrifuged at 2,000 xg for 15 min, followed by at 10,000 xg for 1 min. The lower organic phase was transferred to an amber glass vial while the aqueous phase was transferred to a microcentrifuge tube. Finally, the polar extracts were vacuum dried, and lipophilic extracts were dried under a nitrogen flow, after which they were stored at -80ºC.

At the time of NMR analysis, the dried samples of the aqueous phases were resuspended in 600 µL of deuterated phosphate buffer (PBS 100 mM, pH 7, containing 0.1 mM TSP-d4), and 550 µL of each sample were transferred to 5 mm NMR tubes. Only the aqueous extracts were analyzed by NMR in the scope of this thesis

2.6. ^{1}H-NMR Spectroscopy

Samples were analysed in a Bruker Avance III HD 500 NMR spectrometer (University of Aveiro, PT NMR Network) operating at 500.13 MHz for ^{1}H observation, at 298 K. Standard one-dimensional (1D) ^{1}H NMR spectra with water presaturation (pulse program 'noesypr1d', Bruker library) were recorded for all samples, with 32k points, 7002.8 Hz spectra width, a 2 s relaxation delay and 512 scans. Spectral processing was carried out using TopSpin version 4.0.7 (Bruker Biospin, Rheinstetten, Germany). Each FID was multiplied by a cosine function (with a ssb value of 2), zero filled to 64k data points and Fourier-transformed. The resulting spectra were then manually phased and the baseline corrected, and calibrated to the TSP signal at 0 ppm.

2.7. Multivariate analysis of spectral data

After processing, the spectra were visualized in Amix-Viewer version 4.0.1 (Bruker Biospin, Rheinstetten, Germany). Each spectrum was normalized by its total area, excluding the water-suppression region and some residual contaminant signals (chloroform, ethanol and methanol). The normalized areas were then organized into data matrices containing the information on the signals areas at each chemical shift (columns) in the different spectra (rows).

The data were uploaded into SIMCA-P 11.5 (Umetrics, Umeå, Sweden), where PCA (Principal Component Analysis) and PLS-DA (Partial Least Squares Discriminant Analysis) were applied. Different scaling types were tested, namely unit variance (UV), whereby each variable is divided by the standard deviation of the corresponding column, and Pareto (Par) scaling, where each variable is divided the square root of the standard deviation. These methods allow for variations in less abundant metabolites to have the equal/similar weight (UV/Par) as more intense signals in multivariate models. The results were visualized through scores scatter plots and loadings plots, colored according to variable importance to the projection (VIP).

2.8. Spectral integration and univariate analysis

Spectral integration was carried out in Amix-Viewer version 4.0.1 (Bruker Biospin, Rheinstetten, Germany). Representative signals of each metabolite were integrated and normalized by the total spectral area. For each metabolite, the percentage of variation in treated samples was calculated relative to the respective controls, along with the effect size (ES) and the statistical significance (*p*-value). The variations with large magnitude (|ES|>0.8) were expressed in heatmaps coloured as a function of the percentage of variation, using the R-statistical software 3.6.0 (R Core Team (2017). R: A language and environment for statistical computing. R Foundation for Statistical Computing, Vienna, Austria. http://www.R-project.org/).

2.9. Statistical analysis

Graphs and statistical analysis were performed using GraphPad Prism version 6.0 (GraphPad Software, CA, USA). Differences between average values obtained for different groups were assessed using One-Way Analysis of Variance (one-Way ANOVA), followed by an unpaired parametric *t test*.

CHAPTER 3

RESULTS

3. Results

3.1. Selection of conditions for pDC TLR7-stimulation

TLR7 is an endosomal receptor expressed predominantly in pDCs that induces mainly the IRF pathway and the production of type I Interferon. In this work, we have used the TLR7 agonist CL307 to stimulate type I IFN production in CAL-1 pDCs. As there was little information in the literature regarding stimulation of these cells with CL307, different times of incubation (1h, 3h, 6h, 24h) and concentrations (1 µM and 2 µM) of CL307 were tested. Cellular responses were then assessed in terms of cytokine expression and metabolic variations. In particular, mRNA expression of IFN-β (a type I IFN) and TNF-α (a pro-inflammatory cytokine) was evaluated, along with the ^{1}H-NMR profiles of polar cell extracts.

3.1.1. CL307-induced changes in IFN-β and TNF-α expression

The activation state of pDC induced by 3h, 6h or 24h incubation with CL307 (1 or 2 µM) was carried out through assessment of cytokine mRNA levels. The results are shown in **Figure 7**.

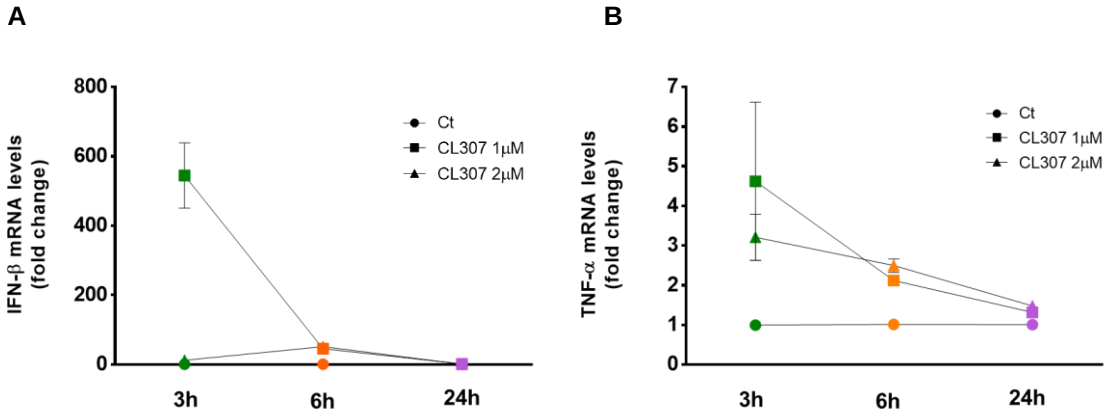

Figure 7 – qRT-PCR results for the transcript levels of (A) IFN-β and (B) TNF-α in pDCs stimulated for 3h, 6h and 24h with 1 or 2 µM CL307. Data represents the mean of 3 technical replicates from one experiment. The results are presented as fold variation in comparison to the experimental control (unstimulated cells).

The highest expression levels of IFN-β and TNF-α were found in samples stimulated with 1 µM CL307 for 3h. Both IFN-β and TNF-α mRNA levels decreased with increasing time of incubation, being almost undetectable for an incubation period of 24h. Moreover, a

dose-dependent effect was observed in 3h samples, as the lowest CL307 concentration (1 μM) stimulated more production of IFN-β and TNF-α relatively to unstimulated controls. This effect was not observed for 6h and 24h of incubation, where IFN-β and TNF-α expression levels were not dependent on the stimulus concentration. Based on these preliminary results, the 24h incubation period was excluded from the metabolomics assay, while a shorter incubation time (1h) was added, as metabolic alterations may precede transcription regulation[197].

3.1.2. CL307-induced changes in pDC metabolic profile

To investigate changes in metabolism, the metabolic profile of pDCs was assessed by ^{1}H-NMR spectroscopy. **Figure 8** shows a representative ^{1}H-NMR spectrum of a polar extract from pDCs. Metabolite assignment was based on matching spectral information to reference spectra available in Chenomx version 8.5, BBIOREFCODE–2–0–0 (Bruker Biospin, Rheinstetten, Germany) and HMDB[198,199]. In total, nearly 30 metabolites were identified (**Table S1** in Supplementary Information). These include several amino acids, organic acids, choline compounds, nucleotides, among others. Most of these metabolites were present in all sample groups, although differing in quantitative levels.

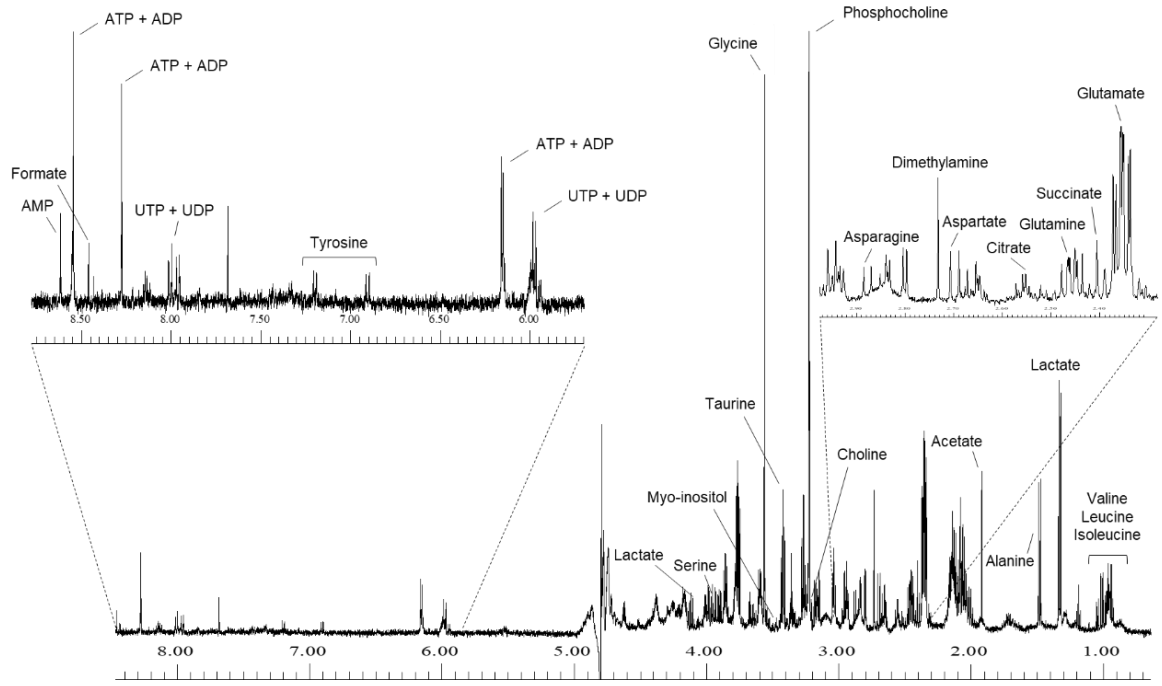

Figure 8 – 500 MHz ^{1}H-NMR spectrum of an aqueous extract from pDCs with some metabolite assignments.

To assess the metabolic differences between CL307-stimulated pDCs and unstimulated controls, their metabolic profiles were compared using multivariate analysis. The PCA scores scatter plot of all samples (**Figure 9**) showed a trend for separation according to incubation time, especially between 1h samples (negative PC1, blue symbols) and 6h samples (positive PC1, orange symbols). The 3h samples (green symbols) were more scattered. Also of notice, 1h and 3h controls were close in space, suggesting their metabolic profiles to be similar, while 6h controls were further away, reflecting the impact of incubation time on the cells metabolic composition, even without stimulus. Regarding the effect of CL307, for a specific incubation period, the separation from controls was especially clear in some cases, for instance between CL307 1 µM 3h and Ct 3h, and less clear for others, reflecting the dependence on time and concentration, as already indicated by PCR results.

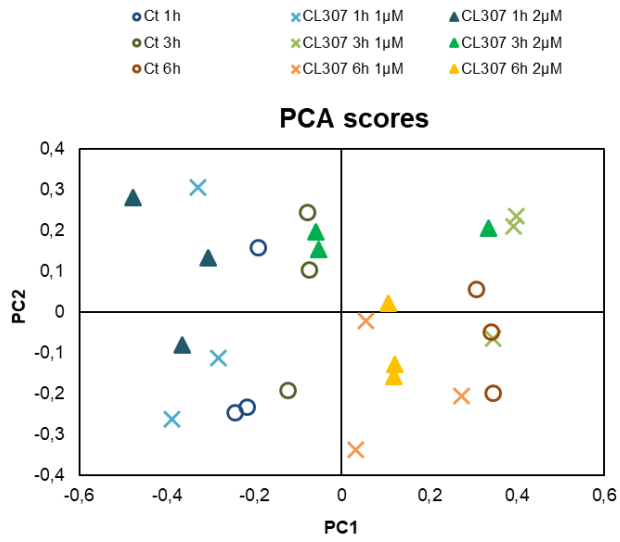

Figure 9 – Principal Component Analysis of ^{1}H-NMR spectra from the polar extracts of pDCs comparing unstimulated pDCs and pDCs stimulated with CL307 (1 or 2 µM), for 1h, 3h, or 6h of incubation.

Then, based on spectral integration, the magnitude and statistical significance of individual metabolite alterations were assessed. Only variations with a large magnitude (|ES| > 0.8) were considered. These results are summarised in a heatmap (**Figure 10**) color-coded according to the percentage of variation of each metabolite relatively to their respective controls. Detailed data is provided in Supplementary **Table S1**.

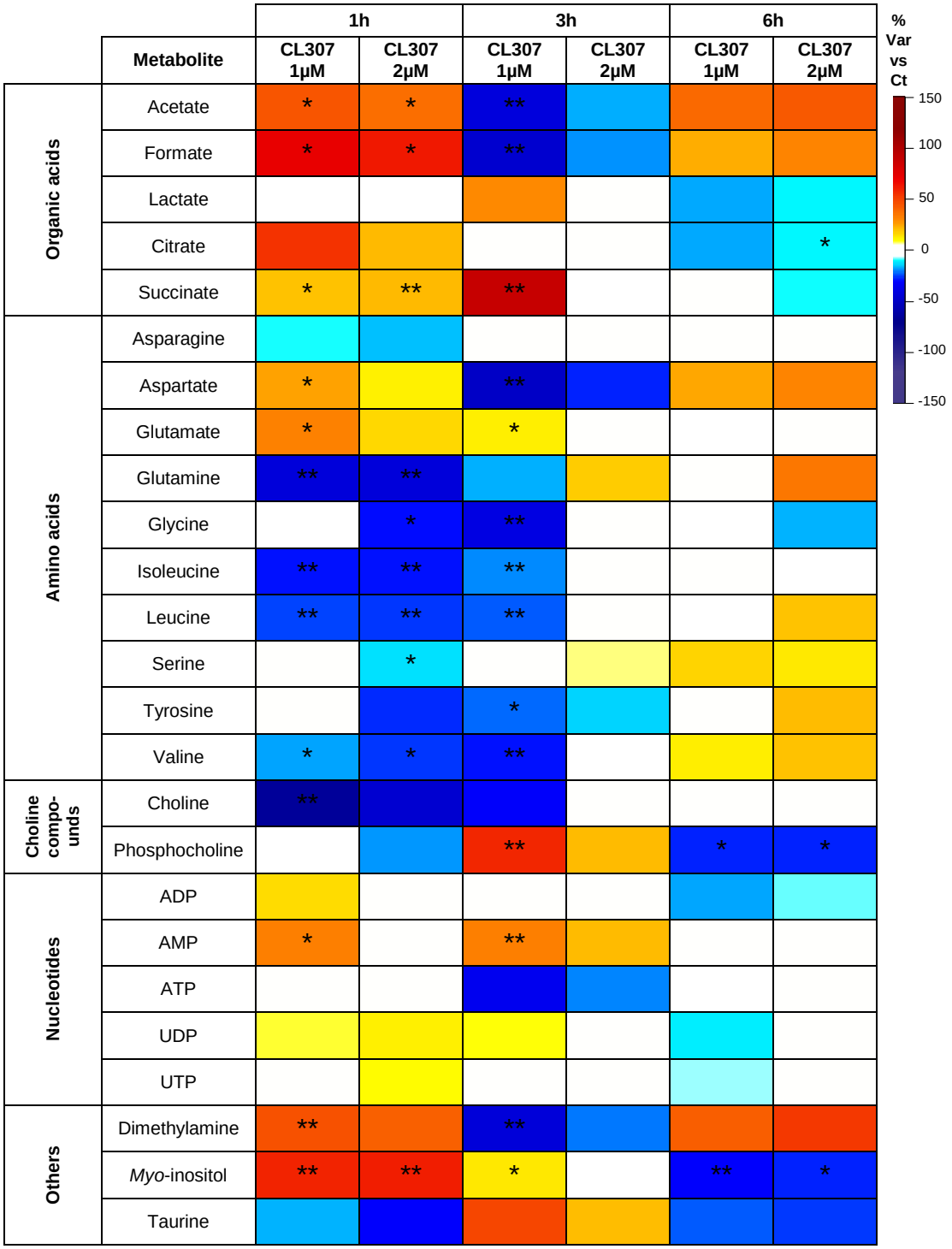

Figure 10 – Heatmap of the main metabolite variations in the polar extracts of pDCs incubated with CL307 for 1h, 3h and 6h at 1 µM and 2 µM. The color scale represents percentage of variation relative to the respective controls (unstimulated cells incubated for 1h, 3h and 6h) (n=3). **p*-value < 0.05; ***p*-value < 0.01.

In a general analysis, for 1h and 6h incubations, most variations were common between samples with either 1 or 2 µM CL307, although there were a few dose-dependent changes. For the 3h incubation period, the 2 µM concentration had a much lower impact on the cells metabolic composition. This agrees with the qRT-PCR results, which showed little change in IFN-β expression for 2 µM 3h samples. Additionally, most changes were clearly time-dependent, with the number of significant variations being attenuated from 1h/3h to 6h. Some metabolites even showed opposite directions of variation for different incubation periods, for instance acetate, formate, aspartate and dimethylamine (increased in cells treated with CL307 for 1h and 6h, but decreased at 3h), taurine and phosphocholine (decreased at 1/6h, increased at 3h), or *myo*-inositol (increased at 1/3h, decreased at 6h).

Taking a closer look at specific metabolic variations, within organic acids, the levels of acetate and formate in CL307-stimulated cells increased at 1h, decreased at 3h and increased again at 6h (relative to respective controls). On the other hand, citrate, succinate and lactate showed increased levels upon 1h/3h stimulation and decreased contents in cells stimulated for 6h. Regarding amino acids, glutamine, asparagine, glycine, leucine, isoleucine, valine, serine and tyrosine showed decreased levels in cells stimulated with CL307 for 1h and/or 3h, while, for some of them, an increasing trend was noted at 6h of stimulation. On the other hand, aspartate and glutamate were increased in 1h-stimulated cells relatively to 1h unstimulated controls. Glutamate remained elevated upon 3h stimulation, whereas aspartate strongly decreased in 3h-stimulated cells. Choline and phosphocholine also showed time-dependent variations. The former was decreased in 1h/3h-stimulated cells but showed no difference in cells treated with CL307 for 6h (compared to respective controls). On the other hand, changes in phosphocholine were more prominent for longer incubation times, being markedly increased in 3h-stimulated cells and decreased in 6h-stimulated cells. As for variations in nucleotides, the most marked changes were in the levels of AMP (increased upon 1h and 3h CL307 stimulation) and ATP (decreased upon 3h CL307 stimulation). Finally, dimethylamine, *myo*-inositol and taurine also showed prominent and time-dependent variations.

Overall, the results showed that pDCs dynamically adapted their metabolism during activation with CL307. The most prominent CL307-induced changes were captured at earlier incubation periods (1h/3h), for which several opposing variations were found. Hence, both these activation periods were selected for subsequent assays (CL307 stimulation in a tumor-mimicking environment). Regarding CL307 concentrations, although there were some dose-dependent changes, the lower concentration was found to be effective in

producing changes both in cytokine mRNA expression and metabolic profiles. Therefore, the experiments that followed were performed with 1 µM CL307.

3.2. Phenotypic and metabolic responses of pDC to TLR7 stimulation under tumor-mimicking conditions

After selecting the conditions for CAL-1 activation (1 µM, 1h and 3h incubation), a more complete study was performed, to assess the behaviour of pDCs in a tumor-mimicking microenvironment (containing TNF-α and TGF-β soluble factors). As schematically represented in **Figure 6B**, the samples compared were: I) unstimulated control pDCs, II) CL307-activated pDCs (1h or 3h stimulation), III) pDCs incubated with TNF-α and TGF-β, IV) pDCs incubated with TNF-α and TGF-β for 16h and activated with CL307 (1h or 3h). The phenotypic and metabolic changes in groups II-IV relatively to group I (controls) are described in the following sections.

3.2.1. Expression of IFN-β and TNF-α in pDCs treated with CL307 and/or TNF-α+TGF-β

In order to assess CAL-1 activation, mRNA levels of IFN-β and TNF-α were measured upon stimulation with CL307, preceded or not by treatment with TNF-α +TGF-β for 16h (**Figure 11**). As observed previously, the cells incubated with CL307 during 3h showed a large increase in IFN-β levels (**Figure 11A**, blue bar). On the other hand, expression of IFN-β was similar to basal levels when CL307 was administered to cells pre-incubated with TNF-α and TGF-β (**Figure 11A**, red bar), confirming the expected immunosuppressive effect of TNF-α and TGF-β. Interestingly, these factors alone (without CL307) also caused increased expression of IFN-β (**Figure 11A**, green bar). Similar variation trends as those described for IFN-β were also found for TNF-α mRNA expression (**Figure 11B**), although the magnitude of effects was much smaller. In the future, these results should be confirmed through measurements in biological replicates.

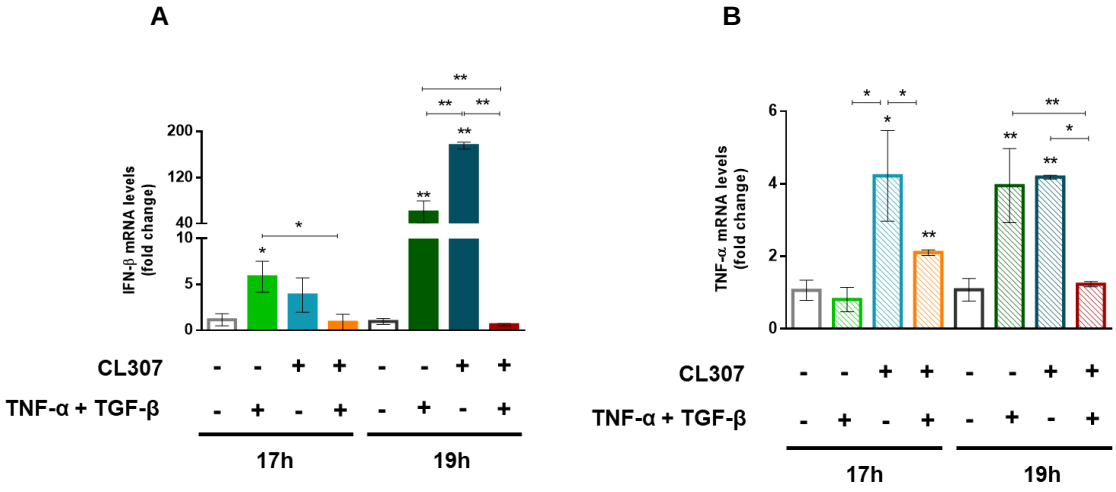

Figure 11 – mRNA levels of (A) IFN-β and (B) TNF-α in cells incubated with TNF-α and TGF-β and/or CL307 during a total time of incubation of 17h and 19h (TNF-α and TGF-β incubated for 16h and CL307 for 1h or 3h) along with the respective control groups (n=1 with 3 technical replicates). The results are presented as fold variation in comparison to the experimental control (unstimulated cells). Significant variations over the bars represented are comparisons to the respective control groups (unstimulated cells incubated 17h and 19h). **p*-value < 0.05; ***p*-value < 0.01.

3.2.2. Changes in pDC metabolic profile induced by CL307 and/or TNF-α +TGF-β

3.2.2.1. Metabolic response of pDCs to CL307 stimulation

The effects of CL307 on the intracellular metabolome of CAL-1 were assessed through ^{1}H-NMR analysis of cell polar extracts, followed by multivariate analysis and spectral integration. The PCA and PLS-DA results obtained for the comparison between untreated pDCs and pDCs incubated with CL307 during 1h or 3h (following 16h incubation in medium with 1% FBS and lacking TNF-α and TGF-β) are shown in **Figure 12**. The PCA scores plot obtained for the 4 sample groups (**Figure 12A**) showed a clear separation between control samples (Ct 17h) and cells incubated with CL307 for 1h (Ct 16h[CL307 1h]), while the separation between the two other groups (Ct 19h and Ct 16h[CL307 3h]) was not as good. In spite of the low number of samples per group (n=3), pairwise PLS-DA was also performed to obtain an immediate picture of the main metabolic effects induced by CL307 activation (**Figure 12B** and **12C**). In the resulting PLS-DA scores plots, samples incubated with CL307 were grouped in the negative side of the LV1 axis, so negative loadings should correspond to metabolites increased in those samples, whereas positive loadings are expected to correspond to metabolites elevated in control groups.

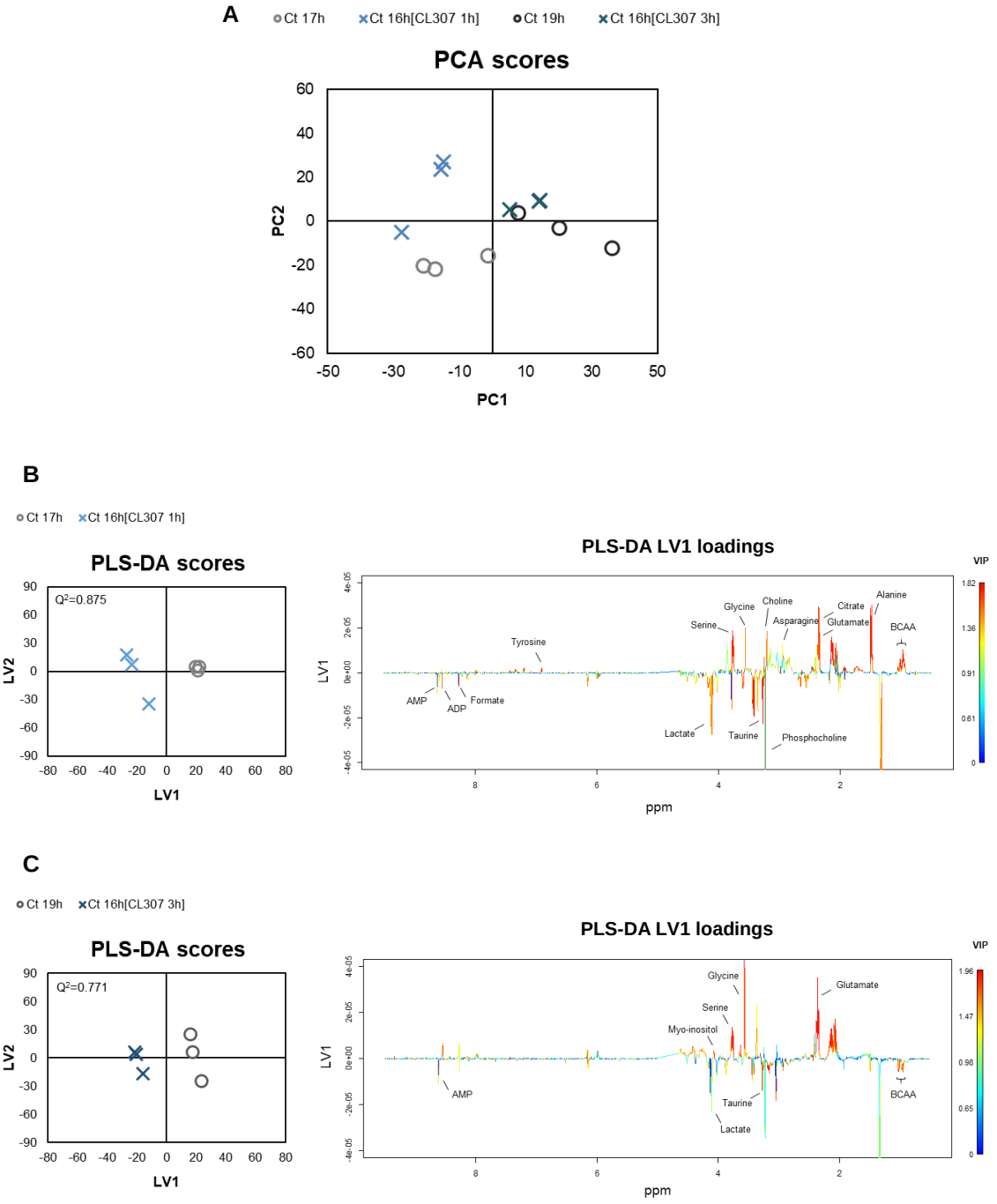

Figure 12 – Multivariate analysis of ^{1}H-NMR spectra from polar extracts of pDCs stimulated with CL307: (A) PCA and (B) and (C) PLS-DA scores scatter plots (left) and LV1 loadings w (right) colored according to variable importance to projection (VIP).

Then, based on spectral integration, the magnitude and statistical significance in individual metabolite alterations highlighted in the PLS-DA loadings were analyzed in more detail. The results of this analysis are summarised in **Figure 13A** (detailed data in Supplementary **Figure S4** and **Table S2**). Only variations with a large magnitude (|ES| > 0.8) were considered. Moreover, variations in the cells exometabolome were also assessed by determining the metabolite variations in cell-conditioned media relative to acellular medium (**Figure 13B** and **13C**; detailed data in Supplementary **Table S3**).

Spectral integration corroborated that the shorter (1h) incubation time with CL307 produced a higher metabolic impact, as cells incubated with CL307 for 3h showed less changes compared to their respective controls (**Figure 13A**). Focusing on the variations induced by 1h CL307 incubation, the intracellular metabolites which increased relatively to controls were formate, lactate, citrate, phosphocholine, ADP, AMP, UDP and taurine, while decreases were found for choline, several amino acids and *myo*-inositol. At the extracellular level (**Figure 13B** and **13C**), 1h CL307-activated cells showed higher consumption of glucose and aspartate. The 3h incubation with CL307 produced a significant increase in pyruvate consumption.

It should also be noticed that some of the changes mentioned above were distinct from those found in the preliminary study (section 2.3). A main experimental difference between the two sets of experiments (represented in **Figure 6A** and **6B**) was the time at which the culture medium was changed from 10% FBS to 1% FBS. In the first study (**Figure 6A**), the cells were incubated in medium with 1% FBS only when CL307 was added, while in the second study (**Figure 6B**), pDCs were incubated in 1% FBS medium for 16h prior to CL307 stimulation. This could have altered the cells basal metabolic profile, hence, their response to the activating stimulus.

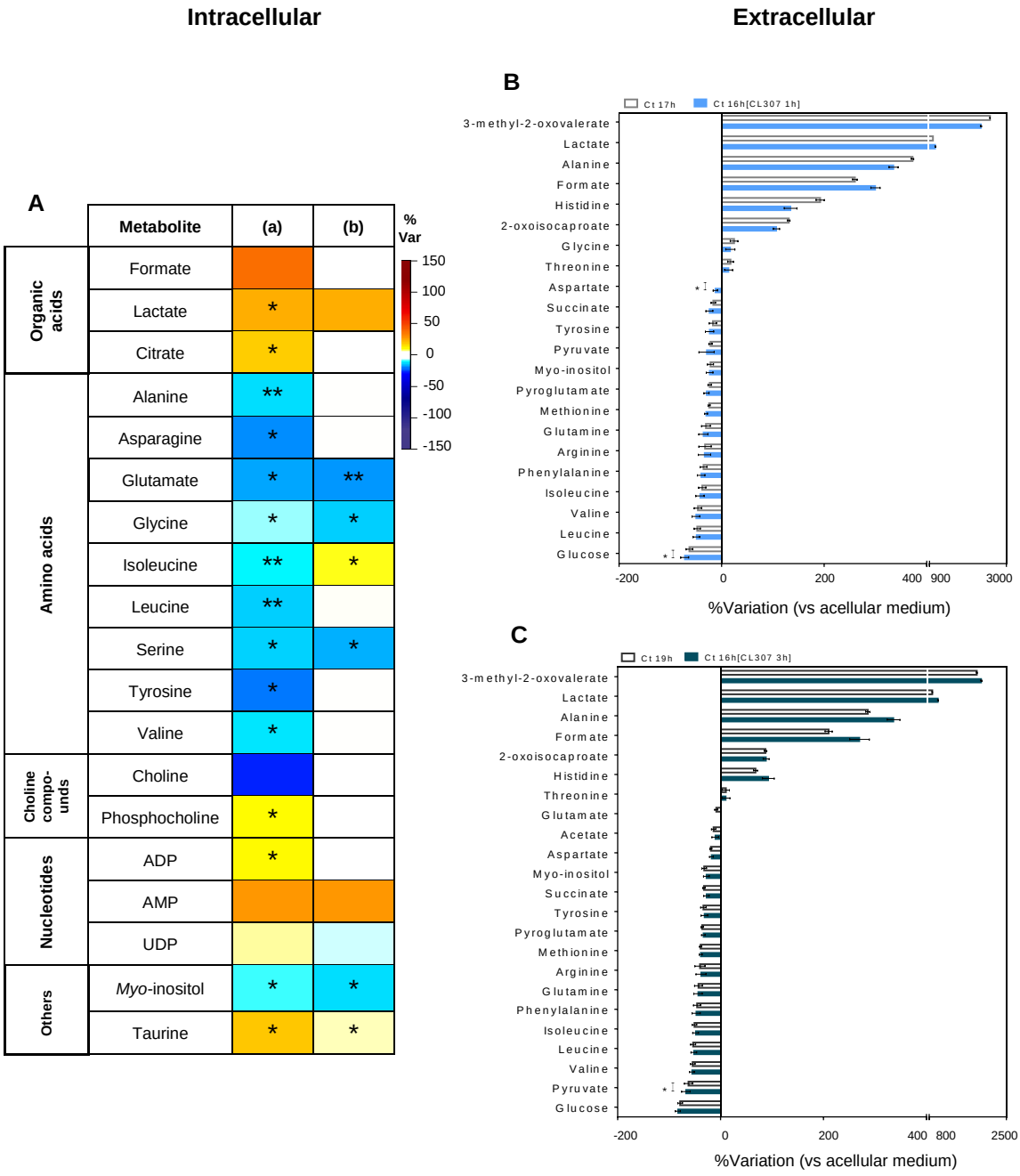

Figure 13 – Intracellular and extracellular metabolite variations in pDCs stimulated with CL307 during 1h and 3h. (A) Heatmap showing the intracellular metabolite variations in pDCs stimulated with CL307, compared to the respective controls. The variations represented in each column were obtained from the following comparisons: (a) Ct 16h[CL307 1h] vs Ct 17h and (b) Ct 16h[CL307 3h] vs Ct 19h. (B) Metabolites consumed (negative bars) and excreted (positive bars) by cells incubated for 17h, with or without 1h stimulation with CL307. (C) The same as in (B) but for 19h incubation, with or without 3h CL307 stimulation. **p*-value < 0.05; ***p*-value < 0.01.

3.2.2.2. Metabolic response of unstimulated pDCs to TNF-α+TGF-β

The effects of TNF-α and TGF-β on the metabolome of pDCs were also assessed through ^{1}H-NMR analysis of cell extracts and culture medium supernatants, followed by multivariate analysis and/or spectral integration, using the same strategy described in the previous section. The PCA and PLS-DA results obtained for the polar extracts are shown in Supplementary **Figure S2**, while quantitative variations are presented in **Figure 14A** for the endometabolome (detailed data in Supplementary **Figure S4** and **Table S2**), and in **Figure 14B** and **14C** for the exometabolome (detailed data in Supplementary **Table S3**). At the intracellular level (**Figure 14A**), the strongest variations induced by incubation with TNF-α+TGF-β for 17h were increases in acetate and formate and a decrease in choline. Milder changes were also seen for other metabolites (e.g. lower lactate, higher AMP). Interestingly, the changes induced by TNF-α+TGF-β upon 19h of incubation were not coincident with the 17h signature, and, in some cases, were even opposite (e.g. decreased acetate and increased choline in 19h TNF-α+TGF-β-treated cells compared to respective controls). At the extracellular level, a high number of significant changes were detected in 17h culture media samples from cells incubated with TNF-α and TGF-β, relatively to medium of control cells (**Figure 14B**). When exposed to these factors, pDCs were found to consume higher amounts of nutrients like glucose, pyruvate, succinate, acetate and some amino acids, but to excrete lower amounts of several metabolites (e.g. formate, alanine, lactate and 3-methyl-2-oxovalerate) when compared to the respective controls. Contrarily, no significant variations were observed in the groups incubated for 19h, except for histidine (**Figure 14C**).

Overall, the results showed that resting (non-activated) pDCs change their metabolism in the presence of TNF-α+TGF-β (tumor-mimicking microenvironment), in a time-dependent manner. The next section addresses the analysis of cells stimulated with CL307 under TNF-α+TGF-β incubation, in order to study the influence of tumor-mimicking conditions in the response of pDCs to TLR7-stimulation.

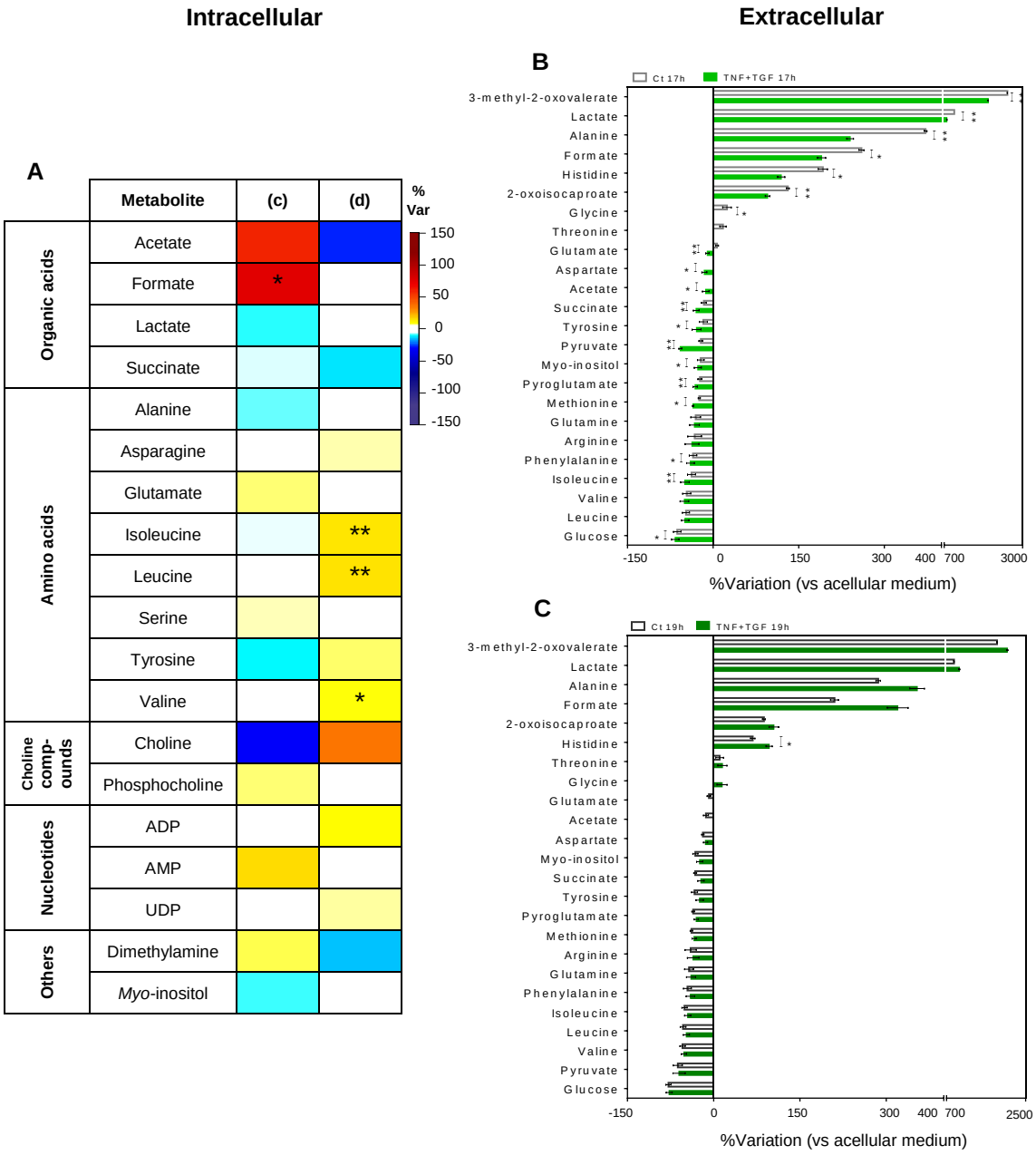

Figure 14 – Intracellular and extracellular metabolite variations in pDCs incubated with TNF-α and TGF-β during 17 and 19h. (A) Heatmap showing the intracellular metabolite variations in pDCs incubated with TNF-α and TGF-β, compared to the respective controls. The variations represented in each column were obtained from the following comparisons: (c) TNF+TGF 17h vs Ct 17h and (d) TNF+TGF 19h vs Ct 19h. (B) Metabolites consumed (negative bars) and excreted (positive bars) by cells incubated for 17h. (C) The same as in (B) but for 19h incubation. **p*-value < 0.05; ***p*-value < 0.01.

3.2.2.3. Influence of TNF-α+TGF-β and CL307 on pDC metabolic responses

The metabolic response of pDCs to CL307 (TLR7-activating stimulus) under the influence of TNF-α and TGF-β (tumor mimicking factors) was assessed through ^{1}H-NMR analysis of cell polar extracts and medium supernatants. The samples compared were: untreated pDCs in culture for 17h or 19h (controls), and pDCs stimulated by CL307 (1h or 3h) after 16h pre-incubation with TNF-α+TGF-β (groups I and IV in **Figure 6B**). Again, multivariate analysis was carried out to have a first overview of differences between sample groups. The results are shown in **Supplementary Figure S3**. Quantitative variations in cells polar extracts and medium supernatants were then measured through spectral integration of metabolite signals. The results are presented in **Figure 15A** and Supplementary **Figure S4** and **Table S2** for the intracellular composition, and in **Figure 15B** and **15C** and Supplementary **Table S3** for the extracellular variations.

The results for the endometabolome (**Figure 15A**) showed a higher number of variations in cells stimulated with CL307 for 3h (after 16h incubation with TNF-α+TGF-β) than in cells stimulated with CL307 for 1h (also under the influence of TNF-α+TGF-β) relatively to respective controls. Also, some variations were common while others were in opposite directions between cells stimulated with CL307 for 1h and for 3h. Formate and citrate were increased in both sample groups. The decrease in choline was also common to the two groups. On the other hand, amino acids, taurine and nucleotides showed different variations. Cells stimulated with CL307 for 1h, under the influence of TNF-α+TGF-β, showed decreased levels of some amino acids (alanine, isoleucine, leucine and tyrosine), compared to untreated controls, while cells stimulated with CL307 for 3h showed increases in several amino acids (asparagine, aspartate, glutamate, isoleucine, leucine, serine, tyrosine, valine). Moreover, AMP and UDP increased upon 1h stimulation with CL307, whereas AMP and ADP decreased in 3h samples.

At the extracellular level, when inspecting medium samples results (**Figure 15B** and **15C**), both 1h and 3h CL307-activated cells showed higher consumption of pyruvate. Regarding other metabolites, there were no significant differences in the cells consumption and excretion patterns.

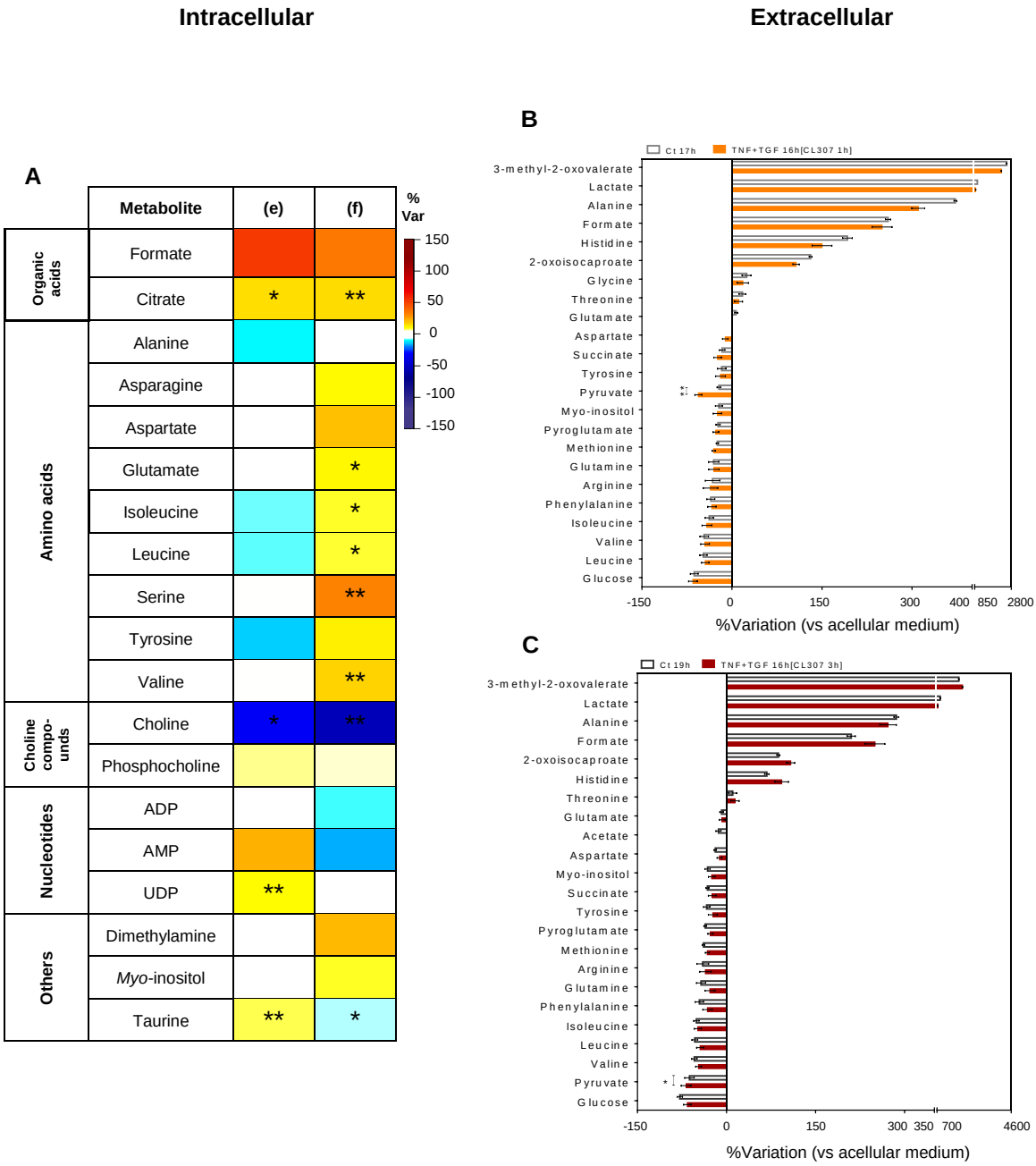

Figure 15 – Intracellular and extracellular metabolite variations in 1h and 3h CL307-stimulated pDCs incubated with TNF-α and TGF-β during 17 and 19h. (A) Heatmap showing the intracellular metabolite variations in pDCs incubated with TNF-α and TGF-β, compared to the respective controls. The variations represented in each column were obtained from the following comparisons: (e) TNF+TGF 16h[CL307 1h] vs Ct 17h and (f) TNF+TGF 16h[CL307 3h] vs Ct 19h. (B) and (C) Variations in consumptions (negative bars) and excretions (positive bars) of several metabolites in the cell culture supernatant. **p*-value < 0.05; ***p*-value < 0.01.

CHAPTER 4

DISCUSSION

4. Discussion

Plasmacytoid dendritic cells comprise a subset of DCs characterized by their ability to produce large amounts of type I IFN, representing important actors in innate immunity. However, when pDCs are recruited to a tumor site, they are maintained in an immature (non-active) state, leading to impaired function with decreased production of type I IFN, while promoting immunosuppression. However, the mechanisms through which pDCs acquire its immunosuppressive phenotype is not well known. Although the field of cancer immunometabolism is just emerging, there is growing evidence suggesting that changes in metabolism following TLR stimulation are essential for pDC activation. However, this metabolic rewiring occurring in response to TLR-stimulation is not known in detail, with no information related to pDCs behavior in the TME. Furthermore, the information available for TLR-stimulated pDCs is, somehow, contrasting, since the metabolic adaptations of pDCs could depend on several factors such as the type of DC subset, its origin, the stimulus used and the time considered upon stimulation. Thus, this project aimed at characterizing the metabolic profile of pDCs by assessing the metabolic changes associated with activation of the immunogenic profile (TLR7 stimulation) and immunosuppression induced by a tumor-mimicking microenvironment.

Activation of pDCs was performed through incubation with the TLR7 agonist CL307, while the soluble factors TNF-α and TGF-β were used to induce a more tolerogenic phenotype, typically observed in tumors. In a first step, as there was little information in the literature about these cells responses to CL307 stimulation, different times of incubation and concentrations of CL307 were tested. After determining the conditions inducing the most significant changes, the second part of this work focused on the study of the influence of tumor-mimicking conditions in pDCs activation. Cellular responses were assessed in terms of IFN-β and TNF-α mRNA expression and metabolic variations.

At a starting point of this work, the activation state of pDC induced by CL307 incubation was carried out through assessment of cytokine mRNA levels. Increases in IFN-β and TNF-α mRNA levels were observed upon CL307 stimulation, showing that this stimulus activated the cells, reaching the highest level of mRNA expression at 3h of CL307 stimulation. Under the influence of TNF-α and TGF-β (tumor-mimicking factors), mRNA expression of IFN-β and TNF-α was suppressed, when compared to the results obtained for 1h and 3h CL307-stimulated cells, which agrees with the expected immunosuppressive effects of a tumor-like microenvironment. Indeed, according to Sisirak *et al.*[88], recombinant

TNF-α and TGF-β synergistically block IFN production of TLR-activated pDC, while their neutralization restores pDCs' IFN production.

The metabolic profile was studied by ^{1}H-NMR analysis of cell extracts and culture medium supernatants. **Figure 16** shows the main results obtained for the intracellular metabolic variations in pDCs incubated with TNF-α+TGF-β and/or CL307 for a total time of incubation of 17h or 19h.

The effects of CL307 on the intracellular metabolome of CAL-1 were assessed through the comparison between untreated pDCs and pDCs incubated with CL307 during 1h or 3h (following 16h incubation in stimuli-free medium). As shown in **Figure 16,** shorter (1h) incubation time with CL307 produced a higher metabolic impact. There were marked increases in AMP and ADP, as well as in lactate and the TCA cycle intermediate, citrate. Apart from these increases, there were also significant decreases in several amino acids, namely alanine, asparagine, glutamate, glycine, isoleucine, leucine, serine, tyrosine and valine. At the extracellular level, cells stimulated with CL307 for 1h showed higher consumption of glucose and aspartate. These data suggest an upregulation of glucose metabolism. This agrees with previous work showing that human pDCs switch to glycolysis to perform antiviral functions[142]. This switch is due to an increased HIF-1α expression that induces early glycolysis (within minutes), as observed by increased rates of lactate production[142]. Also, it was reported that the inhibition of glycolysis in TLR7-activated pDCs by 2-DG decrease type I IFN production and upregulation of surface molecules[142]. The same study showed the involvement of TLR7 pathway in glycolysis, by using chloroquine, which is known to disrupt endosomal acidification required for TLR7 signaling[60,142]. In contrast, TLR9 activation of mouse pDCs has been reported to result in increased OXPHOS and FAO[145].

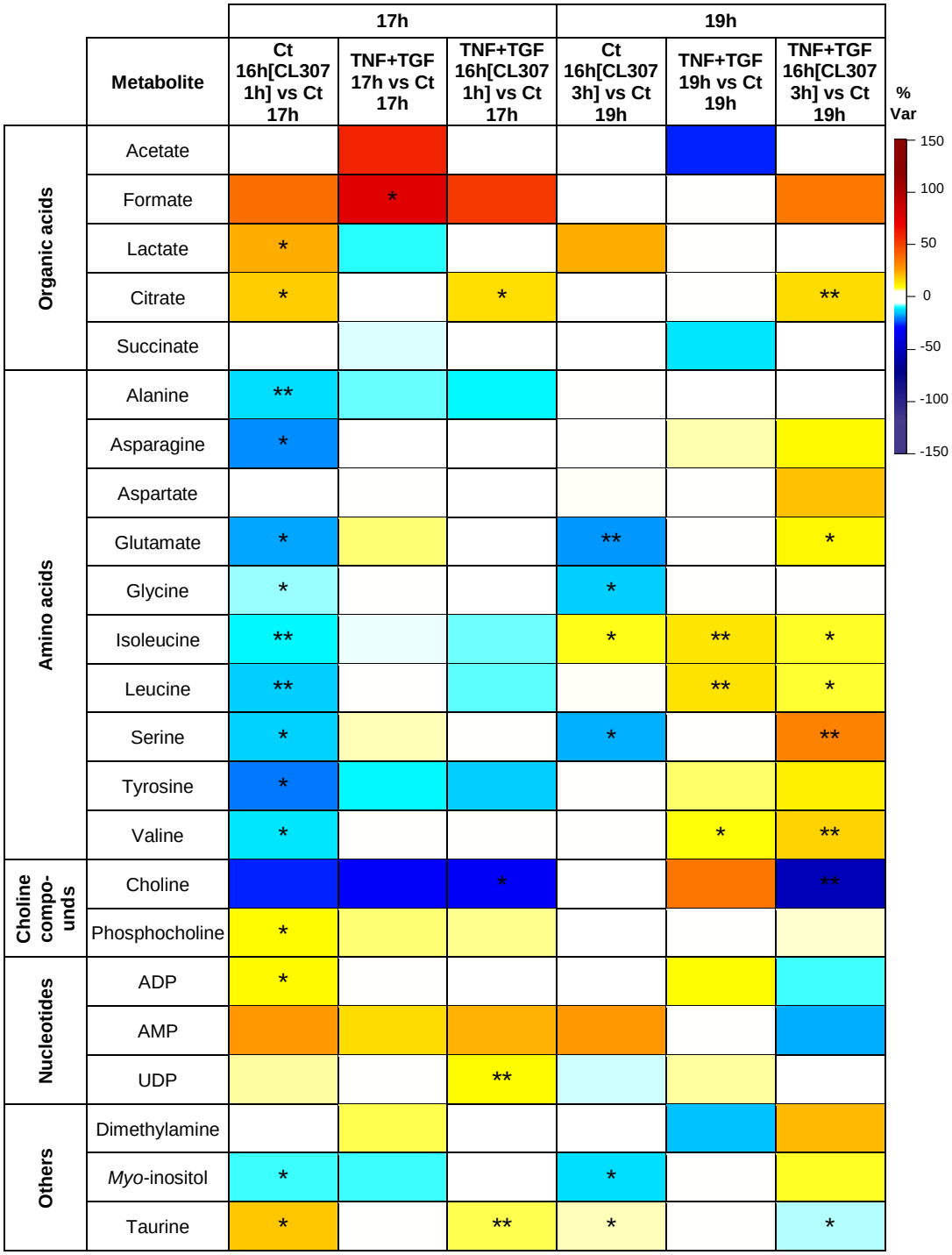

Figure 16 – Heatmap of the main metabolite variations in the polar extracts of pDCs incubated with TNF-α+TGF-β and/or CL307. The color scale represents percentage of variation relative to the respective controls (unstimulated cells) (n=3). **p*-value < 0.05; ***p*-value < 0.01.

TLR stimulation of human cDCs and mouse BMDCs has also been shown to trigger a shift to glycolysis, which is essential for the immune functions of DCs[136]. This induction in glycolysis promotes *de novo* fatty acid synthesis through formation of citrate[200,201]. Disrupting this pathway reduces DC maturation, cytokine secretion and thus T cell immune responses[127]. In this sense, the results obtained in this work showing increased intracellular lactate and citrate, along with increased glucose consumption, suggest an increased glycolysis coupled with intensified TCA cycle. Besides, in 1h CL307-stimulated pDCs, there was also a significant decrease in all amino acids. Such variation is consistent with the anaplerotic fueling of the TCA cycle, suggesting its upregulation. For example, alanine and glycine can be converted into pyruvate, isoleucine into acetyl-CoA, glutamate into α-ketoglutarate and asparagine and aspartate into oxaloacetate. Nevertheless, the decrease in glutamate is also consistent with decreased glutaminolysis caused by TLR7 treatment, being reported to derive from autophagy[127].

In this work, pDCs stimulated for 1h with CL307 additionally showed increased levels of AMP and ADP. These nucleotides may arise from hydrolysis of ATP to generate energy for anabolic processes. This is consistent with the hypothesis presented above, whereby activation involves upregulated glycolysis and TCA cycle to support biosynthesis (e.g. of lipids). On the other hand, increases in the AMP:ATP or ADP:ATP ratios could activate AMPK[147] and shift metabolism to catabolic reactions (such as FAO) to restore ATP levels. This could possibly relate to the attenuation of metabolic changes induced by longer (3h) stimulation with CL307. Assessment of AMPK activation state could help to clarify this question.

Under the influence of TNF-α and TGF-β (tumor-mimicking factors), the metabolic responses to CL307 stimulation was attenuated, which correlated well with the lack of IFN-β and TNF-α mRNA production. There was still an increase in AMP and citrate (related to AMPK regulation and TCA cycle), as well as some decreases in amino acids, mainly alanine, isoleucine, leucine and tyrosine, despite being less pronounced. But, unlike CL307-stimulated pDCs, under the influence of tumor-mimicking conditions, there was no longer an increase in intracellular levels of lactate and ADP, along with no significant variations in the consumption/excretion pattern of glucose. Hence, these results suggest that

upregulation of glycolysis and TCA, suggested to be induced by 1h incubation with CL307, were attenuated in the presence of TNF-α and TGF-β.

Additionally, we could observe changes in *myo*-inositol and taurine, which may relate to their role in osmoregulation[202] and, in the case of taurine, antioxidant protection[203]. Finally, some alterations were common to all stimuli, such as strong increases in formate and strong decreases in choline, suggesting that these metabolites are probably not related to the activation/suppressive phenotype of pDCs.

Regarding the metabolic changes obtained for 3h CL307-stimulated pDCs (following 16h incubation in normal medium) (**Figure 16**), the results showed similar metabolic responses to 1h CL307-stimulated pDCs, although less marked. We could observe an increase in intracellular AMP and lactate, as accompanied by higher pyruvate consumption. On the other hand, levels of some amino acids, such as glutamate, glycine and serine, were decreased. Comparing to the observed for 1h of CL307 stimulation, where it was suggested an increased glycolytic activity coupled to increased TCA cycle, in 3h CL307-stimulated pDCs this metabolic activity is still present, although attenuated. Interestingly, while metabolic alterations were more marked in pDCs incubated with CL307 for 1h than in 3h-stimulated cells, the mRNA expression levels of IFN-β and TNF-α were higher for longer CL307 incubation, suggesting that the metabolic processes involved in pDC activation may indeed precede transcriptional alterations.

Notably, under the influence of TNF-α and TGF-β, most of the changes observed in 3h CL307-stimulated cells are not present. Some metabolites showed no change (e.g. lactate) or opposite variations (e.g. glutamate, serine, AMP, *myo*-inositol, taurine). In fact, there is a strong influence of TNF-α+TGF-β in CL307-stimulated cell, since the results obtained for these conditions are closer to the ones obtained for unstimulated cells incubated under the influence of tumor-mimicking factors. For instance, several amino acids show a marked increase both in cells incubated with TNF-α+TGF-β for 19h and in cells stimulated with CL307 (3h) in the presence of these factors. This suggests that the anaplerotic fueling of the TCA cycle was attenuated, leading to this increase, or the consumption of amino acids from the extracellular media increased. Besides, AMP showed decreased levels under tumor-mimicking conditions in stimulated cells, which could reflect its regeneration into ATP and favoring of ATP-generating catabolic processes associated with a more tolerogenic phenotype. Since these metabolic changes are closer to the ones found in unstimulated cells under the influence of TNF-α and TGF-β, and the cytokine (TNF-

α) and type I interferon (IFN-β) mRNA expression decreased compared to 3h CL307-stimulated cells, we might conclude that, under the influence of tumor-mimicking conditions, 3h CL307-stimulated pDCs acquire a more evident tolerogenic phenotype characterized by a possible prevalence of catabolic processes.

Overall, as expected, CAL-1 metabolism responds to TLR7 stimulation. These changes include variations in some glycolytic metabolites such as lactate and glucose, as well as in TCA cycle intermediates, mainly citrate, significant variations in several amino acids and nucleotides. Furthermore, the suppression of CL307-induced activation, reflected on mRNA expression of type I IFN and TNF-α, is also reflected on the cells metabolic profile.

CHAPTER 5

CONCLUSIONS AND FUTURE PERSPECTIVES

4. Conclusions and future perspectives

In this thesis, ^{1}H-NMR based metabolomics proved to be a very useful tool for characterizing the metabolic profile of a human pDC cell line. Near 30 intracellular metabolites were detected in the cells polar extracts (endometabolome), whereas analysis of cells-conditioned culture medium (exometabolome) was useful to assess the consumption/excretion of several substrates/products. Multivariate analysis and quantitative assessments of metabolic profiles revealed consistent variations upon exposure of pDCs to the activation stimulus CL307 and tumor microenvironment factors, TNF-α and TGF-β.

This study provided novel insights into TLR-stimulated metabolic adaptations in human pDCs. CL307 stimulation was associated with different metabolic profiles, with some time-dependent variations. Overall, pDCs metabolism responded to TLR7 stimulation by changes in the glycolytic activity and TCA cycle, possibly relating to intensified biosynthetic activity and a more immunogenic phenotype. The suppression of CL307-induced activation by the tumor-mimicking environment was confirmed through decreased mRNA expression of type I IFN and TNF-α, and newly found to be reflected on the cells metabolic profile

In the future, in order to confirm and better understand the results obtained, it would be important to evaluate changes in lipid metabolism and the state of some metabolic sensors, namely AMPK and mTOR signaling pathways, important for the metabolic activity of pDCs. Those future developments will contribute to our understanding of pDC biology in the context of cancer and will expand the availability of strategies to improve cancer immunotherapy.

REFERENCES

1. Bray, F., Ferlay, J., Soerjomataram, I., Siegel, R., Torre, L. A. & Jemal, A. Global Cancer Statistics 2018: GLOBOCAN Estimates of Incidence and Mortality Worldwide for 36 Cancers in 185 Countries. *CA Cancer J CLIN* **68**, 394–424 (2018).

2. Hanahan, D. & Weinberg, R. A. The hallmarks of cancer. *Cell* **100**, 57–70 (2000).

3. Hanahan, D. & Weinberg, R. A. Hallmarks of Cancer: The Next Generation. *Cell* **144**, 646–674 (2011).

4. Fouad, Y. A. & Aanei, C. Revisiting the hallmarks of cancer. *Am J Cancer Res* **7**, 1016–1036 (2017).

5. Candeias, S. M. & Gaipl, U. S. The Immune System in Cancer Prevention, Development and Therapy. *Anti-Cancer Agents in Medicinal Chemistry* **16**, 1–14 (2016).

6. Abbas, A. K. & Litchman, A. H. Introduction to the Immune System. in *Basic Immunology* 3 (Saunders, 2004).

7. Mittal, D., Gubin, M. M., Schreiber, R. D. & Smyth, M. J. New insights into cancer immunoediting and its three component phases —elimination, equilibrium and escape. *Curr Opin Immunol* **27**, 16–25 (2014).

8. Gonzalez, H., Hagerling, C. & Werb, Z. Roles of the immune system in cancer: from tumor initiation to metastatic progression. *Genes & Development* **32**, 1267–1284 (2018).

9. Sharma, P., Wagner, K., Wolchok, J. D. & Allison, J. P. Novel cancer immunotherapy agents with survival benefit: recent successes and next steps. *Nat Rev Cancer* **11**, 805–812 (2012).

10. Zitvogel, L., Tesniere, A. & Kroemer, G. Cancer despite immunosurveillance: immunoselection and immunosubversion. *Immunology* **6**, 715–727 (2006).

11. Binnewies, M., Roberts, E. W., Kersten, K., Chan, V., Douglas, F., Merad, M., Coussens, L. M., Gabrilovich, D. I., Ostrand, S., Hedrick, C. C., Vonderheide, R. H., Pittet, M. J. & Rakesh, K. Understanding the tumor immune microenvironment (TIME) for effective therapy. *Nat Med.* **24**, 541–550 (2018).

12. Yu, Y. & Cui, J. Present and future of cancer immunotherapy: A tumor microenvironmental perspective (Review). *Oncology Letters* **16**, 4105–4113 (2018).

13. Chen, J. Disease-Associated Plasmacytoid Dendritic Cells. **8**, 1–12 (2017).

14. Qiao, J., Liu, Z. & Fu, Y. Adapting conventional cancer treatment for immunotherapy. *Journal of Molecular Medicine* **94**, 489–495 (2016).

15. Conforti, F., Pala, L., Bagnardi, V., De Pas, T., Martinetti, M., Viale, G., Gelber, R. D. & Goldhirsch, A. Cancer immunotherapy efficacy and patients' sex: a systematic review and meta-analysis. *Lancet Oncology* **19**, 737–746 (2018).

16. Yu, Y. R. & Ho, P. C. Sculpting tumor microenvironment with immune system: from immunometabolism to immunoediting. *Clinical and Experimental Immunology* **197**, 153–160 (2019).

17. Najafi, M., Goradel, N. H., Farhood, B., Salehi, E., Solhjoo, S., Toolee, H., Kharazinejad, E. & Mortezaee, K. Tumor microenvironment: Interactions and therapy. *J Cell Physiol.* **24**, 5700–5721 (2019).

18. Finotello, F. & Eduati, F. Multi-Omics Profiling of the Tumor Microenvironment: Paving the Way to Precision Immuno-Oncology. *Frontiers in Oncology* **8**, 1–9 (2018).

19. Fu, C. & Jiang, A. Dendritic Cells and CD8 T Cell Immunity in Tumor Microenvironment. *Frontiers in Immunology* **9**, 1–11 (2018).

20. Pitt, J. M., Marabelle, A., Eggermont, A., Soria, J., Kroemer, G. & Zitvogel, L. Targeting the tumor microenvironment: removing obstruction to anticancer immune responses and

immunotherapy. *Annals of Oncology* **27**, 1482–1492 (2016).

21. Collin, M. & Bigley, V. Human dendritic cell subsets: an update. *Immunology* **154**, 3–20 (2018).

22. Palucka, K. & Banchereau, J. Cancer immunotherapy via dendritic cells. *Nat Rev Cancer* **12**, 265–277 (2013).

23. Cells, T. D., Karthaus, N., Torensma, R. & Tel, J. Deciphering the Message Broadcast by Tumor-Infiltrating Dendritic Cells. *The American Journal of Pathology* **181**, 733–742 (2012).

24. Constantino, J., Gomes, C., Falcão, A., Neves, B. M. & Cruz, M. T. Dendritic cell-based immunotherapy: a basic review and recent advances. *Immunol Res* **65**, 798–810 (2017).

25. Wang, M., Zhao, J., Zhang, L., Wei, F., Lian, Y., Wu, Y., Gong, Z., Zhang, S., Zhou, J., Cao, K., Li, X., Li, G., Zeng, Z. & Guo, C. Role of tumor microenvironment in tumorigenesis. *Journal of Cancer* **8**, 761–773 (2017).

26. Oderup, C., Cederbom, L., Makowska, A., Cilio, C. M. & Ivars, F. Cytotoxic T lymphocyte antigen-4-dependent down-modulation of costimulatory molecules on dendritic cells in $CD4^+$ $CD25^+$ regulatory T-cell-mediated suppression. *Immunology* **118**, 240–249 (2006).

27. Larmonier, N., Marron, M., Zeng, Y., Cantrell, J., Romanoski, A., Sepassi, M., Thompson, S., Chen, X., Andreansky, S. & Katsanis, E. Tumor-derived $CD4^+$ $CD25^+$ regulatory T cell suppression of dendritic cell function involves TGF-β and IL-10. *Cancer Immunol Immunother* **56**, 48–59 (2007).

28. Lin, A., Schildknecht, A., Nguyen, L. T. & Ohashi, P. S. Dendritic cells integrate signals from the tumor microenvironment to modulate immunity and tumor growth. *Immunology Letters* **127**, 77–84 (2010).

29. Huang, L.-Y., Reis e Sousa, C., Itoh, Y., Inman, J. & Scott, D. E. IL-12 Induction by a Th1-Inducing Adjuvant In Vivo: Dendritic Cell Subsets and Regulation by IL-10. *The Journal of Immunology* **167**, 1423–1430 (2001).

30. Yang, A. S. & Lattime, E. C. Tumor-induced Interleukin 10 Suppresses the Ability of Splenic Dendritic Cells to Stimulate CD4 and CD8 T-cell Responses. *Cancer Research* **63**, 2150–2157 (2003).

31. Hultkrantz, S., Östman, S. & Telemo, E. Induction of antigen-specific regulatory T cells in the liver-draining celiac lymph node following oral antigen administration. *Immunology* **116**, 362–372 (2005).

32. Hargadon, K. M. Tumor-altered dendritic cell function : implications for anti-tumor immunity. **4**, 1–13 (2013).

33. Rubtsov, Y. P., Rasmussen, J. P., Chi, E. Y., Fontenot, J., Castelli, L., Ye, X., Treuting, P., Siewe, L., Roers, A., Jr, W. R. H., Muller, W. & Rudensky, A. Y. Regulatory T Cell-Derived Interleukin-10 Limits Inflammation at Environmental Interfaces. *Immunity* **28**, 546–558 (2008).

34. Whiteside, T. The tumor microenvironment and its role in promoting tumor growth. *Oncogene* **27**, 5904–5912 (2008).

35. Ziani, L., Chouaib, S. & Thiery, J. Alteration of the Antitumor immune Response by Cancer-Associated Fibroblasts. *Frontiers in Immunology* **9**, 1–14 (2018).

36. Patente, T. A., Pinho, M. P., Oliveira, A. A., Evangelista, G. C. M., Bergami-Santos, P. C. & Barbuto, J. A. M. Human Dendritic Cells: Their Heterogeneity and Clinical Application Potential in Cancer Immunotherapy. *Frontiers in Bioscience* **9**, 1–18 (2019).

37. Hermans, I. F., Silk, J. D., Gileadi, U., Mathew, B., Ritter, G., Schmidt, R., Adrian, L., Old, L. & Cerundolo, V. NKT Cells Enhance $CD4^+$ and $CD8^+$ T Cell Responses to Soluble Antigen In Vivo through Direct Interaction with Dendritic Cells. *J Immunol* **171**, 5140–5147 (2003).

38. Halim, T. Y. F., Hwang, Y. Y., Scalon, S. T., Zaghouani, H., Garbi, N., Fallon, P. G. & Mckenzie, A. N. J. Europe PMC Funders Group Group 2 innate lymphoid cells license dendritic cells to potentiate memory T helper 2 cell responses. **17**, 57–64 (2016).

39. Thordardottir, S., Hangalapura, B. N., Hutten, T., Cossu, M., Spanholtz, J., Schaap, N., Radstake, T. R. D. J., Voort, R. V. D. & Dolstra, H. The Aryl Hydrocarbon Receptor Antagonist StemRegenin 1 Promotes Human Plasmacytoid and Myeloid Dendritic Cell Development from CD34$^+$ Hematopoietic Progenitor Cells. *Stem Cells and Development* **23**, 955–967 (2014).

40. Schreibelt, G., Tel, J., Sliepen, K. H. E. W. J., Benitez-Ribas, D., Figdor, C. G., Adema, G. J. & Vries, I. J. M. Toll-like receptor expression and function in human dendritic cell subsets: implications for dendritic cell-based anti-cancer immunotherapy. *Cancer Immunol Immunother* **59**, 1573–1582 (2010).

41. Brussel, I. Van, Berneman, Z. N. & Cools, N. Optimizing Dendritic Cell-Based Immunotherapy: Tackling the Complexity of Different Arms of the Immune System. *Mediators of Inflammation* **2012**, 1–14 (2012).

42. Bol, K. F., Schreibelt, G., Gerritsen, W. R., Vries, I. J. M. De & Figdor, C. G. Dendritic Cell-Based Immunotherapy: State of the Art and Beyond. *Clin Cancer Res* **22**, 1897–1907 (2016).

43. Macdonald, K. P. A., Munster, D. J., Clark, G, J., Dzionek, A., Schmitz, J., & Hart, D. N. J. Characterization of human blood dendritic cell subsets. *Blood* **100**, 4512–4520 (2002).

44. Lehmann, C., Lafferty, Mark, Garzino-demo, A., Jung, N., Hartmann, P., Wolf, J. S., Lunzen, J. V, & Romerio, F. Plasmacytoid Dendritic Cells Accumulate and Secrete Interferon Alpha in Lymph Nodes of HIV-1 Patients. *PLOS ONE* **5**, 1–12 (2010).

45. Tabarkiewicz, J., Rybojad, P., Jablonka, A. & Rolinski, J. CD1c$^+$ and CD303$^+$ dendritic cells in peripheral blood, lymph nodes and tumor tissue of patients with non-small cell lung cancer. *Oncology Reports* **19**, 237–243 (2008).

46. Rodrigues, P. F., Alberti-servera, L., Eremin, A., Grajales-reves, G. E., Ivanek, R. & Tussiwand, R. Distinct progenitor lineages contribute to the heterogeneity of plasmacytoid dendritic cells. *Nature Immunology* **19**, 711–724 (2018).

47. Mitchell, D., Chintala, S. & Dey, M. Plasmacytoid dendritic cell in immunity and cancer. *Journal of Neuroimmunology* **322**, 63–73 (2018).

48. Siegal, F. P., Kadowaki, N., Shodell, M., Fitzgerald-Bocarsly, P. A., Shah, K., Ho, S., Antonenko, S. & Liu, Y. The Nature of the Principal Type 1 Interferon-Producing Cells in Human Blood. *Science* **284**, 1835–1837 (1999).

49. Liu, Y. IPC: Professional Type 1 Interferon-Producing Cells and Plasmacytoid Dendritic Cell Precursors. *Annu. Rev. Immunol.* **23**, 275–306 (2005).

50. Schettini, J. & Mukherjee, P. Physiological Role of Plasmacytoid Dendritic Cells and Their Potential Use in Cancer Immunity. *Clinical and Developmental Immunology* **2008**, 1–10 (2008).

51. Gehrie, E., Touw, W. Van der, Bromberg, J. S. & Ochando, J. C. Plasmacytoid Dendritic Cells in Tolerance. *Methods Mol Biol.* **677**, 127–147 (2011).

52. Akira, S., Uematsu, S. & Takeuchi, O. Pathogen Recognition and Innate Immunity. *Cell* **124**, 783–801 (2006).

53. Hémont, C., Neel, A., Heslan, M., Braudeau, C. & Josien, R. Human blood mDC subsets exhibit distinct TLR repertoire and responsiveness. *Journal of Leukocyte Biology* **93**, 599–609 (2013).

54. Colletti, N. J., Liu, H., Gower, A. C., Alekseyev, Y. O., Arendt, C. W. & Shaw, M. H. TLR3 signaling promotes the induction of unique human BDCA-3 dendritic cell populations.

Frontiers in Immunology **7**, 1–11 (2016).

55. Edwards, A. D., Diebold, S. S., Slack, E. M. C., Tomizawa, H., Hemmi, H., Kaisho, T., Akira, S. & Reis e Sousa, C. Toll-like receptor expression in murine DC subsets: Lack of TLR7 expresion of CD8α⁺ DC correlates with unresponsiveness to imidazoquinolines. *European Journal of Immunology* **33**, 827–833 (2003).

56. Matsumoto, M., Funami, K., Tanabe, M., Oshiumi, H., Shingai, M., Seto, Y., Yamamoto, A. & Seya, T. Subcellular Localization of Toll-Like Receptor 3 in Human Dendritic Cells. *The Journal of Immunology* **171**, 3154–3162 (2003).

57. Funami, K., Matsumoto, M., Oshiumi, H., Akazawa, T., Yamamoto, A. & Seya, T. The cytoplasmic 'linker region' in Toll-like receptor 3 controls receptor localization and signaling. *International Immunology* **16**, 1143–1154 (2004).

58. T, S., H, O., M, S., T, A. & M., M. TICAM-1 and TICAM-2: toll-like receptor adapters that participate in induction of type 1 interferons. *Int J Biochem Cell Biol* **37**, 524–9 (2005).

59. Klechevsky, E., Kato, H., Sponaas, A., Garra, A. O., Banchereau, J. & New, A. S. Dendritic cells star in Vancouver. *JEM* **202**, 5–10 (2005).

60. Saas, P., Varin, A., Perruche, S. & Ceroi, A. Recent insights into the implications of metabolism in plasmacytoid dendritic cell innate functions: Potential ways to control these functions. *F1000 Research* **6**, 1–24 (2017).

61. Gilliet, M., Cao, W. & Liu, Y. Plasmacytoid dendritic cells: Sensing nucleic acids in viral infection and autoimmune diseases. *Immunology* **8**, 594–606 (2008).

62. Pelka, K. & Latz, E. IRF5, IRF8, and IRF7 in human pDCs - the good, the bad, and the insignificant? *European Journal of Immunology* **43**, 1693–1697 (2013).

63. Britten, C. M., Kreiter, S., Diken, M. & Rammensee, H.-G. *Cancer Immunotherapy Meets Oncology: In Honor of Christoph Huber*.

64. Guiducci, C., Ott, G., Chan, J. H., Damon, E., Calacsan, C., Matray, T., Lee, K., Coff, R. L. & Barrat, F. J. Properties regulating the nature of the plasmacytoid dendritic cell response to Toll-like receptor 9 activation. *JEM* **203**, 1999–2008 (2006).

65. Kerkmann, M., Costa, L. T., Richter, C., Rothenfusser, S., Battianv, J., Hornung, V., Johnson, J., Englert, S., Ketterer, T., Heckl, W., Thalhammer, S., Endres, S. & Hartmann, G. Spontaneous Formation of Nucleic Acid-based Nanoparticles Is Responsible for High Interferon-alpha Induction by CpG-A in Plasmacytoid Dendritic Cells. *The Journal of Biological Chemistry* **280**, 8086–8093 (2005).

66. Combes, A.. Camosseto, V., Guessan, P. N., Arguello, R. J., Mussard, J., Caux, C., Bendriss-vermare, N., Pierre, P. & Gatti, E. BAD-LAMP controls TLR9 trafficking and signalling in human plasmacytoid dendritic cells. *Nature Communications* **8**, 1–18 (2017).

67. Treilleux, I., Blay, J., Bendriss-Vermare, N., Ray-Coquard, I., Bachelot, T., Guastalla, J., Bremond, A., Goddard, S., Pin, J., Barthelemy-Dubois, C. & Lebecque, S. Dendritic Cell Infiltration and Prognosis of Early Stage Breast Cancer. *Clinical Cancer Research* **10**, 7466–7474 (2004).

68. Labidi-Galy, S. I., Treilleux, I., Goddard-Leon, S., Combes, J. D., Blay, J. Y., Caux, C. & Bendriss-Vermare, N. Plasmacytoid dendritic cells infiltrating ovarian cancer are associated with poor prognosis. *OncoImmunology* **1**, 379–381 (2012).

69. Noubade, R., Majri-Morrison, S. & Tarbell, K. V. Beyond CDC1: Emerging Roles of DC Crosstalk in Cancer Immunity. *Frontiers in Immunology* **10**, 1–13 (2019).

70. Schreibelt, G., Bol, K. F., Westdorp, H., Wimmers, F., Aarntzen, E. H. J. G., Duiveman-De Boer, T., Van De Rakt, M. W. M. M., Scharenborg, N. M., De Boer, A. J., Pots, J. M., Olde Nordkamp, M. A. M., Van Oorschot, T. G. M., Tel, J., Winkels, G., Petry, K., Bloky, W. A. M.,

Van Rossum, M. M., Welzen, M. E. B., Mus, R. D. M., Croockewit, S. A. J., Koornstra, R. H. T., Jacobs, J. F. M., Kelderman, S., Blank, C. U., Gerritsen, W. R., Punt, C. J. A., Fidgor, C. G. & De Vries, I. J. M. Effective Clinical Responses in Metastatic Melanoma Patients after Vaccination with Primary Myeloid Dendritic Cells. *Clinical Cancer Research* **22**, 2155–2166 (2016).

71. Salmon, H., Idoyaga, J., Rahman, A., Leboeuf, M., Remark, R., Jordan, S., Casanova-Acebes, M., Khudoynazarova, M., Agudo, J., Tung, N., Chakarov, S., Rivera, C., Hogstad, B., Bosenberg, M., Hashimoto, D., Gniatic, S., Bhardwaj, N., Palucka, A. K., Brown, B. D., Brody, J., Ginhoux, F. & Merad, M. Expansion and activation of $CD103^+$ dendritic cell progenitors at the tumor site enhances tumor responses to therapeutic PD-L1 and BRAF inhibition. *Immunity* **44**, 924–938 (2016).

72. Laoui, D., Keirsse, J., Morias, Y., Van Overmeire, E., Geeraerts, X., Elkrim, Y., Kiss, M., Bolli, E., Lahmar, Q., Sichien, D., Serneels, J., Scott, C. L., Boon, Louis De Baetselier, P., Mazzone, M., Guilliams, M. & Van Ginderachter, J. A. The tumour microenvironment harbours ontogenically distinct dendritic cell populations with opposing effects on tumour immunity. *Nature Communications* **7**, 1–17 (2016).

73. Broz, M., Binnewies, M., Boldajipour, B., Nelson, A., Pollock, J., Erle, D., Barczak, A., Rosenblum, M., Daud, A., Barber, D., Amigorena, S., Veer, L. J. van't, Sperling, A., Wolf, D. & Krummel, M. F. Dissecting the Tumor Myeloid Compartment Reveals Rare Activating Antigen Presenting Cells, Critical for T cell Immunity. *Cancer Cell* **26**, 638–652 (2014).

74. Guilliams, M., Crozat, K., Henri, S., Tamoutounour, S., Grenot, P., Devilard, E., Alexopoulou, L., Dalod, M. & Malissen, B. Skin-draining lymph nodes contain dermis-derived $CD103^-$ dendritic cells that constitutively produce retinoic acid and induce $Foxp3^+$ regulatory T cells. *Blood* **115**, 1958–1968 (2010).

75. Idoyaga, J., Fiorese, C., Zbytnuik, L., Lubkin, A., Miller, J., Malissen, B., Mucida, D., Merad, M. & Steinman, R. M. Specialized role of migratory dendritic cells in peripheral tolerance induction. *The Journal of Clinical Investigation* **123**, 1–11 (2013).

76. Perrot, I., Blanchard, D., Freymond, N., Isaac, S., Guibert, B., Pachéco, Y., Perrot, I., Blanchard, D. & Lebecque, S. Dendritic Cells Infiltrating Human Non-Small Cell Lung Cancer Are Blocked at Immature Stage. *The Journal of Immunology* **178**, 2763–2769 (2007).

77. Bekeredjian-ding, I., Hartmann, E., Parcina, M., Giese, T., Wollenberg, B. & Hatmann, G. Identification and Functional Analysis of Tumor-Infiltrating Plasmacytoid Dendritic Cells in Head and Neck Cancer. *Cancer Research* **63**, 6478–6487 (2003).

78. Vermi, W., Bonecchi, R., Facchetti, F., Bianchi, D., Sozzani, S., Festa, S., Berenzi, A., Cella, M. & Colonna, M. Recruitment of immature plasmacytoid dendritic cells (plasmacytoid monocytes) and myeloid dendritic cells in primary cutaneous melanomas. *Journal of Pathology* **200**, 255–268 (2003).

79. Zou, W., Machelon, V., Coulomb-L'Hermin, A., Borvak, J., Nome, F., Isaeva, T., Wei, S., Krzysiek, R., Durand-Gasselin, I., Gordon, A., Pustilnik, T., Curiel, D. T., Galanaud, P., Capron, F., Emilie, D. & Curiel, T. J. Stromal-derived factor-1 in human tumors recruits and alters the function of plasmacytoid precursor dendritic cells. *Nature Medicine* **7**, 1339–1346 (2001).

80. Menetrier-caux, C., Montmain, G., Dieu, M. C., Bain, C., Favrot, M. C., Caux, C. & Blay, J. Y. Inhibition of the Differentiation of Dendritic Cells From $CD34^+$ Progenitors by Tumor Cells: Role of Interleukin-6 and Macrophage Colony-Stimulating Factor. *Blood* **92**, 4778–4791 (1998).

81. Liu, Y. & Zeng, G. Cancer and Innate Immune System Interactions: Translational Potentials for Cancer Immunotherapy. *Journal of Immunotherapy* **35**, 299–308 (2012).

82. Ghirelli, C., Reyal, F., Jeanmougin, M., Zollinger, R., Sirven, P., Michea, P., Caux, C., Bendriss-Vermare, N., Donnadieu, M. H., Caly, M., Fourchotte, V., Vincent-Salomon, A.,

Sigal-Zafrani, B., Sastre-Garau, X. & Soumelis, V. Breast Cancer Cell-Derived GM-CSF Licenses Regulatory Th2 Induction by Plasmacytoid Predendritic Cells in Aggressive Disease Subtypes. *Cancer Research* **75**, 2775–2787 (2015).

83. Ito, T., Yang, M., Wang, Y., Lande, R., Gregorio, J., Perng, O. A., Qin, X., Liu, Y. & Gilliet, M. Plasmacytoid dendritic cells prime IL-10-producing T regulatory cells by inducible costimulator ligand. *JEM* **204**, 105–115 (2007).

84. Vollmer, A., Blackwell, S. E., Maier, J., Sontheimer, K., Beyer, T., Mandel, B., Lunov, O., Tron, K., Nienhaus, G. U., Simmet, T., Debatin, K., Weiner, G. J. & Fabricius, D. Granzyme B produced by human plasmacytoid dendritic cells suppresses T-cell expansion. *Blood* **115**, 1156–1166 (2010).

85. Munn, D. H., Koni, P. A., Mellor, A. L., Sharma, M. D., Hou, D. & Baban, B. Expression of indoleamine 2,3-dioxygenase by plasmacytoid dendritic cells in tumor-draining lymph nodes. *The Journal of Clinical Investigation* **114**, 280–290 (2004).

86. Aspord, C., Leccia, M. T., Charles, J. & Plumas, J. Plasmacytoid Dendritic Cells Support Melanoma Progression by Promoting Th2 and Regulatory Immunity through OX40L and ICOSL. *Cancer Immunology Research* **1**, 402–415 (2013).

87. Chevolet, I., Speeckaert, R., Schreuer, M., Neyns, B., Krysko, O., Bachert, C., Hennart, B., Allorge, D., van Geel, N., van Gele, M.& Brochez, L. Characterization of the *in vivo* immune network of IDO, tryptophan metabolism, PD-L1, and CTLA-4 in circulating immune cells in melanoma. *OncoImmunology* **4**, 1–8 (2015).

88. Sisirak, V., Vey, N., Goutagny, N., Renaudineau, S., Malfroy, M., Thys, S., Treilleux, I., Labidi-Galy, S. I., Bachelot, T., Dezutter-Dambuyant, C., Ménétrier-Caux, C., Blay, J. Y., Caux, C. & Bendriss-Vermare, N. Breast cancer-derived transforming growth factor-β and tumor necrosis factor-α compromise interferon-α production by tumor-associated plasmacytoid dendritic cells. *International Journal of Cancer* **133**, 771–779 (2013).

89. Beckebaum, S., Zhang, X., Chen, X., Yu, Z., Frilling, A., Dworacki, G., Grosse-Wilde, H., Broelsch, C. E., Gerken, G. & Cicinnati, V. R. Increased Levels of Interleukin-10 in Serum from Patients with Hepatocellular Carcinoma Correlate with Profound Numerical Deficiencies and Immature Phenotype of Circulating Dendritic Cell Subsets. *Clinical Cancer Research* **10**, 7260–7269 (2004).

90. Bekeredjian-ding, I., Hartmann, E., Parcina, M., Giese, T., Wollenberg, B. & Hatmann, G. Tumour-derived prostaglandin E2 and transforming growth factor-β synergize to inhibit plasmacytoid dendritic cell-derived interferon-α. *Immunology* **128**, 439–450 (2009).

91. Ray, A., Das, DS., Song, Y., Macri, V., Richardson, P., Brooks, CL., Chauhan, D. & Anderson, KC. A novel agent SL-401 induces anti-myeloma activity by targeting plasmacytoid dendritic cells, osteoclastogenesis and cancer stem-like cells. *Leukemia* **31**, 2652–2660 (2017).

92. Coukos, G., Benencia, F., Buckanovich, R. J. & Conejo-garcia, J. R. The role of dendritic cell precursors in tumour vasculogenesis. **2**, 1182–1187 (2005).

93. Labidi-Galy, S. I., Sisirak, V., Meeus, P., Gobert, M., Treilleux, I., Bajard, A., Combes, J. D., Faget, J., Mithieux, F., Cassignol, A., Tredan, O., Durand, I., Ménétrier-Caux, C., Caux, C., Blay, J. Y., Ray-Coquard, I. & Bendriss-Vermare, N. Quantitative and Functional Alterations of Plasmacytoid Dendritic Cells Contribute to Immune Tolerance in Ovarian Cancer. *Cancer Research* **71**, 5423–5434 (2011).

94. Sallusto, F. & Lanzavecchia, A. The instructive role of dendritic cells on T-cell responses. 127–132 (2002).

95. Melhaoui, S., Melhaoui, S., Maenhout, S. K. & Locy, H. Dendritic Cells: The Tools for Cancer Treatment. 100–128

96. Merad, M., Sathe, P., Helft, J., Miller, J. & Mortha, A. The Dendritic Cell Lineage: Ontogeny

and Function of Dendritic Cells and Their Subsets in the Steady State and the Inflamed Setting. *Annu Rev Immunol.* **31**, 1–48 (2013).

97. Garg, A. D., Coulie, P. G., Van den Eynde, B. J. & Agostinis, P. Integrating Next-Generation Dendritic Cell Vaccines into the Current Cancer Immunotherapy Landscape. *Trends in Immunology* **38**, 577–593 (2017).

98. Saxena, M. & Bhardwaj, N. Re-Emergence of Dendritic Cell Vaccines for Cancer Treatment. *Trends in Cancer* **4**, 119–137 (2018).

99. Salio, M., Palmowski, M. J., Atzberger, A. & Hermans, I. F. CpG-matured Murine Plasmacytoid Dendritic Cells Are Capable of *In Vivo* Priming of Functional CD8 T Cell Responses to Endogenous but Not Exogenous Antigens. *J. Exp. Med.* **199**, 567–579 (2004).

100. Dey, M. *et al.* Dendritic Cell Based Vaccines that Utilize Myeloid Rather than Plasmacytoid Cells Offer a Superior Survival Advantage in Malignant Glioma. *J Immunol* **195**, 367–376 (2015).

101. Saito, T., Takayama, T., Osaki, T., Nagai, S., Suzuki, T., Sato, M., Kuwano, H. & Tahara, H. Combined mobilization and stimulation of tumor-infiltrating dendritic cells and natural killer cells with Flt3 ligand and IL-18 in vivo induces systemic antitumor immunity. *Cancer Science* **99**, 2028–2036 (2008).

102. Vasquez, M., Sanchez-arraez, A., Teijeira, A. & Melero, I. Cellular immunotherapies for cancer. *Oncoimmunology* **6**, 1–5 (2017).

103. Hatipoglu, I. & Acker, H. H. Van. Human blood myeloid and plasmacytoid dendritic cells cross activate each other and synergize in inducing NK cell cytotoxicity. *Oncoimmunology* **5**, 1–12 (2016).

104. Lou, Y., Liu, C., Kim, G. J., Liu, Y., Hwu, P. & Wang, G. Plasmacytoid Dendritic Cells Synergize with Myeloid Dendritic Cells in the Induction of Antigen-Specific Antitumor Immune Responses. *J Immunol* **178**, 1534–1541 (2007).

105. Brewitz, A., Eickhoff, S., Dähling, S., Quast, T., Bedoui, S., Kroczek, R.A., Kurts, C., Garbi, N., Barchet, W., Iannacone, M., Klauschen, F., Kolanus, W., Kaisho, T., Colonna, M., Germain, R. N. & Kastenmüller, W. $CD8^+$ T cells orchestrate pDC-$XCR1^+$ dendritic cell spatial and functional cooperativity to optimize priming. *Immunity* **46**, 205–219 (2017).

106. Piccioli, D., Sammicheli, C., Tavarini, S., Nuti, S., Frigimelica, E., Manetti, A. G. O., Nuccitelli, A., Aprea, S., Valentini, S., Borgogni, E., Wack, A. & Valiante, N. M. Human plasmacytoid dendritic cells are unresponsive to bacterial stimulation and require a novel type of cooperation with myeloid dendritic cells for maturation. *Blood* **113**, 4232–4240 (2009).

107. Saxena, M. & Bhardwaj, N. Turbocharging Vaccines: Emerging Adjuvants for Dendritic Cell Based Therapeutic Cancer Vaccines. *Curr Opin Immunol* **47**, 35–43 (2017).

108. Rehman, H., Silk, A. W., Kane, M. P. & Kaufman, H. L. Into the clinic: Talimogene laherparepvec (T-VEC), a first-in-class intratumoral oncolytic viral therapy. *Journal for ImmunoTherapy of Cancer* **4**, 1–8 (2016).

109. Galluzzi, L., Buqué, A., Kepp, O., Zitvogel, L. & Kroemer, G. Immunogenic cell death in cancer and infectious disease. *Nature Reviews Immunology* **17**, 97–111 (2017).

110. Jongbloed, S. L., Kassianos, A. J., McDonald, K. J., Clark, G. J., Ju, X., Angel, C. E., Chen, C. J. J., Dunbar, P. R., Wadley, R. B., Jeet, V., Vulink, A. J.E., Hart, D. N.J. & Radford, K. J. Human $CD141^+$ $(BDCA\text{-}3)^+$ dendritic cells (DCs) represent a unique myeloid DC subset that cross-presents necrotic cell antigens. *Journal of Experimental Medicine* **207**, 1247–1260 (2010).

111. Sánchez-Paulete, A. R., Cueto, F. J., Martínez-López, M., Labiano, S., Morales-Kastresana, A., Rodríguez-Ruiz, M. E., Jure-Kunkel, M., Azpilikueta, A., Aznar, M. A., Quetglas, J. I.,

Sancho, D. & Melero, I. Cancer immunotherapy with immunomodulatory anti-CD137 and anti–PD-1 monoclonal antibodies requires BATF3-dependent dendritic cells. *Cancer Discovery* **6**, 71–79 (2016).

112. Dummer, R., Urosevic, M., Kempf, W., Hoek, K., Hafner, J. & Burg, G. Imiquimod in basal cell carcinoma: how does it work? *British Journal of Dermatology* **149**, 57–58 (2003).

113. Wuest, M., Dummer, R. & Urosevic, M. Induction of the members of Notch pathway in superficial basal cell carcinomas treated with imiquimod. *Arch Dermatol Res* **299**, 493–498 (2007).

114. Hofmann, M. A., Kors, C., Audring, H., Walden, P., Sterry, W. & Trefzer, U. Phase 1 Evaluation of Intralesionally Injected TLR9-agonist PF-3512676 in Patients With Basal Cell Carcinoma or Metastatic Melanoma. *Journal of Immunotherapy* **31**, 520–527 (2008).

115. Chauhan, D., Singh, A. V., Brahmandam, M., Carrasco, R., Bandi, M., Hideshima, T., Bianchi, G., Podar, K., Tai, Y., Mitsiades, C., Raje, N., Jaye, D. L., Kumar, S. K., Richardson, P., Munshi, N. & Anderson, K. C. Functional Interaction of Plasmacytoid Dendritic Cells with Multiple Myeloma Cells: A Therapeutic Target. *Cancer Cell* **16**, 309–323 (2009).

116. Liu, C., Wang, G., Hwu, P., Liu, C., Lou, Y., Lizée, G., Qin, H., Liu, S., Rabinovich, B., Liu, Y., Wang, G. & Hwu, P. Plasmacytoid dendritic cells induce NK cell-dependent, tumor antigen-specific T cell cross-priming and tumor regression in mice. *The Journal of Clinical Investigation* **118**, 1165–1175 (2008).

117. Cao, W., Bover, L., Cho, M., Wen, X., Hanabuchi, S., Bao, M., Rosen, D. B., Wang, Y., Shaw, J. L., Du, Q., Li, C., Arai, N., Yao, Z., Lanier, L. L. & Liu, Y. Regulation of TLR7/9 responses in plasmacytoid dendritic cells by BST2 and ILT7 receptor interaction. *JEM* **206**, 1603–1614 (2009).

118. Von Bubnoff, D., Scheler, M., Wilms, H., Fimmers, R. & Bieber, T. Identification of IDO-Positive and IDO-Negative Human Dendritic Cells after Activation by Various Proinflammatory Stimuli. *The Journal of Immunology* **186**, 6701–6709 (2011).

119. Manches, O., Munn, D., Fallahi, A., Lifson, J., Chaperot, L., Plumas, J. & Bhardwaj, N. HIV-activated human plasmacytoid DCs induce Tregs through an indoleamine 2,3-dioxygenase-dependent mechanism. *The Journal of Clinical Investigation* **118**, 3431–3439 (2008).

120. Ito, H., Ando, T., Arioka, Y., Saito, K. & Seishima, M. Inhibition of indoleamine 2,3-dioxygenase activity enhances the anti-tumour effects of a Toll-like receptor 7 agonist in an established cancer model. *Immunology* **144**, 621–630 (2015).

121. Yamahira, A., Narita, M., Iwabuchi, M., Uchiyama, T., Iwaya, S., Ohiwa, R. I. E., Nishizawa, Y., Suzuki, T. & Yokoyama, Y. Activation of the Leukemia Plasmacytoid Dendritic Cell Line PMDC05 by Toho-1, a Novel IDO Inhibitor. *Anticancer Research* **34**, 4021–4028 (2014).

122. Rodríguez, Y. D., Cordeiro, P. & Belounis, A. *In vitro* differentiated plasmacytoid dendritic cells as a tool to induce anti-leukemia activity of natural killer cells. *Cancer Immunology, Immunotherapy* **66**, 1307–1320 (2017).

123. O'Neill, L. A. J., Kishton, R. J. & Rathmell, J. A guide to immunometabolism for immunologists. *Nat Rev Immunol.* **16**, 553–565 (2016).

124. Wculek, S. K., Khouili, S. C., Priego, E., Heras-Murillo, I. & Sancho, D. Metabolic Control of Dendritic Cell Functions: Digesting Information. *Frontiers in immunology* **10**, 1–20 (2019).

125. R, Kratchmarov, S, Viragova, MJ, Kim, NJ, Rothman, K, Liu, B, Reizis & SL, Reiner Metabolic control of cell fate bifurcations in a hematopoietic progenitor population. *Immunol Cell Biol* **96**, 863–871 (2018).

126. Everts, B., Amiel, E., Huang, S. C., Smith, A. M., Chang, C., Lam, W. Y., Redmann, V., Freitas, T. C., Blagih, J., Windt, G. J. W., Artyomov, M. N., Jones, R. G., Pearce, E. L. &

Pearce, E. J. TLR-driven early glycolytic reprogramming via the kinases TBK1-IKKε supports the anabolic demands of dendritic cell activation. *Nat Immunol.* **15**, 323–332 (2014).

127. Basit, F., Mathan, T., Sancho, D. & De Vries, J. M. Human dendritic cell subsets undergo distinct metabolic reprogramming for immune response. *Frontiers in Immunology* **9**, 1–17 (2018).

128. Du, X., Wen, J., Wang, Y., Karmaus, P., Khatamian, A., Tan, H., Li, Y., Guy, C., Nguyen, T. M., Dhungana, Y., Neale, G., Peng, J., Yu, J. & Chi, H. Hippo/Mst signaling couples metabolic state and immune function of CD8α+ dendritic cells. *Nature* **558**, 141–145 (2018).

129. Buck, M. D., Sowell, R. T., Kaech, S. M. & Pearce, E. L. Metabolic Instruction of Immunity. *Cell* **169**, 570–586 (2017).

130. Guak, H., Al Habyan, S., Ma, E. H., Aldossary, H., Al-Masri, M., Won, S. Y., Ying, T., Fixman, E. D., Jones, R. G., McCaffrey, L. M. & Krawczyk, C. M. Glycolytic metabolism is essential for CCR7 oligomerization and dendritic cell migration. *Nature Communications* **9**, 1–12 (2018).

131. Song, M., Sandoval, T. A., Chae, C., Chopra, S., Rutkowski, M. R., Raundhal, M., Chaurio, R. A., Payne, K. K., Konrad, C., Bettigole, S. E., Shin, H. R., Crowley, M. J. P., Juan, P., Conejo-garcia, J. R., Glimcher, L. H. & Cubillos-Ruiz, J. R. IRE1α-XBP1 controls T cell function in ovarian cancer by regulating mitochondrial activity. *Nature* **562**, 423–428 (2018).

132. Kelly, B. & Neill, L. A. J. O. Metabolic reprogramming in macrophages and dendritic cells in innate immunity. *Cell Research* **25**, 771–784 (2015).

133. Cross, J. R., DeBerardinis, R. J., Krawczyk, C. M., Thompson, C. B., Sun, J., Holowka, T., Amiel, E., Jung, E., Pearce, E. J., Blagih, J. & Jones, R. G. Toll-like receptor-induced changes in glycolytic metabolism regulate dendritic cell activation. *Blood* **115**, 4742–4749 (2010).

134. Du, X., Chapman, N. M. & Chi, H. Emerging roles of cellular metabolism in regulating dendritic cell subsets and function. *Frontiers in Cell and Developmental Biology* **6**, 1–8 (2018).

135. Pantel, A., Teixeira, A., Haddad, E., Wood, E. G., Steinman, R. M. & Longhi, M. P. Direct Type I IFN but Not MDA5/TLR3 Activation of Dendritic Cells Is Required for Maturation and Metabolic Shift to Glycolysis after Poly IC Stimulation. *PLoS Biology* **12**, 1–11 (2014).

136. Cross, J. R., DeBerardinis, R. J., Krawczyk, C. M., Thompson, C. B., Sun, J., Holowka, T., Amiel, E., Jung, E., Pearce, E. J., Blagih, J. & Jones, R. G. Toll-like receptor-induced changes in glycolytic metabolism regulate dendritic cell activation. *Blood* **115**, 4742–4749 (2010).

137. Waickman, A. T. & Powell, J. D. mTOR, metabolism, and the regulation of T-cell differentiation and function. *Immunological Reviews* **249**, 43–58 (2012).

138. LA, O. & DG, H. Metabolism of inflammation limited by AMPK and pseudo-starvation. *Nature* **493**, 346–355 (2013).

139. Williams, N. C. & O'Neill, L. A. J. A Role for the Krebs Cycle Intermediate Citrate in Metabolic Reprogramming in Innate Immunity and Inflammation. *Frontiers in Immunology* **9**, 1–11 (2018).

140. Ryan, D. G. & O'Neill, L. A. J. Krebs cycle rewired for macrophage and dendritic cell effector functions. *FEBS Letters* **591**, 2992–3006 (2017).

141. Rubic, T., Lametschwandtner, G., Jost, S., Hinteregger, S., Kund, J., Carballido-Perrig, N., Schwärzler, C., Junt, T., Voshol, H., Meingassner, J. G., Mao, X., Werner, G., Rot, A. & Carballido, J. M. Triggering the succinate receptor GPR91 on dendritic cells enhances immunity. *Nature Immunology* **9**, 1261–1269 (2008).

142. Bajwa, G., DeBerardinis, R. J., Shao, B., Hall, B., Farrar, J. D. & Gill, M. A. Critical Role of Glycolysis in Human Plasmacytoid Dendritic Cell Antiviral Responses Gagan. *J Immunol.* **196**, 2004–2009 (2015).

143. Wang, F., Zhang, S., Vuckovic, I., Jeon, R., Lerman, A., Folmes, C. D., Dzeja, P. P. & Herrmann, J. Glycolytic Stimulation Is Not a Requirement for M2 Macrophage Differentiation. *Cell Metabolism* **28**, 463–475 (2018).

144. Kužnik, A., Benčina, M., Švajger, U., Jeras, M., Rozman, B. & Jerala, R. Mechanism of Endosomal TLR Inhibition by Antimalarial Drugs and Imidazoquinolines. *The Journal of Immunology* **186**, 4794–4804 (2011).

145. Wu, D., Sanin, D. E., Everts, B., Chen, Q., Qiu, J., Michael, D., Patterson, A., Smith, A. M., Chang, C., Liu, Z., Maxim, N., Pearce, E. L., Cella, M. & Pearce, E. J. Type 1 interferons induce changes in core metabolism that are critical for immune function. *Immunity* **44**, 1325–1336 (2016).

146. Pearce, E. J. & Everts, B. Dendritic cell metabolism. *Nat Rev Immunol* **15**, 18–29 (2015).

147. Sim, W. J., Ahl, P. J. & Connolly, J. E. Metabolism Is Central to Tolerogenic Dendritic Cell Function. *Mediators of Inflammation* **2016**, 1–10 (2016).

148. Munn, D. H. & Mellor, A. L. IDO in the Tumor Microenvironment: Inflammation, Counter-regulation and Tolerance. *Trends Immunol.* **37**, 193–207 (2016).

149. Zhao, F., Xiao, C., Evans, K. S., Theivanthiran, T., DeVito, N., Holtzhausen, A., Liu, J., Liu, X., Boczkowski, D., Nair, S., Locasale, J. W. & Hanks, B. A. Paracrine Wnt5a-β-catenin Signaling Triggers a Metabolic Program That Drives Dendritic Cell Tolerization. *Immunity* **48**, 147–160 (2018).

150. Routy, J. P., Routy, B., Graziani, G. M. & Mehraj, V. The Kynurenine Pathway is a Double-Edged Sword in Immune-Privileged Sites and in Cancer: Implications for Immunotherapy. *International Journal of Tryptophan Research* **9**, 67–77 (2016).

151. Li, Q., Harden, J. L., Anderson, C. D. & Egilmez, N. K. Tolerogenic Phenotype of IFN-γ–Induced IDO^+ Dendritic Cells Is Maintained via an Autocrine IDO–Kynurenine/AhR–IDO Loop. *The Journal of Immunology* **197**, 962–970 (2016).

152. Belladonna, M. L., Orabona, C., Grohmann, U. & Puccetti, P. TGF-β and kynurenines as the key to infectious tolerance. *Trends in Molecular Medicine* **15**, 41–49 (2009).

153. Rodriguez, P. C., Ochoa, A. C. & Al-Khami, A. A. Arginine Metabolism in Myeloid Cells Shapes Innate and Adaptive Immunity. *Frontiers in Immunology* **8**, 1–12 (2017).

154. Casero, R. A. & Marton, L. J. Targeting polyamine metabolism and function in cancer and other hyperproliferative diseases. *Nature Reviews Drug Discovery* **6**, 373–390 (2007).

155. Mondanelli, G., Bianchi, R., Pallotta, M. T., Orabona, C., Albini, E., Iacono, A., Belladonna, M. L., Vacca, C., Fallarino, F., Macchiarulo, A., Ugel, S., Bronte, V., Gevi, F., Zolla, L., Verhaar, A., Peppelenbosch, M., Mazza, E. M. C., Bicciato, S., Laouar, Y., Santambrogio, L., Puccetti, P., Volpi, C. & Grohmann, U. A Relay Pathway between Arginine and Tryptophan Metabolism Confers Immunosuppressive Properties on Dendritic Cells. *Immunity* **46**, 233–244 (2017).

156. Kim, S. H., Roszik, J., Grimm, E. A. & Ekmekcioglu, S. Impact of L-Arginine Metabolism on Immune Response and Anticancer Immunotherapy. *Frontiers in Oncology* **8**, 1–5 (2018).

157. Norian, L. A., Rodrigues, P. C., O´Mara, L. A., Zabaleta, J., Ochoa, A. C., Cella, M. -& Allen, P. M. Tumor-infiltrating regulatory dendritic cells inhibit $CD8^+$ T cell function via L-arginine metabolism. *Cancer Res* **69**, 3086–3094 (2009).

158. Friberg, M., Jennings, R., Alsarraj, M., Dessureault, S., Cantor, A., Extermann, M., Mellor, A. L., Munn, D. H. & Antonia, S. J. Indoleamine 2,3-dioxygenase contributes to tumor cell evasion of T cell-mediated rejection. *International Journal of Cancer* **101**, 151–155 (2002).

159. Grohmann, U., Volpi, C., Fallarino, F., Bozza, S., Bianchi, R., Vacca, C., Orabona, C., Belladonna, M. L., Ayroldi, E., Nocentini, G., Boon, L., Bistoni, F., Fioretti, M. C., Romani, L.,

Riccardi, C. & Puccetti, P. Reverse signaling through GITR ligand enables dexamethasone to activate IDO in allergy. *Nature Medicine* **13**, 579–586 (2007).

160. Grohmann, U., Orabona, C., Fallarino, F., Vacca, C., Calcinaro, F., Falorni, A., Candeloro, P., Belladonna, M. L., Bianchi, R., Fioretti, M. C. & Puccetti, P. CTLA-4-Ig regulates tryptophan catabolism *in vivo*. *Nature Immunology* **3**, 1097–1101 (2002).

161. Fallarino, F., Grohmann, U., Hwang, K. W., Orabona, C., Vacca, C., Bianchi, R., Belladonna, M. L., Fioretti, M. C., Alegre, M. L. & Puccetti, P. Modulation of tryptophan catabolism by regulatory T cells. *Nature Immunology* **4**, 1206–1212 (2003).

162. Pallotta, M. T., Orabona, C., Volpi, C., Vacca, C., Belladonna, M. L., Bianchi, R., Servillo, G., Brunacci, C., Calvitti, M., Bicciato, S., Mazza, E. M.C., Boon, L., Grassi, F., Fioretti, M. C., Fallarino, F., Puccetti, P. & Grohmann, U. Indoleamine 2,3-dioxygenase is a signaling protein in long-term tolerance by dendritic cells. *Nature Immunology* **12**, 870–878 (2011).

163. Maroof, A., English, N. R., Bedford, P. A., Gabrilovich, D. I. & Knight, S. C. Developing dendritic cells become 'lacy' cells packed with fat and glycogen. *Immunology* **115**, 473–483 (2005).

164. Cubillos-Ruiz, J. R., Silberman, P. C., Rutkowski, M. R., Chopra, S., Perales-Puchalt, A., Song, M., Zhang, S., Bettigole, S. E., Gupta, D., Holcomb, K., Ellenson, L. H., Caputo, T., Lee, A. H., Conejo-Garcia, J. R. & Glimcher, L. H. ER Stress Sensor XBP1 Controls Anti-tumor Immunity by Disrupting Dendritic Cell Homeostasis. *Cell* **161**, 1527–1538 (2015).

165. Cubillos-Ruiz, J. R., Bettigole, S. E. & Glimcher, L. H. Tumorigenic and Immunosuppressive Effects of Endoplasmic Reticulum Stress in Cancer. *Cell* **168**, 692–706 (2017).

166. Schumann, T., Adhikary, T., Wortmann, A., Finkernagel, F., Lieber, S., Schnitzer, E., Legrand, N., Schober, Y., Nockher, W. A., Toth, P. M., Diederich, W. E., Nist, A., Stiewe, T., Wagner, U., Reinartz, S., Muller-Brusselbach, S. & Muller, R. Deregulation of PPARβ/δ target genes in tumor-associated macrophages by fatty acid ligands in the ovarian cancer microenvironment. *Oncotarget* **6**, 13416–13433 (2015).

167. Gardner, J. K., Mamotte, C. D. S., Patel, P., Yeoh, T. L., Jackaman, C. & Nelson, D. J. Mesothelioma Tumor Cells Modulate Dendritic Cell Lipid Content, Phenotype and Function. *PLoS ONE* **10**, 1–29 (2015).

168. Cao, W., Ramakrishnan, R., Tuyrin, V. A., Veglia, F., Condamine, T., Amoscato, A., Mohammadyani, D., Johnson, J. J., Zhang, L. M., Klein-Seetharaman, J., Celis, V. E. & Gabrilovich, D. I. Oxidized lipids block antigen cross-presentation by dendritic cells in cancer1 Oxidized lipids and DCs in cancer. *J Immunol.* **192**, 2920–2931 (2014).

169. Veglia, F., Tyurin, V. A., Mohammadyani, D., Blasi, M., Duperret, E. K., Donthireddy, L., Hashimoto, A., Kapralov, A., Amoscato, A., Angelini, R., Patel, S., Alicea-Torres, K., Weiner, D., Murphy, M. E., Klein-Seetharaman, J., Celis, E., Kagan, V. E. & Gabrilovich, D. I. Lipid bodies containing oxidatively truncated lipids block antigen cross-presentation by dendritic cells in cancer. *Nature Communications* **8**, 1–16 (2017).

170. Herber, D. L., Cao, W., Nefedova, Y., Novitskiy, S. V., Nagaraj, S., Tyurin, V. A., Corzo, A., Cho, H. I., Celis, E., Lennox, B., Stella, C., Padhya, T., Mccaffrey, T. V., Mccaffrey, J. C., Antonia, S., Fishman, M., Ferris, R. L., Kagan, V. E., Gabrilovich, D. I. Lipid accumulation and dendritic cell dysfunction in cancer. *Nat Med.* **16**, 880–886 (2010).

171. Bougnères, L., Helft, J., Tiwari, S., Vargas, P., Chang, B. H. J., Chan, L., Campisi, L., Lauvau, G., Hugues, S., Kumar, P., Kamphorst, A. O., Dumenil, A. M. L., Nussenzweig, M., MacMicking, J. D., Amigorena, S., Guermonprez, P. A Role for Lipid Bodies in the Cross-presentation of Phagocytosed Antigens by MHC Class I in Dendritic Cells. *Immunity* **31**, 232–244 (2009).

172. Ibrahim, J., Nguyen, A. H., Rehman, A., Ochi, A., Jamal, M., Graffeo, C. S., Henning, J. R., Zambirinis, C. P., Fallon, N. C., Barilla, R., Badar, S., Mitchell, A., Rao, R. S., Acehan, D.,

Frey, A. B. & Miller, G. Dendritic cell populations with different concentrations of lipid regulate tolerance and immunity in mouse and human liver. *Gastroenterology* **143**, 1061–1072 (2012).

173. Kratchmarov, R., Viragova, S., Kim, M. J., Rothman, N. J., Liu, K., Reizis, B. & Reiner, S. L. Metabolic control of cell fate bifurcations in a hematopoietic progenitor population. *Immunology and Cell Biology* **8**, 863–871 (2018).

174. Andrejeva, G. & Rathmell, J. C. Similarities and Distinctions of Cancer and Immune Metabolism in Inflammation and Tumors. *Cell Metab.* **26**, 49–70 (2017).

175. Márquez, S., Fernández, J. J., Terán-Cabanillas, E., Herrero, C., Alonso, S., Azogil, A., Montero, O., Iwawaki, T., Cubillos-Ruiz, J. R., Fernández, N. & Crespo, M. S. Endoplasmic Reticulum Stress Sensor IRE1α Enhances IL-23 Expression by Human Dendritic Cells. *Frontiers in Immunology* **8**, 1–19 (2017).

176. Hong, Y., Manoharan, I., Survawanshi, A., Majumdar, T., Angus-Hill, M. L., Koni, P. A., Manicassamy, B., Mellor, A. L., Munn, D. H. & Manicassamy, S. β-Catenin Promotes Regulatory T-cell Responses in Tumors by Inducing Vitamin a Metabolism in Dendritic Cells. *Cancer Research* **75**, 656–665 (2015).

177. Tong, D., Liu, Q., Wang, L. A., Xie, Q., Pang, J., Huang, Y., Wang, L., Liu, G., Zhang, D., Lan, W. & Jiang, J. The roles of the COX2/PGE2/EP axis in therapeutic resistance. *Cancer and Metastasis Reviews* **37**, 355–368 (2018).

178. Wang, D. & DuBois, R. N. Eicosanoids and cancer. *Nat Rev Cancer* **10**, 181–193 (2010).

179. Kalinski, P. Regulation of Immune Responses by Prostaglandin E2. *J Immunol.* **188**, 21–28 (2012).

180. Zelenay, S., Van Der Veen, A. G., Bottcher, J. P., Snelgrove, K. J., Rogers, N., Acton, S. E. Chakravarty, P., Girotti, M. R., Marais, R., Quezada, S. A., Sahai, E. & Reis E Sousa, C. Cyclooxygenase-Dependent Tumor Growth through Evasion of Immunity. *Cell* **162**, 1257–1270 (2015).

181. Oberkampf, M., Guillerev, C., Mouriès, J., Rosenbaum, P., Favolle, C., Bobard, A., Savina, A., Ogier-Denis, E., Enninga, J., Amigorena, S., Leclerc, C., Dadaglio, G. Mitochondrial reactive oxygen species regulate the induction of $CD8^+$ T cells by plasmacytoid dendritic cells. *Nature Communications* **9**, 1–14 (2018).

182. Nicholson, J. K., Lindon, J. C. & Holmes, E. 'Metabonomics': understanding the metabolic responses of living systems to pathophysiological stimuli via multivariate statistical analysis of biological NMR spectroscopic data. *Xenobiotica* **29**, 1181–1189 (1999).

183. Duarte, I. F., Lamego, I., Rocha, C. & Gil, A. M. NMR metabonomics for mammalian cell metabolism studies. *Bioanalysis* **1**, 1597–1614 (2009).

184. Griffin, J. L. & Shockcor, J. P. Metabolic profiles of cancer cells. *Nature Reviews Cancer* **4**, 551–561 (2004).

185. Merz, A. L. & Serkova, N. J. Use of nuclear magnetic resonance-based metabolomics in detecting drug resistance in cancer. *Biomark Med.* **3**, 289–306 (2009).

186. Gowda, G. A. N. & Raftery, D. Can NMR solve some significant challenges in metabolomics? *J Mag Reson.* **260**, 144–160 (2015).

187. Frédérich, M., Pirotte, B., Fillet, M. & Tullio, P. De. Metabolomics as a Challenging Approach for Medicinal Chemistry and Personalized Medicine. *Journal of Medicinal Chemistry* **59**, 8649–8666 (2016).

188. Fan, T. W. & Lane, A. N. Applications of NMR Spectroscopy to Systems Biochemistry. *Progress in Nuclear Magnetic Resonance Spectroscopy* 1–59 (2016).

189. Zhang, A., Sun, H., Wang, P., Hana, Y. & Wang, X. Modern analytical techniques in

metabolomics analysis. *Analyst* **137**, 293–300 (2012).

190. Alonso, A., Marsal, S. & Julià, A. Analytical methods in untargeted metabolomics: state of the art in 2015. *Frontiers in Bioengineering and Biotechnology* **3**, 1–20 (2015).

191. Xia, J., Broadhurst, D. I., Wilson, M. & Wishart, D. S. Translational biomarker discovery in clinical metabolomics: an introductory tutorial. *Metabolomics* **9**, 280–299 (2013).

192. Everts, B. Metabolomics in Immunology Research. *Methods in Molecular Biology* **1730**, 29–42 (2018).

193. Li, S., Park, Y., Duraisingham, S., Strobel, F. H., Khan, N., Soltow, O. A., Jones, D. P. & Pulendran, B. Predicting Network Activity from High Throughput Metabolomics. *PLoS Computational Biology* **9**, 1-11 (2013).

194. Ravindran, R., Khan, N., Nakaya, H. I, Li, S., Maddur, M. S., Park, Y., Jones, D. P., Chappert, P., Davoust, J., Weiss, D. S., Virgin, H. W., Ron, D. & Pulendran, B. Vaccine Activation of the Nutrient Sensor GCN2 in Dendritic Cells Enhances Antigen Presentation. *Science* **343**, 313–317 (2014).

195. Vanherwegen, A. S., Eelen, G., Ferreira, G. B., Ghesquière, B., Cook, D. P., Nikolic, T., Roep, B., Carmeliet, P., Telang, S., Mathieu, C., Gysemans, C. Vitamin D controls the capacity of human dendritic cells to induce functional regulatory T cells by regulation of glucose metabolism. *Journal of Steroid Biochemistry and Molecular Biology* **187**, 134–145 (2019).

196. Kostidis, S., Addie, R. D., Morreau, H., Mayboroda, O. A. & Giera, M. Quantitative NMR analysis of intra- and extracellular metabolism of mammalian cells: A tutorial. Anal. Chim. Acta 980, 1–24 (2017).

197. Conaway, R. C. Metabolic Regulation of Transcription and Chromatin. *Annual Review of Biochemistry* **87**, 23–25 (2018).

198. Wishart, D. S., Feunang, Y. D., Marcu, A., Guo, A. C., Liang, K., Vázquez-Fresno, R., Sajed, T., Johnson, D., Li, C., Karu, N., Saveeda, Z., Lo, E., Assempour, N., Berjanskii, M., Singhal, S., Arndt, D., Liang, Y., Badran, H., Grant, J., Serra-Cavuela, A., Liu, Y., Mandal, R., Neveu, V., Pon, A., Knox, C., Wilson, M., Manach, C. & Scalbert, A. HMDB 4.0: The human metabolome database for 2018. *Nucleic Acids Research* **46**, 608–617 (2018).

199. Weljie, A. M., Newton, J., Mercier, P., Carlson, E. & Slupsky, C. M. Targeted Profiling: Quantitative Analysis of ^{1}H-NMR Metabolomics Data. *Anal. Chem.* **78**, 4430–4442 (2006).

200. Amiel, E., Everts, B., Fritz, D., Beauchamp, S., Ge, B. & Erika, L. Mechanistic Target of Rapamycin Inhibition Extends Cellular Lifespan in Dendritic Cells by Preserving Mitochondrial Function. *J Immunol* **193**, 2821–2830 (2014).

201. Rehman, A., Hemmert, A., Ochi, A., Jamal, M., Henning, J. R., Rao, R. S., Greco, S., Deutsch, M. & Narayan, S. Role of Fatty-acid Synthesis in Dendritic Cell Generation and Function. *J Immunol* **190**, 4640–4649 (2013).

202. Balla T. Phosphoinositides: tiny lipids with giant impact on cell regulation. *Physiological reviews*, **93**, 1019–1137 (2013)

203. Jong, C. J., Azuma, J. & Schaffer, S. Mechanism underlying the antioxidant activity of taurine: Prevention of mitochondrial oxidant production. *Amino acids*. **42**. 2223-2232 (2011)

204. Salyer, A. C. D. & Davied, S. A. Transcriptomal signatures of vaccine adjuvants and accessory immunostimulation of sentinel cells by toll-like receptor 2/6 agonists. *Human Vaccines and Immunotherapeutics*. **0**. 1-11 (2018)

SUPPLEMENTARY INFORMATION

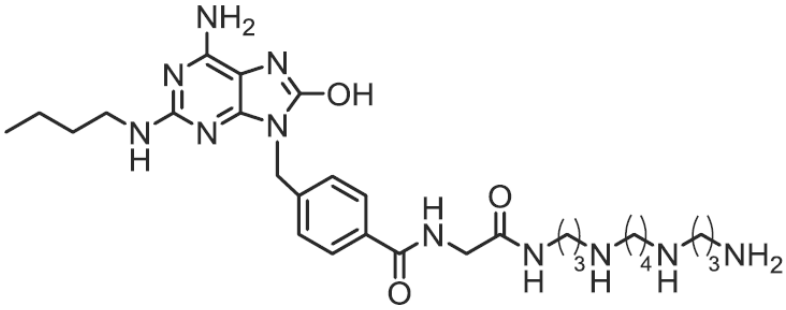

Figure S1 – Chemical Structure of CL307. Source: Salyer et al. (2018)[204].

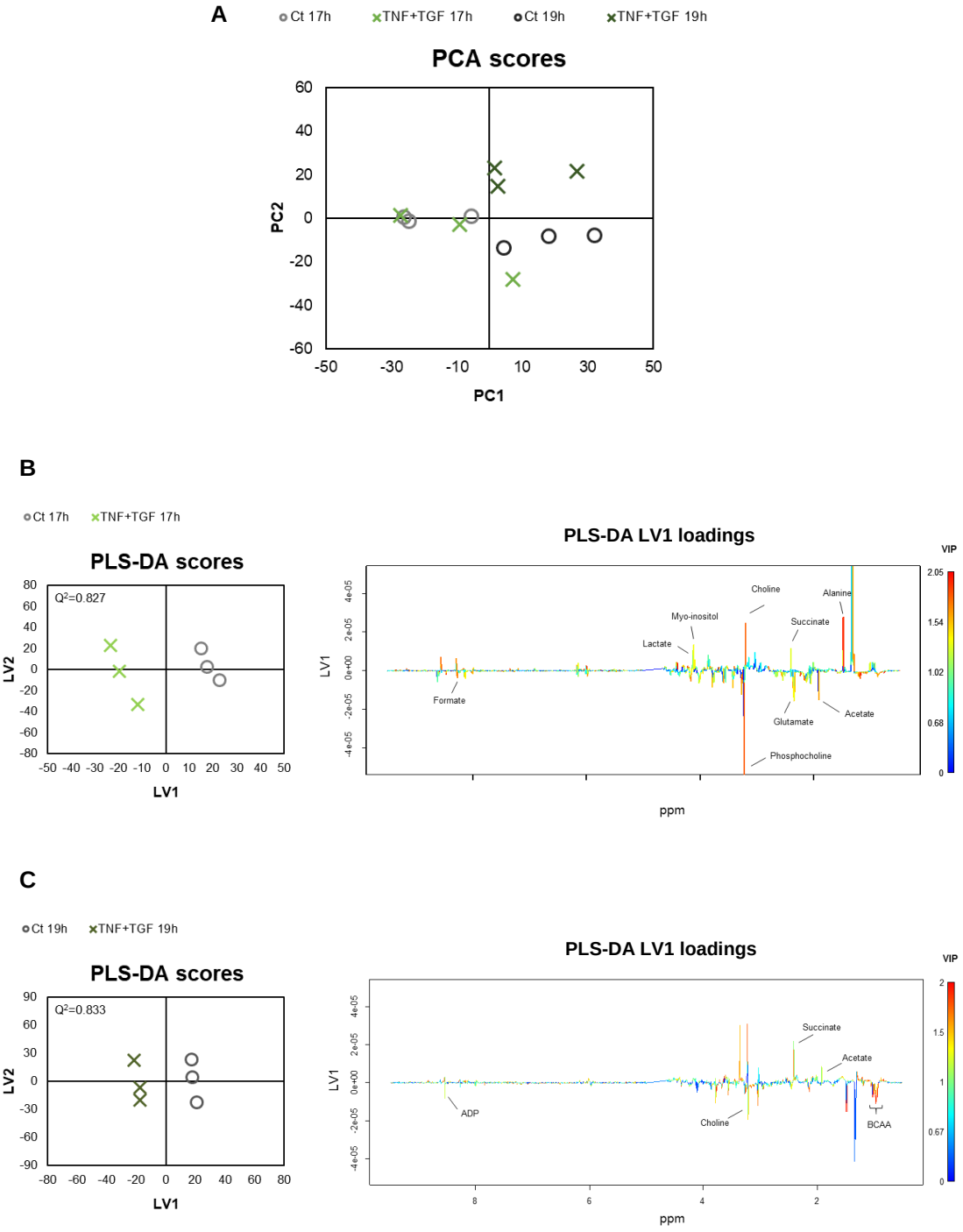

Figure S2 – Multivariate analysis of ^{1}H-NMR spectra from polar extracts of pDCs incubated with TNF-α and TGF-β for 17h and 19h: (A) PCA and (B) and (C) PLS-DA scores scatter plots and LV1 loadings w (right) colored according to variable importance to projection (VIP).

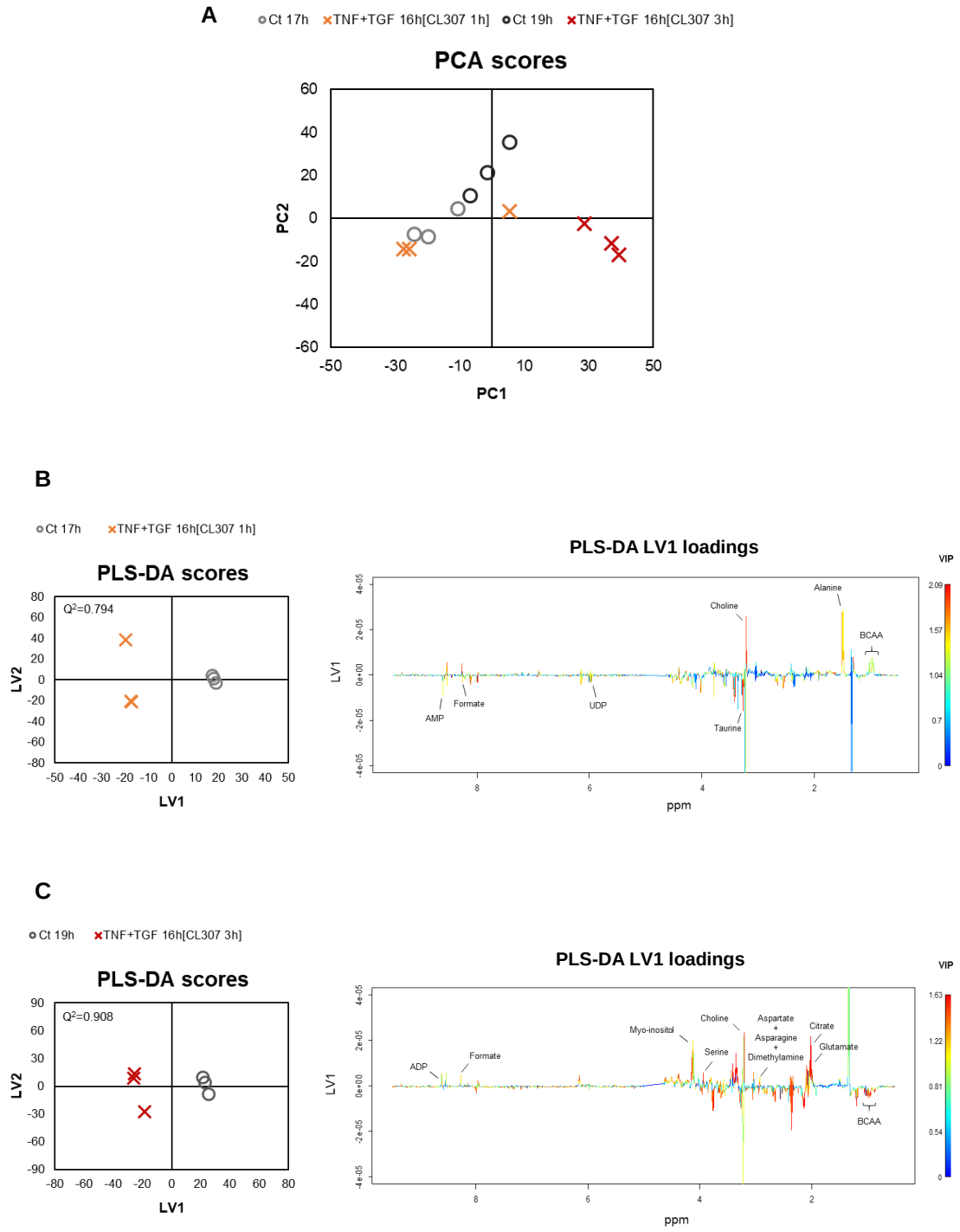

Figure S3 – Multivariate analysis of ^{1}H-NMR spectra from polar extracts of pDCs incubated with TNF-α and TGF-β and CL307 for 17h and 19h: (A) PCA and (B) and (C) PLS-DA scores scatter plots and LV1 loadings w (right) colored according to variable importance to projection (VIP).

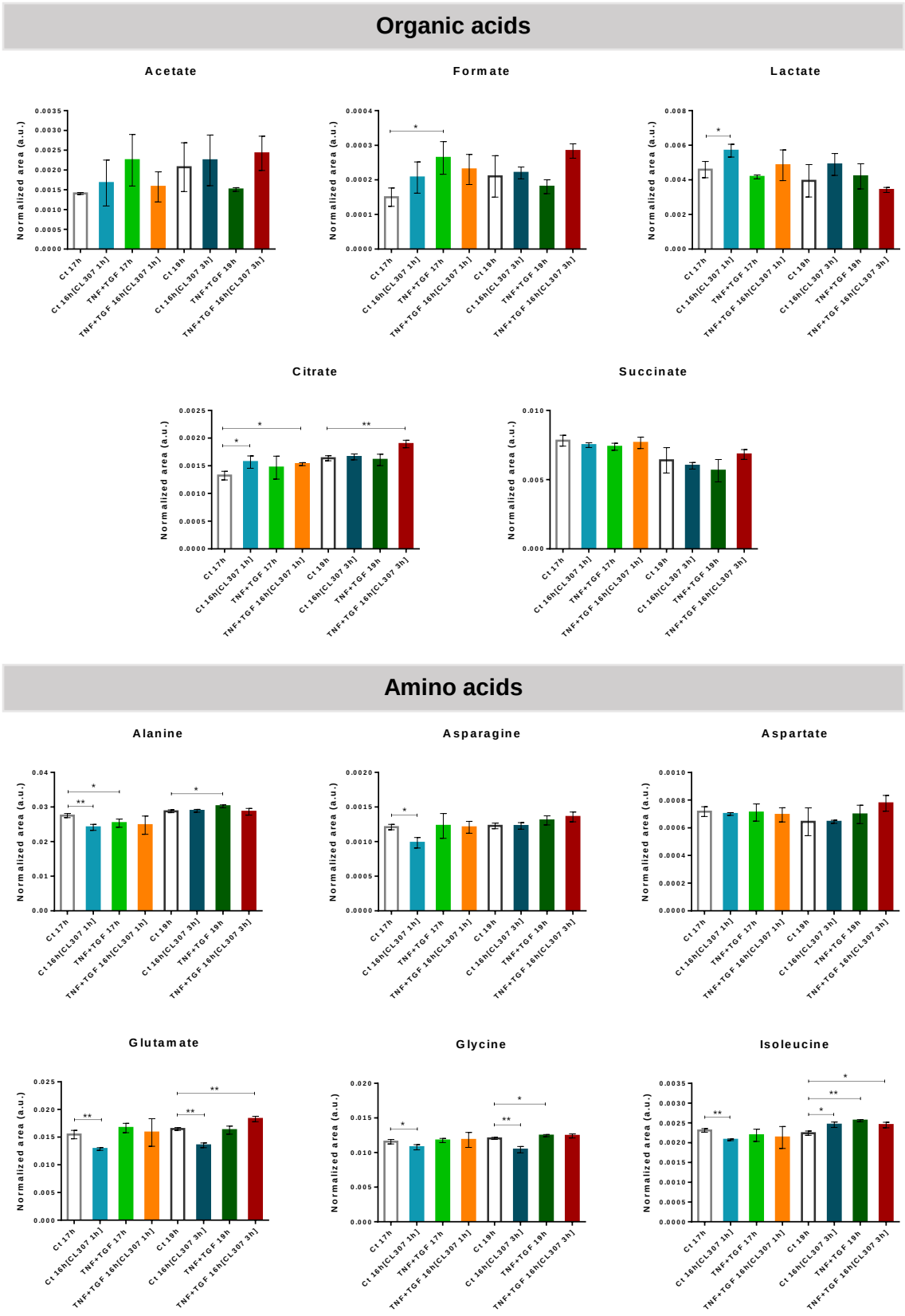

Figure S4 – Variations in intracellular metabolites in unstimulated pDCs (control groups) and pDCs incubated with TNF-α and TGF-β (16h) and/or stimulated with CL307 (1h and 3h). **p*-value < 0.05; ***p*-value < 0.01.

Amino acids (Cont.)

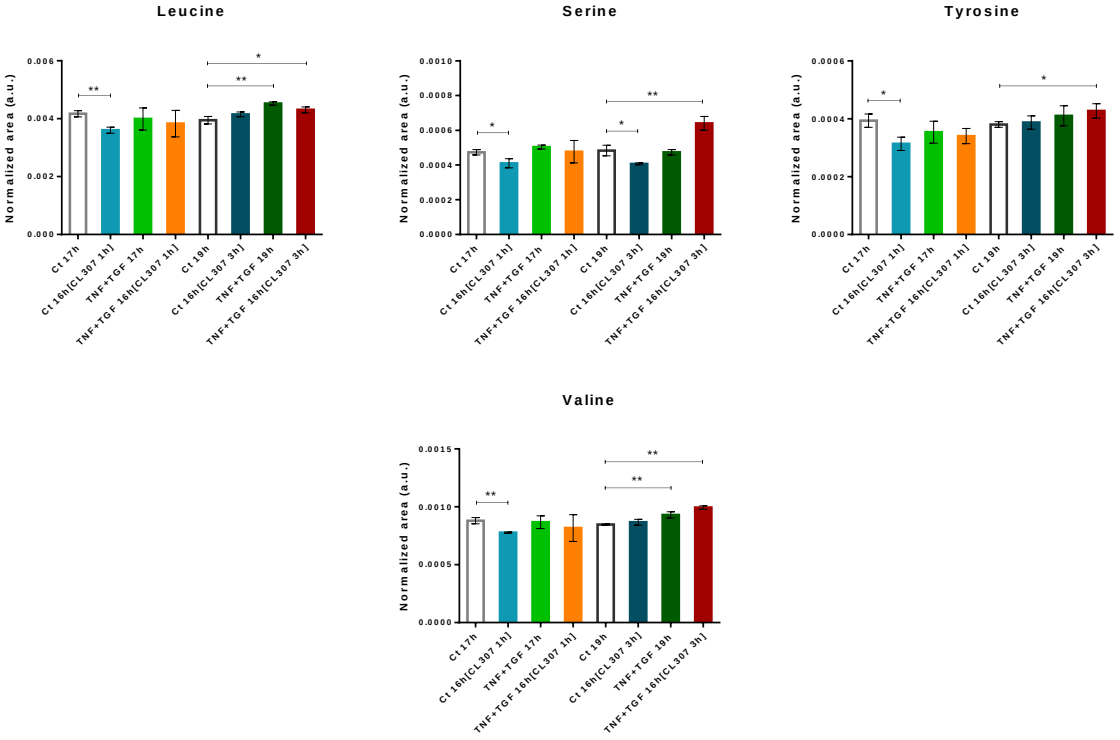

Choline compounds

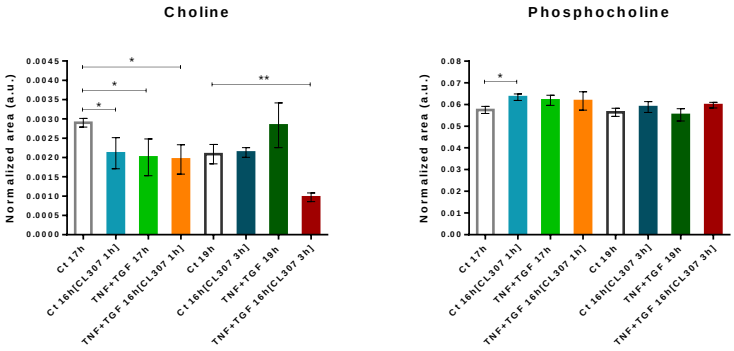

Nucleotides

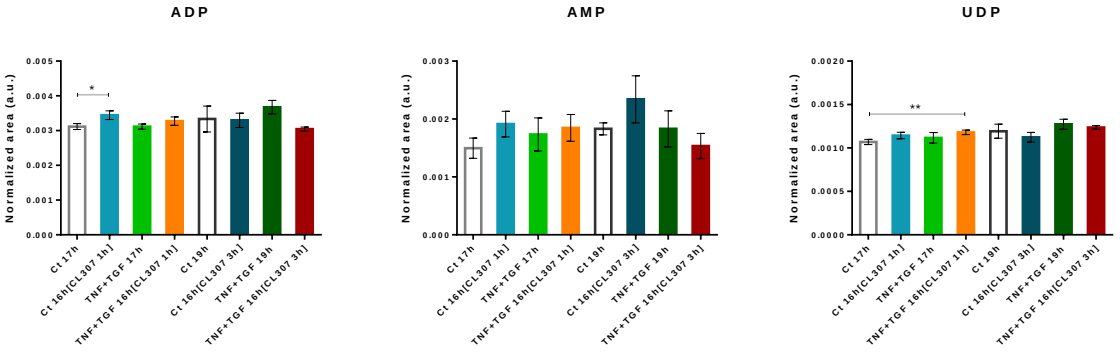

Figure S4 (Cont.)

Others

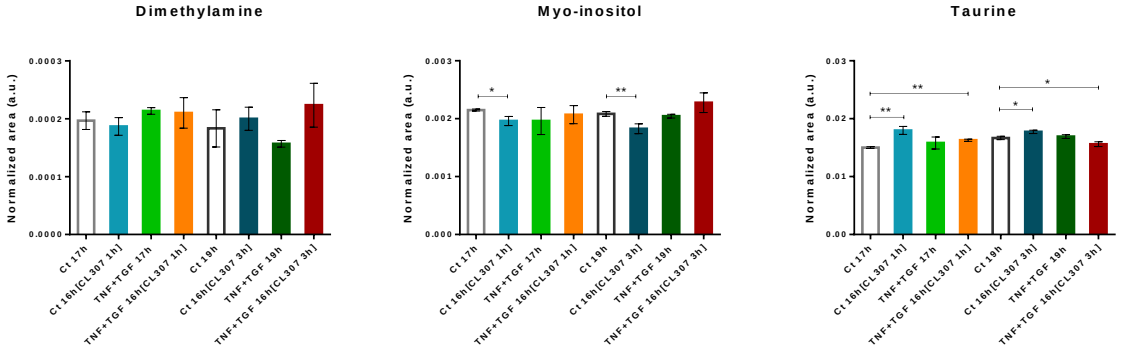

Figure S4 (Cont.)

Table S1 – Main metabolite variations in aqueous extracts of cells exposed to 1 and 2 µM of CL307 for 1, 3 and 6h, in relation to control cells, expressed as percentage of variation (%Var) and respective error (±), effect size (ES) and *p*-value. The variations with |ES| < 0.8 were not considered relevant.

Time		1h		3h		6h	
Conc. (µM)		CL307 1 µM	CL307 2 µM	CL307 1 µM	CL307 2 µM	CL307 1 µM	CL307 2 µM
Acetate	%Var	45.19	37.87	-41.62	-16.20	39.59	44.09
	±	5.99	4.99	3.08	13.68	13.69	13.99
	ES	4.02	4.17	-11.13	0	1.58	1.69
	p-value	0.0175	0.0130	0.0012	0.3191	0.0922	0.0816
ADP	%Var	15.69	0	0	0	-16.69	-7.96
	±	6.22	7.60	4.21	6.64	7.71	6.73
	ES	1.53	0	0	0	-1.54	-0.80
	p-value	0.0801	0.7516	0.3683	07852	0.1251	0.3261
Alanine	%Var	0	0	-5.36	0	0	0
	±	4.65	2.90	1.50	2.70	13.57	10.96
	ES	0	0	-2.40	0	0	0
	p-value	0.9927	0.3520	0.0216	0.8757	0.9309	0.9176
AMP	%Var	33.21	0	33.09	21.58	0	0
	±	6.68	12.23	6.30	8.94	20.50	16.13
	ES	2.79	0	2.95	1.42	0	0
	p-value	0.0448	0.4223	0.0142	0.0992	0.8801	0.7696
Asparagine	%Var	-9.56	-14.75	0	0	0	0
	±	4.40	9.10	3.55	3.68	8.29	7.62
	ES	-1.49	-1.14	0	0	0	0
	p-value	0.1425	0.1739	0.4118	0.5783	0.9706	0.6977
Aspartate	%Var	26.07	12.06	-49.13	-27.27	25.13	31.94
	±	7.66	8.07	2.61	13.98	10.65	11.34
	ES	1.97	0.92	-16.27	-1.47	1.37	1.59
	p-value	0.0461	0.2394	0	0.1492	0.1579	0.1252
ATP	%Var	0	7.46	-35.14	-19.38	-13.23	0
	±	12.04	6.10	8.06	14.43	13.06	17.53
	ES	0	0	-3.46	-0.97	0	0
	p-value	0.7021	0.3561	0.0083	0.2396	0.3878	0.6315
Choline	%Var	-64.99	-45.75	-30.47	0	0	0
	±	13.52	16.00	14.38	14.29	27.27	29.50
	ES	-4.65	-2.42	-1.63	0	0	0
	p-value	0.0079	0.0503	0.0926	0.8819	0.8822	0.9393
Citrate	%Var	55.21	21.79	0	0	-16.61	-10.25
	±	21.64	6.96	3.26	3.94	6.48	3.17
	ES	1.31	1.84	0	0	-1.83	-2.22
	p-value	0.1811	0.0800	0.9596	0.7650	0.0678	0.0474
Dimethylamine	%Var	46.27	41.83	-42.62	-20.34	42.55	53.45
	±	6.02	11.73	9.37	11.00	16.60	15.51
	ES	4.08	1.93	-3.78	-1.34	1.38	1.78
	p-value	0.0034	0.0720	0.0061	0.1360	0.1255	0.0716
Formate	%Var	72.03	62.94	-45.77	-18.54	24.05	31.65
	±	12.35	7.47	3.42	13.74	16.91	15.91
	ES	2.80	4.19	-11.35	-0.96	0.83	1.12
	p-value	0.0218	0.0045	0.0001	0.2748	0.3199	0.2135
Glutamate	%Var	32.75	16.48	12.53	0	0	0
	±	8.02	7.74	2.58	4.20	5.15	8.31
	ES	2.29	1.28	2.98	0	0	0
	p-value	0.0469	0.1484	0.0272	0.3192	0.3343	0.4967
Glycine	%Var	-42.17	-42.17	-15.95	18.54	0	35.51
	±	2.69	3.73	6.25	9.38	20.56	13.95
	ES	-12.97	-9.36	-1.81	1.18	0	1.41
	p-value	0.0004	0.0021	0.0663	0.1947	0.8579	0.1107

Table S1 (Cont.)

Time		1h		3h		6h	
Conc. (µM)		CL307 1 µM	CL307 2 µM	CL307 1 µM	CL307 2 µM	CL307 1 µM	CL307 2 µM
Isoleucine	%Var	-28.78	-28.78	-18.94	0	0	0
	±	4.76	6.28	2.36	7.39	9.36	9.38
	ES	-4.61	-3.49	-5.79	0	0	0
	p-value	0.0024	0.0076	0.0012	0.4722	0.8328	0.3814
Lactate	%Var	0	23.81	30.38	0	0	0
	±	18.34	18.23	17.35	22.66	32.97	13.34
	ES	0	0	0.99	0	0	0
	p-value	0.5902	0.3507	0.2641	0.9274	0.7412	0.5431
Leucine	%Var	-24.74	-25.63	-22.81	0	0	20.24
	±	3.25	3.84	2.62	8.54	9.58	8.85
	ES	-5.67	-5.00	-6.41	0	0	1.36
	p-value	0.0013	0.0033	0.0006	0.4552	0.3941	0.1382
Myo-inositol	%Var	59.71	61.16	13.82	0	-30.37	-27.34
	±	5.55	7.35	2.95	3.30	6.43	7.36
	ES	5.41	4.16	2.86	1.20	-3.64	-2.81
	p-value	0.0066	0.0031	0.0148	0.1527	0.0088	0.0128
Phosphocholine	%Var	-8.26	-17.92	58.95	21.70	-27.30	-27.34
	±	8.20	7.75	1.57	14.40	8.75	8.30
	ES	0	-1.66	18.94	0.89	-2.36	-2.49
	p-value	0.3537	0.0642	0.0000	0.3046	0.0226	0.0189
Serine	%Var	0	-12.20	0	7.48	17.13	13.55
	±	2.96	3.57	2.15	4.76	5.14	5.68
	ES	0	-2.38	0	0.99	2.01	1.46
	p-value	0.4063	0.0274	0.4254	0.2657	0.0561	0.0978
Succinate	%Var	20.34	21.78	89.34	0	0	-9.74
	±	5.64	4.22	3.25	20.73	13.64	7.44
	ES	2.14	3.04	12.40	0	0	-0.90
	p-value	0.0389	0.0096	0.0002	0.4207	0.9574	0.2466
Taurine	%Var	-15.75	-30.32	49.77	21.30	-22.86	-25.47
	±	5.54	4.53	2.52	15.04	7.78	3.03
	ES	-2.02	-5.15	10.34	0.84	-2.17	-6.30
	p-value	0.0371	0.0046	0.0006	0.3275	0.0574	0.0030
Tyrosine	%Var	0	-26.67	-21.70	-13.21	0	21.33
	±	20.90	20.70	7.25	10.30	14.71	14.66
	ES	0	-0.97	-2.19	-0.90	0	0.86
	p-value	0.4174	0.2121	0.0330	0.2525	0.6871	0.2731
UDP	%Var	9.01	12.42	9.89	0	-11.15	0
	±	4.44	5.42	3.81	6.27	6.11	8.04
	ES	1.27	1.41	1.62	0	-1.26	0
	p-value	0.1468	0.0973	0.0911	0.4484	0.1328	0.9409
UTP	%Var	0	10.32	0	0	-6.92	0
	±	8.06	5.57	4.00	7.39	4.53	4.83
	ES	0	1.15	0	0	-1.03	0
	p-value	0.6204	0.1830	1.0000	0.7841	0.2250	0.8708
Valine	%Var	-17.06	-25.59	-28.61	0	12.74	20.46
	±	5.93	7.10	2.74	8.70	9.21	10.07
	ES	-2.05	-2.70	-7.97	-0.80	0.85	1.20
	p-value	0.0448	0.0148	0.0032	0.3450	0.3168	0.1575

Table S2 – Main metabolite variations in aqueous extracts of cells exposed to TNF-α+TGF-β and/or CL307 for 1 and 3h, in relation to control groups (17h and 19h), expressed as percentage of variation (%Var) and respective error (±), effect size (ES) and *p*-value. The variations with |ES| < 0.8 were not considered relevant.

Total time		17h			19h		
		Ct 16h[CL307 1h] vs Ct 17h	TNF+TGF 17h vs Ct 17h	TNF+TGF 16h[CL307 1h] vs Ct 16h[CL307 1h]	Ct 16h[CL307 3h] vs Ct 19h	TNF+TGF 19h vs Ct 19h	TNF+TGF 16h [CL307 3h] vs Ct 19h
Acetate	%Var	0	59.72	0	0	-27.21	0
	±	21.82	20.61	14.79	23.81	19.99	19.39
	ES	0	1.46	0	0	-1.03	0
	p-value	0.5146	0.1550	0.5278	0.7527	0.2543	0.4713
ADP	%Var	10.48	0	5.03	0	10.20	-8.70
	±	2.68	2.13	2.67	7.41	6.92	6.83
	ES	2.42	0.00	1.20	0	0.92	-0.87
	p-value	0.0252	0.9625	0.1469	0.8905	0.2550	0.3089
Alanine	%Var	-12.35	-7.96	-10.08	0	5.02	0
	±	2.36	2.89	5.98	1.16	1.14	2.13
	ES	-3.64	-1.88	-1.16	0	2.80	0
	p-value	0.0069	0.0638	0.2058	0.7033	0.0128	0.8158
AMP	%Var	27.84	15.81	23.39	27.87	0	-16.21
	±	9.56	11.94	10.01	11.62	10.39	8.29
	ES	1.67	0.80	1.37	1.38	0	-1.39
	p-value	0.0661	0.2993	0.1098	0.1549	1.0000	0.1273
Asparagine	%Var	-18.73	0.00	0.00	0	6.52	10.60
	±	4.54	8.69	4.54	2.96	3.52	3.65
	ES	-2.97	0.00	0.00	0	1.17	1.80
	p-value	0.0196	0.8882	0.9556	1.0000	0.1597	0.0642
Aspartate	%Var	0	0	0	0	0	20.73
	±	2.98	5.80	5.09	9.05	10.36	9.37
	ES	0	0	0	0	0	1.31
	p-value	0.5019	0.8818	0.5555	1.0000	0.4913	0.1338
Choline	%Var	-27.24	-30.92	-32.76	0	35.78	-53.51
	±	9.64	11.53	9.46	7.66	14.81	10.35
	ES	-2.14	-2.07	-2.70	0	1.34	-4.61
	p-value	0.0674	0.0755	0.0405	0.8062	0.1422	0.0076
Citrate	%Var	18.39	0	15.62	0	0	15.68
	±	5.46	9.20	3.32	2.44	3.99	2.67
	ES	2.01	0	2.85	0	0	3.56
	p-value	0.0430	0.3581	0.0332	0.5929	0.6772	0.0082
Dimethylamine	%Var	0	8.47	0	0	-14.55	21.82
	±	6.51	4.60	8.67	11.40	11.09	14.10
	ES	0	1.15	0	0	-0.92	0.91
	p-value	0.4676	0.1908	0.5015	0.4959	0.2858	0.2373
Formate	%Var	37.78	75.56	53.33	0	0	34.92
	±	16.93	15.13	15.49	16.77	18.73	14.86
	ES	1.23	2.37	1.78	0	0	1.31
	p-value	0.1505	0.0335	0.0655	0.8042	0.4839	0.1585

Table S2 (Cont.)

Total time		17h			19h		
		Ct 16h[CL307 1h] vs Ct 17h	TNF+TGF 17h vs Ct 17h	TNF+TGF 16h[CL307 1h] vs Ct 16h[CL307 1h]	Ct 16h[CL307 3h] vs Ct 19h	TNF+TGF 19h vs Ct 19h	TNF+TGF 16h [CL307 3h] vs Ct 19h
Glutamate	%Var	-16.84	7.70	0	-17.94	0	10.90
	±	3.25	4.09	9.62	1.87	2.71	1.82
	ES	-3.70	1.18	0	-6.87	0	3.72
	p-value	0.0195	0.1453	0.8256	0.0012	0.6694	0.0108
Glycine	%Var	-6.94	0	0	-13.48	0	0
	±	2.55	2.21	5.61	2.48	1.01	1.54
	ES	-1.84	0	0	-3.81	2.15	1.27
	p-value	0.0486	0.5448	0.7348	0.0183	0.0306	0.1493
Isoleucine	%Var	-10.25	-5.34	0	9.52	14.14	9.23
	±	1.33	4.15	7.31	2.12	1.41	2.17
	ES	-5.32	-0.86	0	2.80	6.11	2.66
	p-value	0.0050	0.3004	0.3775	0.0145	0.0031	0.0176
Lactate	%Var	23.80	-9.22	0	23.90	0	0
	±	6.72	6.37	12.29	14.75	16.80	14.84
	ES	2.07	-0.99	0	0.95	0	0
	p-value	0.0366	0.2561	0.6951	0.2307	0.7279	0.4303
Leucine	%Var	-13.59	0	-8.15	5.06	14.51	9.03
	±	2.21	5.61	6.80	2.19	1.93	2.32
	ES	-4.31	0	-0.82	1.47	4.57	2.44
	p-value	0.0027	0.5042	0.3274	0.0997	0.0080	0.0223
Myo-inositol	%Var	-8.84	-8.84	0	-12.32	0	9.28
	±	2.30	6.60	4.30	2.80	1.47	4.65
	ES	-2.63	-0.91	0	-3.07	-0.86	1.25
	p value	0.0487	0.2951	0.4690	0.0196	0.2623	0.1828
Phosphocholine	%Var	10.23	7.71	7.20	0	0	5.90
	±	2.15	2.76	4.43	3.14	3.51	2.26
	ES	2.96	1.76	1.02	0.89	0	1.66
	p-value	0.0107	0.0611	0.2288	0.2526	0.5853	0.0713
Serine	%Var	-13.38	6.34	0	-15.86	0	32.41
	±	3.99	2.26	8.03	4.03	4.12	5.17
	ES	-2.35	1.77	0	-2.79	0	3.52
	p-value	0.0333	0.0576	0.9376	0.0448	0.6477	0.0069
Succinate	%Var	0	-5.63	0	0	0	0
	±	3.24	3.56	4.26	8.80	11.69	8.57
	ES	-0.84	-1.06	0	0	0	0
	p-value	0.2944	0.1907	0.6596	0.5347	0.3476	0.5198

Table S2 (Cont.)

Total time		17h			19h		
		Ct 16h[CL307 1h] vs Ct 17h	TNF+TGF 17h vs Ct 17h	TNF+TGF 16h[CL307 1h] vs Ct 16h[CL307 1h]	Ct 16h[CL307 3h] vs Ct 19h	TNF+TGF 19h vs Ct 19h	TNF+TGF 16h [CL307 3h] vs Ct 19h
Taurine	%Var	19.69	5.26	8.41	6.32	0	-6.46
	±	2.46	3.92	0.88	1.39	1.49	1.79
	ES	4.76	0.85	5.96	2.88	0	-2.44
	p-value	0.0137	0.3160	0.0008	0.0116	0.3863	0.0240
Tyrosine	%Var	-20.34	-10.17	-13.56	0.00	7.89	12.28
	±	5.34	6.86	5.53	3.79	5.27	3.88
	ES	-2.77	-1.02	-1.72	0.00	0.94	1.95
	p-value	0.0132	0.2078	0.0592	0.6805	0.2693	0.0693
UDP	%Var	6.85	0	10.28	-5.87	6.70	0
	±	2.52	3.56	2.05	4.85	4.60	3.94
	ES	1.72	0	3.11	-0.81	0.92	0
	p-value	0.0613	0.3179	0.0092	0.2888	0.2389	0.4508
Valine	%Var	-11.74	0	0	0.00	9.84	17.32
	±	1.89	4.04	8.06	1.74	1.76	1.02
	ES	-4.32	0	0	0.88	3.48	10.16
	p-value	0.0175	0.7316	0.4441	0.3009	0.0274	0.0013

Table S3 - Main metabolite variations in the medium of cell samples exposed to TNF-α+TGF-β and/or 1μM of CL307 for 1 and 3h, in relation to the acellular culture medium, expressed as percentage of variation (%Var) and respective error (±), effect size (ES) and *p*-value. The variations with |ES| < 0.8 were not considered relevant.

		Medium samples							
Sample		Ct 17h	TNF+TGF 17h	Ct 16h[CL307 1h]	TNF+TGF 16h[CL307 1h]	Ct 19h	TNF+TGF 19h	Ct 16h[CL307 3h]	TNF+TGF 16h[CL307 3h]
2-oxoisocaproate	%Var	131.03	95.40	106.90	106.90	87.36	104.60	88.51	108.05
	±	2.41	3.89	6.09	5.19	2.53	8.40	5.75	6.76
	ES	21.50	10.84	7.48	8.77	15.70	5.34	6.97	6.78
	p-value	0	0.0001	0.0026	0.0011	0.0001	0.0127	0.0057	0.0071
3-methyl-2-oxovalerate	%Var	2554.55	1990.91	2309.09	2272.73	1850.00	2083.33	1950.00	2041.67
	±	1.87	5.87	12.34	12.95	7.32	13.64	13.22	14.13
	ES	64.89	20.23	9.74	9.27	16.11	8.74	8.96	8.42
	p-value	0	0.0008	0.0043	0.0048	0.0016	0.0055	0.0053	0.0060
Acetate	%Var	0	-12.81	0	0	-13.48	0	-10.28	0
	±	4.92	5.70	6.46	6.51	4.29	6.31	6.48	7.40
	ES	0	-1.57	0	0	-2.20	0	-1.09	0
	p-value	0.8463	0.1057	0.4555	0.5529	0.0588	0.3815	0.1735	0.4315
Alanine	%Var	372.33	240.06	335.45	310.37	286.05	353.71	336.20	272.11
	±	2.38	5.91	8.84	10.83	4.03	12.69	12.26	13.95
	ES	35.66	12.07	9.26	7.33	19.09	6.58	6.68	5.40
	p-value	0	0.0003	0.0027	0.0053	0.0001	0.0088	0.0084	0.0130
Arginine	%Var	-32.27	-36.94	-33.33	-35.67	-40.00	-35.67	-37.94	-35.46
	±	11.99	12.17	12.06	12.05	9.87	10.00	9.78	9.71
	ES	-2.10	-2.43	-2.17	-2.35	-3.31	-2.84	-3.13	-2.90
	p-value	0.0774	0.0633	0.0728	0.0680	0.0359	0.0365	0.0390	0.0425
Aspartate	%Var	0	-15.35	-1220	-11.02	-18.82	-14.12	-17.65	-11.76
	±	3.57	4.29	4.21	4.60	1.98	3.65	3.72	4.08
	ES	0	-2.53	-2.01	-1.66	-6.84	-2.72	-3.39	-2.00
	p-value	0.5042	0.0250	0.0468	0.0667	0.0005	0.0302	0.0173	0.0675
Formate	%Var	260.0	190.00	300.00	250.00	210.00	320.00	270.00	250.00
	±	4.35	7.25	8.94	16.63	6.90	18.04	19.03	16.63
	ES	16.98	8.78	8.76	4.36	9.70	4.46	3.94	4.36
	p-value	0.0015	0.0002	0.0010	0.0148	0.0001	0.0163	0.0207	0.0148

Table S3 (Cont.)

Medium samples									
Sample		Ct 17h	TNF+TGF 17h	Ct 16h[CL307 1h]	TNF+TGF 16h[CL307 1h]	Ct 19h	TNF+TGF 19h	Ct 16h[CL307 3h]	TNF+TGF 16h[CL307 3h]
Glucose	%Var	-62.84	-66.36	-71.98	-64.94	-78.61	-77.38	-82.96	-65.89
	±	6.50	6.66	7.73	7.30	4.51	5.13	5.06	6.29
	ES	-9.21	-9.74	-9.50	-8.60	-18.75	-16.08	-18.31	-10.20
	p-value	0.0038	0.0035	0.0007	0.0010	0.0010	0.0001	0.0002	0.0001
Glutamate	%Var	6.88	-9.92	0	0	-8.28	0	0	-7.34
	±	2.48	2.96	3.87	4.47	3.02	4.38	4.96	4.85
	ES	1.75	-2.30	0	0	-1.87	0	0	-1.03
	p-value	0.1129	0.0425	0.8481	0.9342	0.0867	0.8637	0.8017	0.1974
Glutamine	%Var	-30.47	-32.67	-35.55	-30.06	-42.86	-39.32	-43.76	-27.88
	±	8.46	8.60	8.97	8.74	7.65	7.97	8.17	8.38
	ES	-2.78	-2.97	-3.15	-2.64	-4.66	-4.01	-4.48	-2.53
	p-value	0.0468	0.0401	0.0295	0.0409	0.0172	0.0129	0.0100	0.0227
Glycine	%Var	24.32	0	16.99	18.15	0.00	14.60	0	0
	±	7.47	9.00	8.89	9.40	5.37	8.63	8.34	9.98
	ES	1.90	0	1.15	1.16	0.00	1.03	0	0
	p-value	0.0959	0.8021	0.1690	0.1581	0.8441	0.1999	0.4835	0.3612
Histidine	%Var	19.31	119.23	134.62	150.00	67.86	96.43	92.86	92.86
	±	8.08	6.38	12.38	16.45	3.77	5.39	11.44	11.44
	ES	7.92	7.65	4.25	3.40	8.78	7.89	3.62	3.62
	p-value	0.0010	0.0003	0.0110	0.0256	0.0002	0.0013	0.0253	0.0253
Isoleucine	%Var	-37.76	-49.48	-42.06	-41.67	-50.74	-45.11	-48.46	-48.19
	±	7.02	7.71	8.19	8.04	4.50	5.50	5.58	5.98
	ES	-4.33	-5.57	-4.25	-4.27	-9.88	-6.92	-7.49	-6.94
	p-value	0.0219	0.0107	0.0069	0.0077	0.0041	0.0006	0.0005	0.0005
Lactate	%Var	996.17	777.78	1063.41	902.11	870.00	991.27	996.73	749.09
	±	0.99	5.09	5.91	7.11	3.23	9.85	9.24	8.55
	ES	110.26	20.43	18.61	15.03	32.88	11.04	11.77	12.06
	p-value	0	0.0010	0.0012	0.0018	0.0002	0.0034	0.0030	0.0028

Table S3 (Cont.)

Medium samples									
Sample		Ct 17h	TNF+TGF 17h	Ct 16h[CL307 1h]	TNF+TGF 16h[CL307 1h]	Ct 19h	TNF+TGF 19h	Ct 16h[CL307 3h]	TNF+TGF 16h[CL307 3h]
Leucine	%Var	-47.51	-48.97	-49.09	-44.41	-53.28	-47.43	-51.98	-44.35
	±	6.09	6.52	6.50	6.29	4.87	5.27	5.53	6.09
	ES	-6.68	-6.50	-6.54	-5.93	-9.74	-7.71	-8.30	-6.12
	p-value	0.0087	0.0043	0.0044	0.0057	0.0012	0.0005	0.0004	0.0007
Methionine	%Var	-24.29	-35.00	-30.36	-30.36	-38.71	-34.05	-38.71	-32.26
	±	1.82	0.97	2.76	2.76	2.18	3.61	2.88	3.31
	ES	-9.93	-28.63	-8.47	-8.47	-14.40	-7.42	-10.89	-7.59
	p-value	0.0007	0	0.0028	0.0028	0.0005	0.0007	0.0001	0.0005
Myo-inositol	%Var	-21.63	-26.74	-23.49	.24.19	-31.85	-24.28	-27.62	-24.94
	±	5.85	6.14	6.56	6.81	4.48	5.35	5.53	5.48
	ES	-2.71	-3.28	-2.65	-2.64	-5.52	-3.37	-3.78	-3.40
	p-value	0.0479	0.0280	0.0267	0.0231	0.0057	0.0069	0.0045	0.0066
Phenylalanine	%Var	-35.15	-39.59	-39.93	-33.45	-45.64	-40.42	-47.39	-32.06
	±	6.60	6.81	7.34	7.04	6.88	7.38	7.94	7.85
	ES	-4.22	-4.74	-4.44	-3.73	-5.62	-4.48	-5.11	-3.18
	p-value	0.0201	0.0152	0.0084	0.0135	0.0122	0.0068	0.0036	0.0100
Pyroglutamate	%Var	-23.14	-31.40	-29.48	.26.72	-35.78	-30.24	-33.43	-27.05
	±	3.40	3.74	4.98	4.77	2.26	3.70	3.44	4.30
	ES	-5.02	-6.50	-4.53	-4.22	-12.60	-6.29	-7.62	-4.75
	p-value	0.0148	0.0046	0.0023	0.0030	0.0001	0.0038	0.0018	0.0101
Pyruvate	%Var	-21.60	-57.49	-29.27	-55.92	-62.37	-60.22	-67.38	-67.92
	±	3.22	2.38	14.80	5.81	7.88	10.64	8.34	8.29
	ES	-4.92	-22.12	-1.51	-8.72	-7.51	-5.29	-7.96	-8.10
	p-value	0.0115	0.0001	0.1455	0.0043	0.0068	0.0013	0.0045	0.0050
Succinate	%Var	-16.24	-29.60	-23.85	-23.85	-32.17	-22.13	-27.51	-24.02
	±	4.37	4.93	6.76	6.47	2.47	5.41	5.25	6.53
	ES	-2.64	-4.61	-2.62	-2.73	-10.16	-3.00	-3.97	-2.73
	p-value	0.0503	0.0103	0.0165	0.0139	0.0016	0.0411	0.0235	0.0504

Table S3 (Cont.)

Medium samples									
Sample		Ct 17h	TNF+TGF 17h	Ct 16h[CL307 1h]	TNF+TGF 16h[CL307 1h]	Ct 19h	TNF+TGF 19h	Ct 16h[CL307 3h]	TNF+TGF 16h[CL307 3h]
Threonine	%Var	17.43	0	13.76	11.01	10.38	15.09	10.38	14.15
	±	5.60	4.99	7.68	6.68	6.83	7.85	7.82	7.10
	ES	1.87	0	1.10	1.02	0.94	1.17	0.82	1.22
	p-value	0.0549	0.4639	0.1724	0.1934	0.2535	0.1518	0.2809	0.1545
Trans-4-hydroxy-L-proline	%Var	11.90	0	0	0	0	0	0	0
	±	5.95	6.90	7.75	8.09	6.55	8.90	6.92	8.55
	ES	1.23	0	0	0	0	0	0	0
	p-value	0.1494	0.8726	0.3608	0.5153	0.7385	0.5648	0.8740	0.7110
Tyrosine	%Var	-17.01	-28.96	-23.58	-19.10	-33.33	-24.46	-31.50	-22.94
	±	7.03	7.80	8.16	8.12	5.22	6.48	6.42	7.71
	ES	-1.73	-2.83	-2.14	-1.70	-5.01	-2.81	-3.80	-2.20
	p-value	0.1144	0.0359	0.0463	0.0758	0.0114	0.0129	0.0049	0.0308
Valine	%Var	-46.17	-50.27	-50.00	-44.81	-54.15	-51.58	-55.59	-46.99
	±	7.10	7.57	7.62	7.17	4.60	4.52	4.79	4.97
	ES	-5.52	-5.80	-5.71	-5.26	-10.55	-10.05	-10.49	-8.07
	p-value	0.0135	0.0078	0.0072	0.0120	0.0030	0.0033	0.0017	0.0009